January 1977

Seedability of Winter Orographic Storms in Utah

Geoffrey E. Hill

Seedability of Winter Orographic Storms in Utah

By
Geoffrey E. Hill

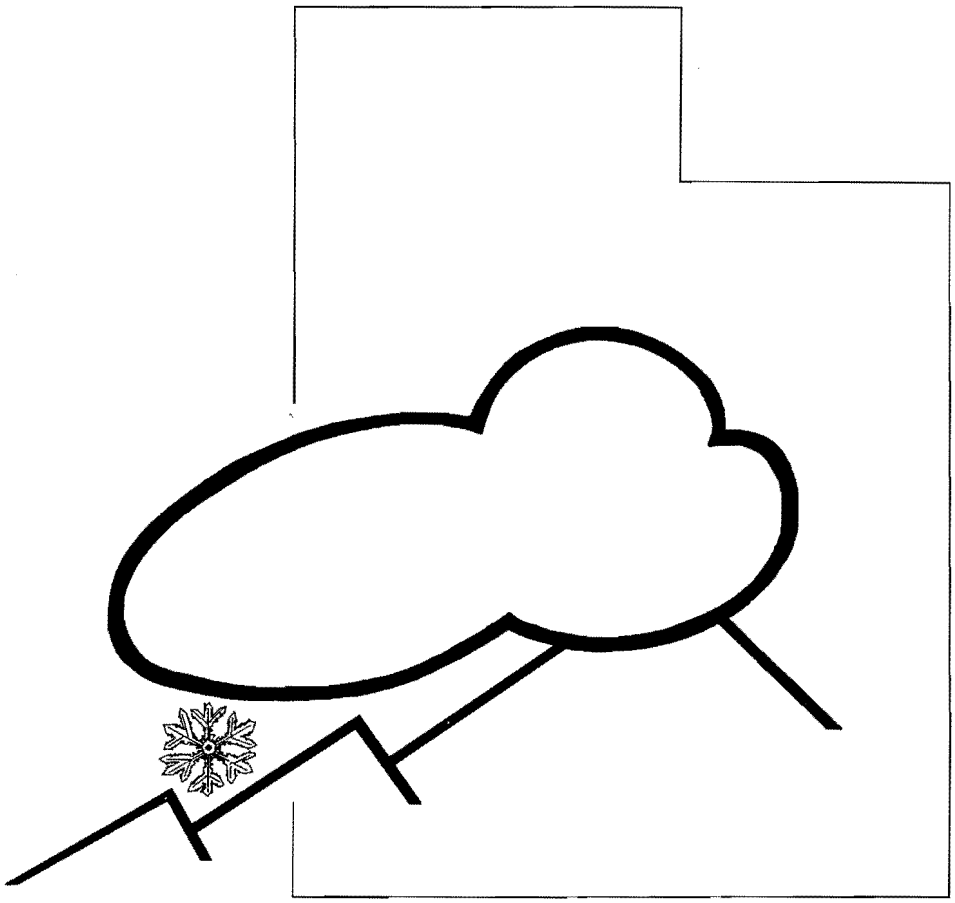

Utah Water Research Laboratory
College of Engineering
Utah State University
Logan, Utah 84322

ATMOSPHERIC WATER RESOURCES SERIES

Report A2

December 1977

SEEDABILITY OF WINTER OROGRAPHIC STORMS IN UTAH

by
Geoffrey E. Hill

Final Report

December 15, 1977

for the

Division of Atmospheric Water Resources Management
U.S. Bureau of Reclamation
Denver, Colorado

under
Contract No. 14-06-D-7184
Dated July 1, 1971

Utah Water Research Laboratory
College of Engineering
Utah State University
Logan, Utah 84322
December 1977

ATMOSPHERIC WATER RESOURCES SERIES

Report A2

ABSTRACT

The primary objective of this research has been to collect and analyze data from (randomized) seeded and unseeded winter storms over the Wasatch Mountains for the purpose of developing and designing cloud seeding technology. Two field programs were conducted sequentially; the first was done by airborne seeding and the second by seeding from mountaintop generators.

Analysis of precipitation estimators based upon radar and/or rawinsonde data and target precipitation show that increased precipitation due to seeding may occur under certain meteorological conditions. Favorable conditions were found when the supercooled water concentration as measured by aircraft icing rates was high. Precipitation in these particular seeded storms was several times the amount estimated from relationships derived from meteorological parameters and unseeded precipitation. Based upon these *a posteriori* results, it is hypothesized that winter season orographic precipitation may be increased by about thirty percent by seeding about one sixth of the storms. Analysis of seeding effects using cloud top temperature on an *a priori* basis of stratification yielded inconclusive results. Other meteorological aspects related to cloud seeding technology are presented in the report.

ACKNOWLEDGMENTS

The assistance and cooperation of the following are acknowledged gratefully: Atmospherics, Inc., Fresno, California for their effective participation in the airborne seeding program; U.S. Forest Service for their cooperation and permission in establishing field installations; U.S. Soil Conservation Service for cooperative field sites; National Weather Service, NOAA, Salt Lake City Airport for data acquisition; U.S. Air Force Air Weather Service, Hill Air Force Base for data acquisition; NCAR which is sponsored by the National Science Foundation, for the loan of an ice nuclei counter; Mountain Fuel Supply for sharing facilities atop Cache Peak; and Mr. Alton Cooper for permission to setup a rawinsonde field site at Mendon, Utah during the three year ground seeding program.

TABLE OF CONTENTS

TABLE OF CONTENTS (CONTINUED)

TABLE OF CONTENTS (CONTINUED)

LIST OF FIGURES

LIST OF FIGURES (CONTINUED)

LIST OF FIGURES (CONTINUED)

LIST OF FIGURES (CONTINUED)

LIST OF TABLES

1.0 INTRODUCTION

1.1 Overview of Project

1.1.1 Review. As part of the Bureau of Reclamtion's Project Skywater, a network of precipitation gages was set up in the Northern Wastach during the years 1967 through 1969. This network of precipitation gages was operated by remote control, so detailed data from an extensive mountainous region could be obtained during winter storms (Chadwick, 1968). By 1969 the results of the Climax experiment (Grant and Mielke, 1967), and other work, led to the idea that the temperature at 500 mb, and later, the temperature at cloud top could be used to discriminate storms in which seeding would increase precipitation. Thus, a number of seeding experiments in the mountains of Western United States were initiated. One of these experiments was carried out by the Utah State University.

Seeding was to be done, in this experiment, by aircraft on a randomized basis. The extensive network of precipitation gages was expected to provide most of the data, from which seeding effects would be found. Other supporting meteorological data such as obtained from rawinsondes were considered basic to the program. After two years of the randomized experimentation, the present contract began. A third year of experimentation was continued. Thus, the airborne seeding program was carried out during the three winters of 1969-70, 1970-71, and 1971-72. After a year of preparation, and under greatly reduced funding, a ground based seeding program was initiated. This ground seeding program which was carried out during the three winters of 1973-74, 1974-75, and 1975-76, was funded in its third year primarily by the Utah Division of Water Resources (UDWR).

Although the first two years of airborne seeding were carried out prior to the current contract and the last year of the ground seeding program was supported by UDWR, a complete analysis of both programs is given in this report. Otherwise only a partial analysis could be made.

1.1.2 Basic Objectives. The objectives of the project emphasized the establishment of a seeding technology which could be used in precipitation management. Efforts were to be concentrated in two main areas: 1) collection and analysis of data needed to develop the techniques for treating winter storms over the Wasatch Mountains, and 2) design and application of the precipitation management system, with such research as necessary to refine the system to full operational capability.

To establish this technology, randomized seeding was carried out using airborne generators in storms declared suitable. Rawinsonde data were used to stratify storms according to cloud top temperature. Later, ground seeding was carried out with various improvements in the data collection system, especially concerning the cloud top temperature determination.

1.2 Summary

1.2.1 Summary of Work. During the last year of the airborne seeding program, 27 storms were studied. Seeding material was delivered in each storm, either during the first or second half of an eight hour period; the choice of which half was seeded was made on a randomized basis. Airborne seeding was carried out for only the first two hours of the seeded half, so that the purge time would be about two hours. In addition to the seeding effort, rawinsondes were released either once or twice during the eight hour period. Precipitation data were received from around the network at intervals of about once a half hour. Silver samples and ice nuclei data were also collected on many of the storms. During the off winter months, maintenance, calibration of precipitation gages, and other field work were carried out. This phase of activity, when added to the two previous years, resulted in a total of 80 storms studied in the airborne program. In addition to the field work, modeling and other physical studies were made in support of the overall program. Analysis of data, of course, constituted a large effort.

Following completion of the airborne seeding program, a ground based seeding program was carried out. In this program three remotely controlled mountaintop seeders were used to deliver silver iodide particles into the clouds. Storms selected for study were primarily orographic. Because the distribution of seeding material released from the ground is much less predictable than when released from the air, a given storm was either seeded or left unseeded for the full period of measurement. In the analysis of cloud top temperatures from the airborne seeding program, a high degree of natural variability was found. Therefore, in the later effort, releases of rawinsondes were made at two hourly intervals during periods of study. Again, during off winter periods, maintenance,

calibration of precipitation gages, and other field work were performed. Other studies, such as development of simple predictors, to account for some of the natural variability of precipitation, were carried out.

Several theoretical studies were made in support of the experimental programs. One investigation concerns the physical basis of cloud seeding; in this development a simple model of orographic flow and its effect on a three phase water budget is considered. The result yields an estimate of the amount of ice nuclei required for an efficient production of precipitation. The next study analyzes the time required to glaciate a supercooled water cloud under various meteorological conditions, such as temperature, updraft velocity and concentration of ice crystals. In another development, a formula relating ice saturation to the dew point depression is given. It turns out that, to a close approximation, the dew point depression at ice saturation is one-tenth the negative of the air temperature in degrees Celsius. With this formula, estimated ice cloud top temperatures can be found by inspection of the vertical distribution of temperature and dew point, as usually plotted on thermodynamic charts. Diffusion studies were also made, one for a line source and another for point sources. The first was used to aid in the analysis of aircraft seeding which was done along a line, and the second study was applied to the mountain top generators.

Other studies included an analysis of the data collection system, calibration procedures for precipitation data, a data quality analysis, and standardization procedures for precipitation data. Use of other supporting meteorological data is also discussed. In this connection a preliminary analysis of cloud structure and its variability is made. Based upon such an analysis, the frequency of rawinsonde releases required to adequately represent cloud top temperatures is estimated. In addition, the use of other parameters derived from rawinsonde data is discussed. Another important step taken in the study is the classification of storm periods into types, i.e., orographic, convective, frontal, or cyclonic. In an analysis using precipitation estimates, or covariates, to reduce unexplained natural variability, a classification system is not only useful, but probably necessary.

1.2.2 Summary of Results. A review of previous evaluations of the three year airborne seeding program along with an analysis of cloud top temperatures shows that the positive seeding effects reported earlier were fortuitous. The reason is that a free choice of limits-of-effect, such as an upper and lower cloud top temperature within which seeding is thought to increase precipitation, enhances artificially any apparent effects. In the analysis of cloud top temperatures, it was found that daytime values were much warmer than at night by around 12°C or 13°C on the average. The difference is due to the use of rawinsondes, which at that time were poorly shielded from effects of solar radiation. Cloud top temperatures based upon continuous vertical incidence radar observations at Hill AFB were used as a basis of stratification rather than those found from rawinsondes.

When only orographic clouds were considered, it was found that at cloud top temperatures warmer than -30°C the seeded precipitation was about 65 percent greater than the unseeded precipitation; however, a precipitation estimator defined as the difference between the cloud base and cloud top mixing ratio (water vapor content) also was higher in the seeded precipitation than the unseeded by over 100 percent. The relationship between the estimator and precipitation for seeded and unseeded precipitation showed no increase in precipitation from seeding. In the cold cloud top temperature category a similar situation was found.

In the non-orographic cases, the precipitation was much higher and more variable with respect to the estimator than in the orographic cases. No seeding effects in these cases were evident. However, the importance of separating various meteorological types is pointed out, because if a few highly variable precipitation events were included in a group of orographic events, the former could produce apparent seeding effects that might appear significant with the large total sample. Finally, use is made of icing reports on the seeding aircraft as a means of identifying cases of high supercooled water concentrations, instead of using cloud top temperatures. Precipitation was found to be higher in the seeded cases than in the unseeded, but statistical significance at the 0.1 level was not achieved.

In the three year ground seeding experiment it was postulated that increases in precipitation would be found in orographic clouds if the ice cloud top temperature were warmer than -28°C. Frequent (solar shielded) rawinsonde releases were to be made and non-orographic clouds were to be eliminated from the data. The precipitation network was reduced to 11 key high altitude gages. Several improvements in the gages were made in order to reduce both the occurrence of snow sticking to the outside of a weighing gage and the mechanical sticking of the weighing mechanism itself. The improvements proved to be successful. Improvements were also made on the seeders to ensure their reliable operation. One such is an automatic ignition system which was activated when the propane flame was supposed to be on but was extinguished, usually by wind.

As in the airborne experiment each event was classified according to type; however, in the ground seeding study, effort was made to exclude non-orographic types before the fact. For the identification of convection, an objective method was developed, based upon the rawinsonde data. A comparison of radar and rawinsonde cloud top temperatures showed a weak relationship, but when only single layered orographic clouds are considered a well defined relationship was found between the two temperatures. Cloud top temperature variability of two-hourly averages expressed by the standard deviation was found to be 5.5°C for two hours time difference in

successive measurements, 13°C for four hours, and 22°C for six hours. Data for cases with scattered clouds or highly variable tops due to multilayers are not included in this analysis. Thus, when all clouds are considered, variations in cloud top temperature are even higher than the amount given here.

Besides cloud top temperatures, two other measures of seedability are explored. One measure is simply the concentration of supercooled cloud water. The rate of aircraft icing is used as an index to the supercooled water concentration. Another measure of seedability is the ratio of the concentrations of supercooled water to ice crystals. The latter quantity is represented by the precipitation rate. Because the precipitation rate may be affected by seeding, analysis of seeding effects is made according to the simple definition of seedability, i.e., the rate of aircraft icing.

An estimator of orographic precipitation is defined as the product of two factors, the cloud top and cloud base mixing-ratio difference and the 9000 foot wind speed normal to the mountain barrier axis. The square of this estimator is found to greatly improve the relationship with precipitation. To achieve statistically normal distributions, the fourth root of precipitation and the square root of the linear estimator are used.

As in the airborne seeding program, analysis is made of events classified as having present substantial amounts of supercooled water. Aircraft reports (PIREPS) are used to make the classification. Because relatively few events are available, events from the airborne seeding program are included in the analysis. Data from the airborne program are made compatible with the ground program by calculating both the precipitation and the precipitation estimator the same way for the two programs.

When ground/air unseeded precipitation is compared with seeded precipitation of the ground program, the seeded precipitation is greater than the unseeded for a given value of the estimator with a significance level of 0.05. In a comparison of unseeded precipitation with the seeded precipitation of the airborne seeding program similar increases of precipitation in seeded events are found, but statistical significance is not achieved at the 0.10 level. When the two programs are combined, the seeded precipitation is found to be greater by a factor of two to three (in the range of most frequent values of the estimator) with a significance level of 0.03. A seasonal increase in precipitation from seeding is estimated to be about thirty percent of the total precipitation. Only about one sixth of the storms are seeded to realize this increase.

Although the foregoing results appear to be statistically significant, it is pointed out that in the airborne experiment the original plan called for a simple comparison between seeded and unseeded precipitation (Chappell et al., 1971). In the first year of the project the cloud top temperature should have been warmer than -22°C for an operational period to be carried out. Later this criterion was abandoned, and stratification according to cloud top temperature was attempted. However, no clear-cut procedure was established beforehand to obtain these temperatures. In the ground seeding experiment such procedures were clearly established; that is upper-level soundings were made according to a fixed schedule and specific criteria for finding cloud top temperatures were formulated. On the other hand in neither experiment was the use of aircraft-icing rates planned as a basis of stratification. Therefore, these apparent seeding effects are regarded as tentative, and it is concluded that further study of stratification based upon supercooled water concentrations is warranted.

2.0 OBSERVATION SYSTEM

2.1 Telemetry System

2.1.1 ARC and Precipitation Network. The telemetering precipitation measurement system is made up of the following four major components (Chappell et al., 1971):

1. The automatic readout console (ARC) located at the Utah Water Research Laboratory (Figure 1).

2. The cable that carries the signals between the automatic readout console and the Mt. Logan translator. There are 27 quarter-mile sections in each of two, four-wire cables. The second cable provides a backup in the event that the first cable fails.

3. The Mt. Logan translator which relays the information from the automatic readout console to the remote telemetering stations and vice versa.

4. The remote telemetering stations. Each installation includes: a) the support assembly on which the precipitation collection weighing system is mounted; b) a standard can-type precipitation collector, with Alter wind shields; c) the weighing transducer, which converts the accumulated precipitation into an electromagnetic signal; d) the electronics housing (a cylindrical can), which is buried in the ground; e) the electronics unit, which is capable of both receiving and sending signals; and f) an antenna for receiving and transmitting electromagnetic signals.

Although some of the components of the telemetering system are extremely complicated, the general principle of operation is quite simple. The automatic readout console interrogates a remote station. The query is carried by the cable to the Mt. Logan translator which electronically transmits the message. The appropriate remote station responds with an electromagnetic frequency which is received by the translator. This signal is then converted and sent via the cable to the automatic readout console, where it is printed out.

The order of station interrogation is programmed into the automatic readout console. However, stations can be omitted from this order at the discretion of the operator. Once the stations to be queried have been selected and the switch turned on, the automatic readout console automatically interrogates the stations in turn until all have been queried. The programmer returns immediately to the first station, repeating the cycle over and over until the switch is turned off. If, during a cycle, a station does not respond, it is automatically queried a set number of times up to three. If there is still no response, the next station is automatically interrogated.

The data printout is in systems units, either electromagnetic periods or frequencies (Figure 2). These printed values are punched and computer converted and edited to precipitation values.

The telemetering network along with station latitude, longitude and elevation, and can capacity is listed in Table 1.

The telemetry base station can be considered as the center of the telemetering system. Interrogations are initiated and replies are recorded by this unit. The system is automatic in that it will automatically interrogate and record data without human intervention. The system has the capacity to handle up to 200 remote stations.

In simplified form, in the command phase, the base station actuates a program sequencer, an address locater, and an interrogation generator. Upon station selection and interrogation, the data-receive mode goes into effect, and an automatic tracking filter starts searching for the received signal lying within the audio spectrum. Once located, the signal is matched in frequency and phase by a locally generated signal. The frequency of the locally generated signal, locked in phase with the remote signal, is counted by a digital counter. Tests conducted on the readout system indicate that tracking error of the base station is less than $\pm$ 1 part in 50,000.

Data are read out to five significant figures by taking a time period average of the incoming frequency. Thus a 2000.00 Hz signal would be read out as a time period of 500.00 microseconds. Theoretical resolution obtainable in the system described is the difference in numerical digits between 1/1100.00 and 1/2500.00 or 50,909 (with the decimal point omitted). Fractions of a cycle can be measured by period measurements whereas only whole cycles are counted on a frequency basis.

The remote station broadcasts and receives using a single 5-element Yagi antenna. The antenna is usually 6 m in height and is placed about 3 m to 5 m from the instrument housing. Vertical polarization is

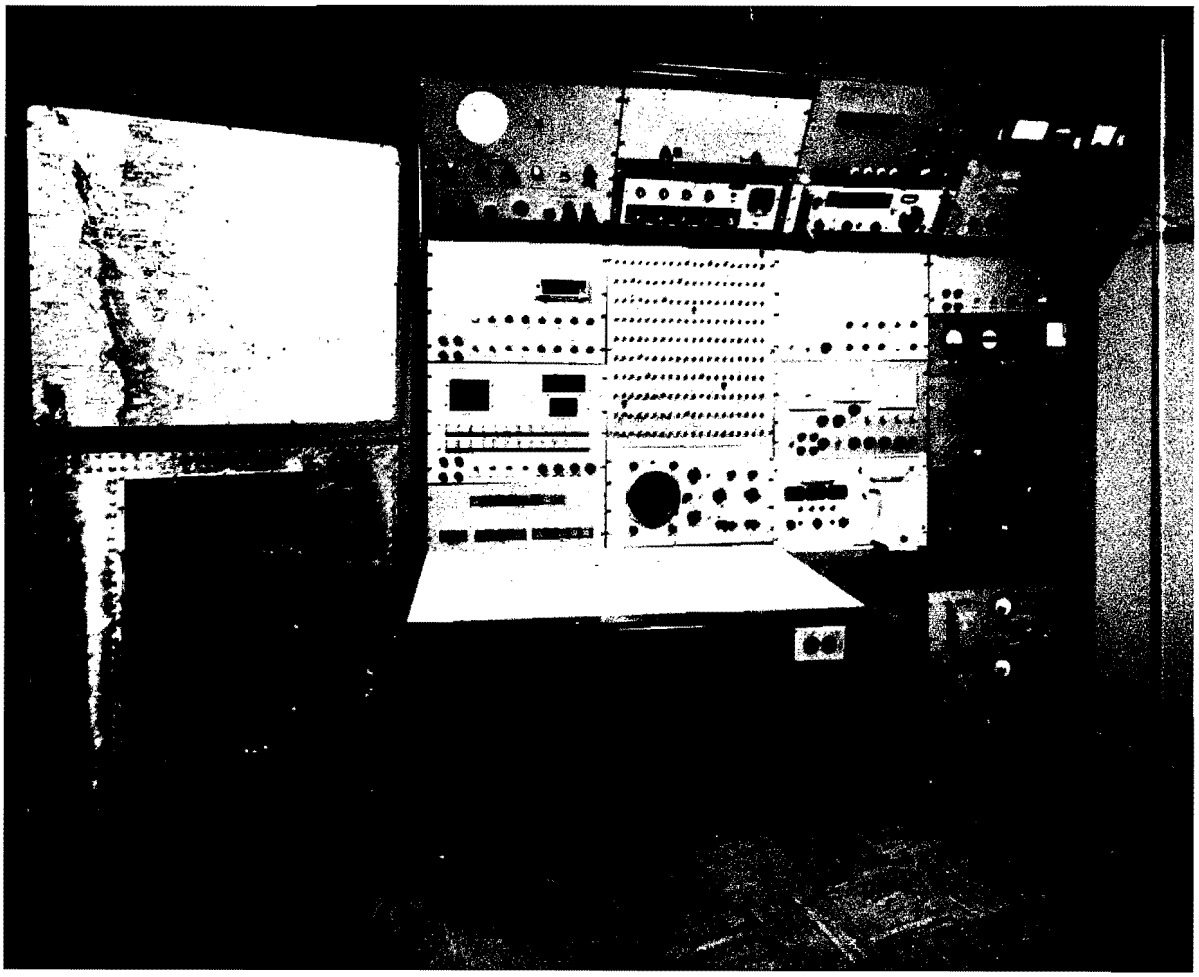

Figure 1. Automatic readout console.

used to be compatible with the vertical omni-direction antenna installed at the mountaintop translator.

Radio transmission is quasi line-of-sight; the radio signals are about 2 meters in wavelength. The radio transmitters operate in the hydrologic telemetering band at 170-174 MHz. Signals, transmitted from a remote site, are beamed to the Mt. Logan translator which lies about 6.4 air kilometers from the Utah Water Research Laboratory. Signals are thence transmitted via land line to the base station located at the laboratory.

The basic remote telemetry station is simple in design, and incorporates a unique transducer sensing technique. The system operates for extended periods of time unattended and requires little maintenance during the snow season. The station is relatively free of problems associated with icing, freezing, thawing, or snow accumulation.

These stations were designed to provide other needed hydrologic or meteorologic data, such as

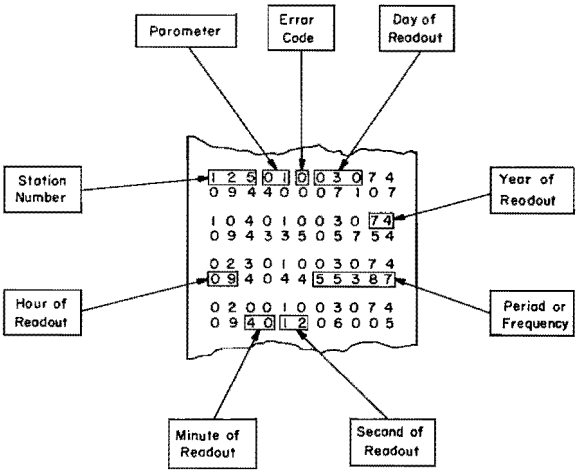

Figure 2. Sample automatic readout of precipitation.

Table 1. Wasatch Weather Modification Project precipitation telemetering stations.

Station No.	Station Name	Latitude	Longitude	Elevation	Can Size
201	Dayton	42°08'51"	112°04'03"	7550'	36 inch
602 & 03	Tony Grove Ranger Station	41°53'10"	111°36'10"	6800'	36 inch
801	Petersboro	41°46'45"	111°59'00"	4450'	36 inch
1001	Gold Hill	40°50'03"	110°53'55"	9800'	70 inch
1202[a] & 03	Cinnamon Creek	41°28'	111°48'	7300'	70 inch
1501	Clarkston	41°55'09"	112°05'45"	6300'	70 inch
1602[a] & 03	Franklin Basin	42°03'08"	111°35'55"	8100'	70 inch
1701	Hell Canyon	41°40'22"	112°00'30"	6400'	70 inch
2001	Curtis Creek	41°36'05"	111°24'30"	8500'	70 inch
2101	Magpie Flats	41°13'57"	111°38'37"	7600'	70 inch
2301	Highline Trail	40°48'24"	109°43'55"	10110'	70 inch
2501	Herd Hollow	41°43'12"	111°35'42"	7350'	70 inch
2609	Providence Traps	41°42'08"	111°41'40"	8800'	70 inch
2901	Hoodoo	41°09'30"	111°35'12"	8350'	70 inch
4401	Hyrum Dam	41°37'17"	111°50'45"	4795'	36 inch
4501	Hardscrabble	40°53'15"	111°43'15"	6720'	70 inch
4602[a] & 03	Tony Grove Lake	41°54'00"	111°37'50"	8400'	70 inch
4701	Lily Lake	40°51'17"	110°46'50"	9300'	70 inch
4902[a] & 03	Ben Lomond	41°21'49"	111°55'05"	8800'	70 inch
5002[a] & 03	Dry Bread Pond	41°24'50"	111°32'46"	8250'	70 inch
5702[a] & 03	George Peak	41°52'56"	113°27'31"	8800'	70 inch
6301	Francis Canyon	41°08'27"	111°17'45"	7360'	70 inch
6501	Guilder's Peak	41°13'53"	111°30'00"	8000'	70 inch
6601	Hardware Ranch	41°36'04"	111°32'29"	5700'	36 inch
6801	Paradise Canyon	41°33'47"	111°40'18"	7650'	70 inch
7001	Bug Lake	41°41'00"	111°25'05"	7950'	70 inch
7101	Deer Springs	41°33'02"	111°27'50"	8450'	70 inch
7801	Sargent Lakes	40°49'39"	111°16'40"	8350'	70 inch
8002[a] & 03	Monte Cristo	41°25'29"	111°30'54"	8880'	70 inch
9501	Chalk Creek No. 2	40°53'52"	111°05'25"	7850'	70 inch
9701	McCoy Park	40°50'57"	110°04'10"	10600'	70 inch
10401	Shingle Mill Flat	40°44'12"	110°07'55"	9900'	70 inch
10903	Chalk Creek No. 1	40°50'58"	110°05'12"	8800'	70 inch
11101	Kelley Ranger Station	42°16'07"	110°47'55"	8750'	70 inch
11301	South Canyon Lower	41°29'48"	111°49'08"	5260'	36 inch
12401	Little Bear Upper	41°24'20"	111°49'25"	6600'	70 inch
12501	Porcupine	40°59'00"	111°09'05"	8100'	70 inch
13201	Middle Fork Ogden	41°20'50"	111°43'35"	8420'	70 inch
14601	Woodruff	41°31'20"	111°10'40"	6350'	36 inch
14701	Klondike Narrows	41°58'05"	111°35'55"	7400'	70 inch
15201	Trigara Springs	41°45'25"	111°30'18"	7200'	70 inch
15501	UWRL	41°44'	111°47'	4600'	36 inch
16202[a] & 03	Steel Creek Park	40°55'00"	111°29'58"	10100'	70 inch
16301	Round Valley	41°47'	111°21'	6000'	70 inch
16403 & 06	Sinks	41°52'00"	111°30'10"	8600'	70 inch
17001	Deseret Peak	40°27'57"	112°36'14"	9250'	70 inch

[a]Snow pillow.

temperature, barometric pressure, or solar radiation by the simple adaptation of commercially available instruments. This results in a system having maximum utility and minimum cost. Lower costs make it possible to place more stations in a given study area, and especially in remote regions having a high variability of precipitation.

2.1.2 Precipitation Weighing Gages. Precipitation data in the form of electronic period were transmitted at intervals ranging from about 15 to 30 minutes from 46 stations located in the Wasatch and Uinta Mountains. A few stations were located outside these regions. A map showing station locations is shown in Figure 3.

A typical remote station is illustrated in Figure 4. The station consists of a precipitation can and stand. The stand is made from 6.35 cm (2½ inch) galvanized pipe with a standard Alter shield. The Alter shield, used to enhance the show catch, consists of 30 baffles placed on a 107 cm (42 inch) diameter 1 cm (3/8 inch) steel rod.

The single-pipe stand is used at low elevation stations where the snowfall is not as great as it is in

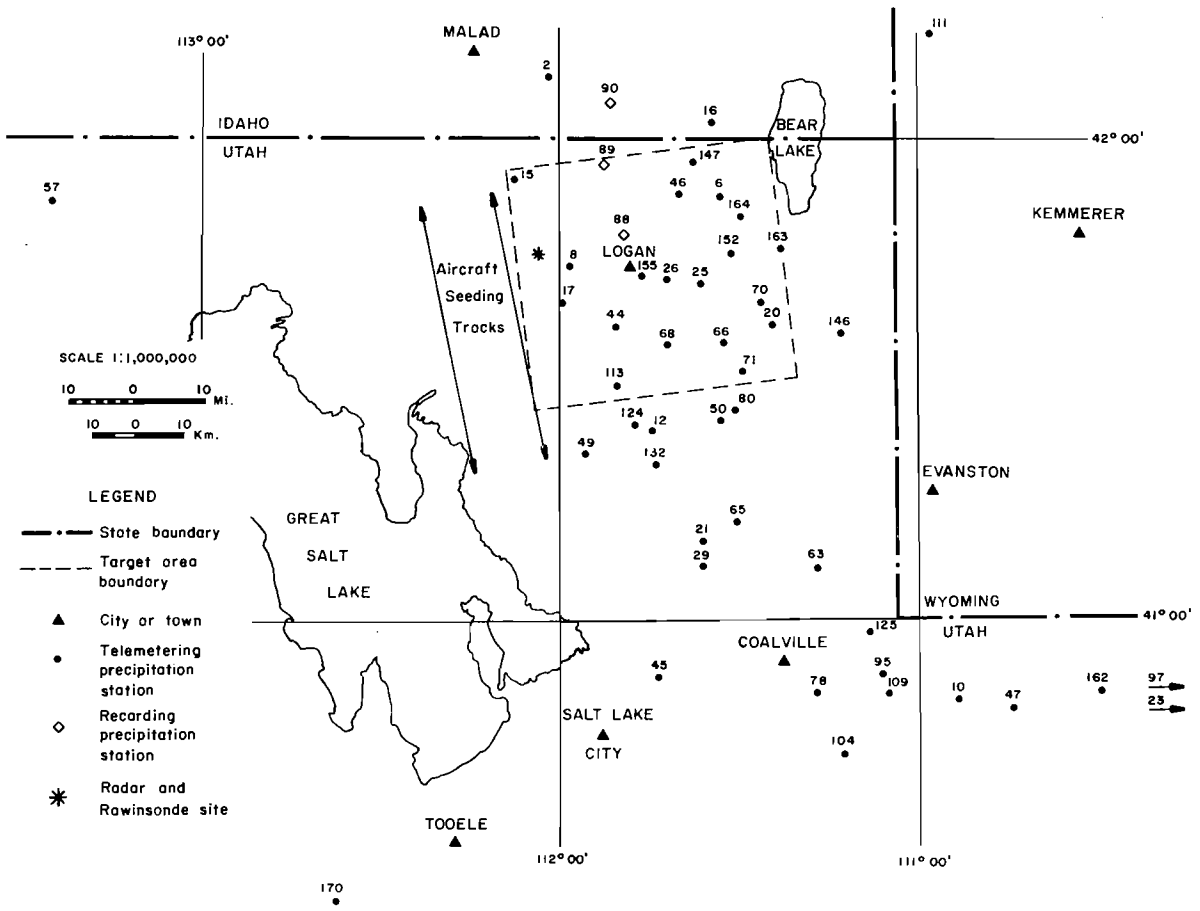

Figure 3. Experimental area and precipitation observing network for airborne weather modification project.

the high mountain regions. For the higher elevations and larger snow accumulations, a three-legged stand patterned after the Soil Conservation Service stands, is used. This type of stand uses 3.8 cm (1½ inch) pipe for each of the three legs.

The precipitation can is placed upon a weighing transducer which changes an audio frequency as the precipitation accumulates in the can; the heavier the can the lower the audio frequency. An electrical cable passes from the transducer down through the pipe leg. The cable then runs from the tower to the instrument container, entering through a watertight fitting. The instrument container houses the main electrical equipment of the station and the batteries which supply the station power. A cable also runs from the metal instrument container through another watertight fitting to a Yagi-type antenna.

The precipitation catchment devices are cylindrical metal containers. The cans are of two basic configurations. The opening in either configuration is 20 cm (8 inches) in diameter. One is 89 cm (36 inches) long having straight sides, and is used at lower elevations where precipitation is not expected to exceed the capacity of the can. The other precipitation can, for higher elevations and less accessible regions, has a 30.5 cm (12 inch) diameter reservoir, giving a total capacity of 178 cm (70 inches). This capacity is adequate for a year's accumulation of precipitation at nearly all of the sites located in Utah.

It is desirable to keep the snow catch in at least a semi-liquid state so that the snow does not accumulate and overflow. To accomplish this, the can is precharged with an antifreeze and water mixture. A small quantity of motor oil, which floats on the top of the liquid mixture, is added to prevent loss of water through evaporation. The cans are painted black so that solar radiation absorption can be enhanced thereby thawing the ice and snow accumulation periodically.

The weighing transducer is located directly underneath the precipitation catchment can, and its function is to weigh the can's contents. The positional sensing element of the transducer consists of a metal plunger which can be lowered into an inductive coil without friction. As weight increases by the accumulation of precipitation, the springs are compressed and the plunger lowers into the coil of wire, causing the inductance of the coil to increase. An increase in inductance changes the frequency of oscillation of the

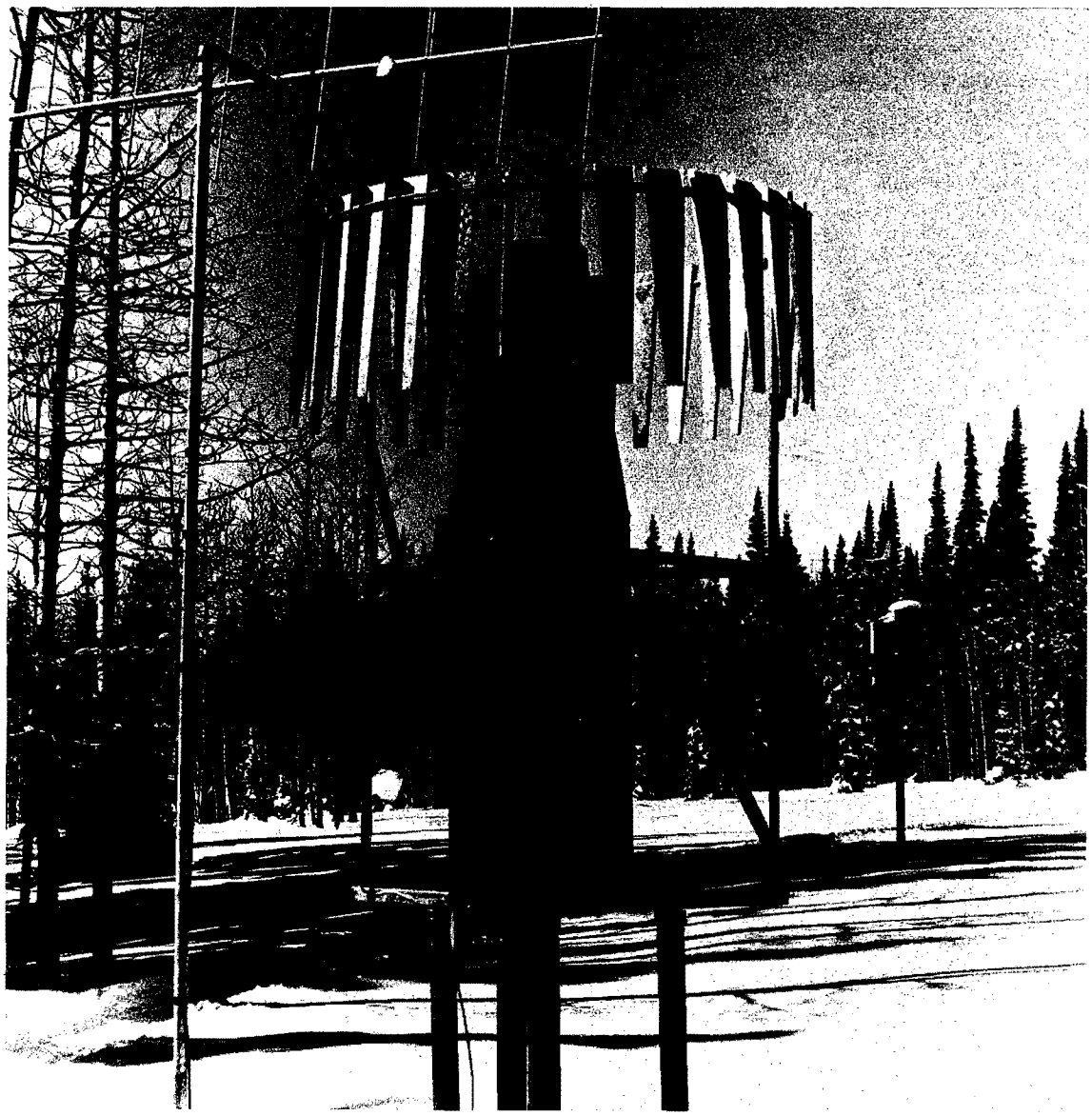

Figure 4. Typical remote precipitation station: Sinks location; station no. 164.

subcarrier oscillator. The frequency has a known relationship to the amount of precipitation in the can.

Variations in the deflection of the springs due to differences in temperature are largely overcome by using springs made of Ni Span C material. This material has the lowest temperature coefficient of any known spring alloy.

The weighing transducer and catchment can, which monitor the amount of precipitation, normally being free of friction, provide a sensitive system. As a consequence, wind may have a tendency to cause some fluctuations in the data.

The transponder electronics consist of a radio transmitter and receiver, a SCO (subcarrier oscillator), a timer, and a parameter commutator. The receiver remains on at all times except when the transmitter is operating. The transmitter turns on when the receiver is signaled with two distinct tones from the terminal readout station at a frequency coded for that particular station. The signal, with its frequency modulated by a parameter transducer, is then broadcast for 15 seconds. After all parameters are reported sequentially, a timer turns the transmitter off. The terminal readout station can reinterrogate as desired.

Power is supplied to the remote station by three or six, six-volt batteries, Battery life is variable; being a function of the number of station interrogations. The receiver standby power is 4 ma. at 12-18 volts which is supplied by readily available disposable or recharge-

able batteries. Six disposable batteries will last at least one year.

2.2 Supporting Observation System

2.2.1 Rawinsonde and Radar. A Bureau of Reclamation RD-65 unit was used throughout the experimental periods to obtain observations of temperature, humidity, pressure-height and wind velocity. Two primary locations were used. During most of the aircraft seeding experiment the unit was located at Cache Peak (elevation about 1740 m); for the ground seeding experiment the unit was located at Mendon (elevation 1372 m). For the aircraft seeding experiment one or two rawinsondes were released, and Salt Lake City data were used to supplement this information. For the ground seeding experiment a rawinsonde was released every two hours for a total of five per storm.

A modified, three centimeter, T-9 tracking radar was operated during the aircraft seeding experiment on Cache Peak near the western border of the target area. This equipment was used to provide flight control information to the pilot, determine regions of cell genesis, and provide information and photography of cell intensity and movement. The radar was also employed in a vertical pointing mode in order to obtain cloud depth and cloud top populations for the area. A method was devised for photographing continuously a vertical cross-section of the cloud system.

2.2.2 Facsimile Data Collection. An Alden weather facsimile machine was placed in operation at UWRL during the winter season. The output from this equipment was used to control operational activities and subsequent analyses of the experiments. A service A teletype machine was also installed in order to obtain hourly surface data and other special reports.

2.2.3 Ice Nucleus Counts. A Summit Hut was designed and built on the Wasatch Ridge east of Logan. This hut is a 6 m x 8.5 m A-frame type structure with a loft for storage and sleeping quarters. The hut is at an elevation of 2650 m and lies within the primary target area. This structure served as a base for monitoring ice nuclei, cloud condensation nuclei and ice crystal characteristics during seeded and non-seeded periods.

Ice nuclei data were collected at the ground during winter seasons using a borrowed NCAR counter and from the air using a cold box furnished by Atmospherics, Inc. Counts were taken at a temperature of -20°C. The NCAR counter was mounted in a stationwagon and counts were obtained at several locations during operational events. The aircraft cold box was used for plume tracking the Mt. Pisgah-based seeding generator.

2.2.4 Silver Concentration of Snow. As part of the observing system, a network of silver sampling sites was established. Snow-chemistry sampling sites for the three-year aircraft seeding experiment are shown in Figure 5.

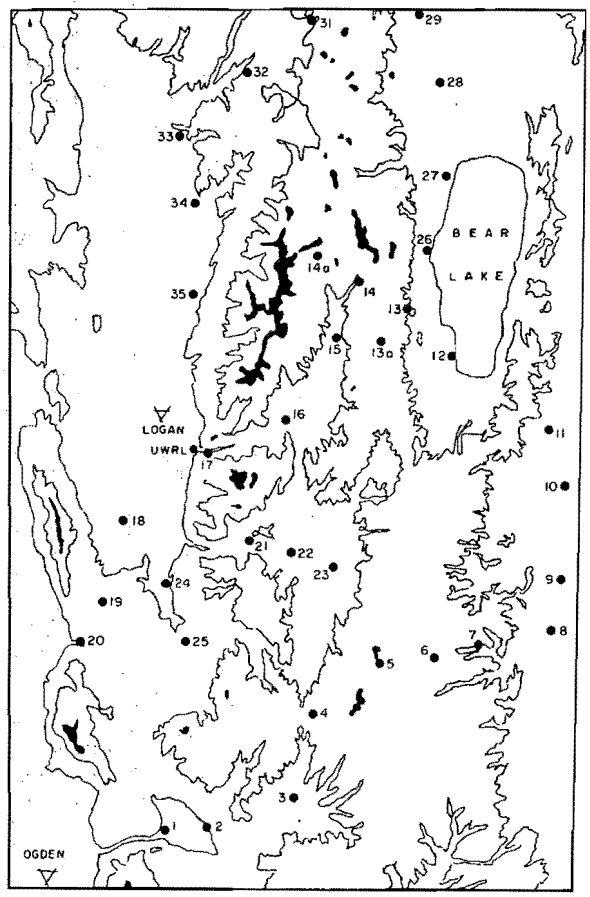

Figure 5. Snow chemistry sampling sites (FY 70-71).

Snow samples were generally taken whenever the snow depth on the route exceeded 8 cm (3 inches) during a storm. Each sample was taken by a technician who placed a fresh conventional polyethylene bag over his hand and scooped new snow into a wide mouthed 4½ liter polypropylene bottle previously stabilized with 5 ml of glacial acetic acid. The tightly closed containers were taken to the laboratory. Analysis of these data will be discussed in Section 6.1.3.

3.0 SEEDING DELIVERY SYSTEM

3.1 Airborne Seeding

3.1.1 Description of Equipment. The airborne seeding component of the Wasatch Weather Modification Project was subcontracted to Atmospherics, Inc. The aircraft supplied to the project was a turbocharged Piper Aztec "C" (N178A). This aircraft was fully licensed for IFR (instrument flight rules) flights and equipped with deicing systems on propellers, wings, and tail surfaces (Henderson et al., 1970).

The aircraft was permanently stationed at the Ogden Municipal Airport during the four-month operational periods. It was available for operations on a 24-hour basis. The decision to base the aircraft at Ogden was based, in part, on considerations of air traffic control centers at Salt Lake City and Hill Air Force Base, flight safety requirements, aircraft service facilities, position of VORTAC installations in relation to seeding flight paths, relationship between radar facilities and aircraft flight operations, and the climatology at airfields throughout the Salt Lake Valley.

In view of the high density aircraft traffic existing in the area of the seeding tracks it was necessary in the initial stages of project development to contact the Federal Aviation Agency in Salt Lake City and Hill Air Force Base near Ogden, in order to organize the flight activities in this area.

Installed on the aircraft were mounting racks of special design for holding a variety of pyrotechnic seeding devices. On this particular aircraft, two racks were mounted vertically on the side of the fuselage. These were used primarily for holding and burning pyrotechnics which did not produce large quantities of corrosive by-products believed to react with the aircraft skin. Two additional racks were installed in the airstream immediately aft of the flaps and outboard of the engine nacelles. These were used for higher output pyrotechnics which could produce corrosive material or heat problems in the first 10 cm, or so, downwind from the end-burning units. Output concentrations of all chemical constituents were such that turbulent mixing one or two meters behind the aircraft provides a dilution below any level which might affect materials or life forms. The output of the airborne seeding was approximately 120 gm h^{-1} of silver iodide.

The selection of seeding tracks was based mainly on combinations of wind speed and direction at seeding level. Careful thought was given to safety considerations, FAA regulations, terrain features, commercial aircraft traffic, location of primary and alternate airfields, radar field headquarters, location of USU telemetry system stations, and storm types within the total operational area.

The seeding track designations A_1 through C_5, related to various wind speeds and directions, are shown in Table 2. If major changes in wind speed and direction during any seeding period occurred, the aircraft track selected was altered to fit the changing weather conditions. Seeding tracks charts with appropriate flight information are depicted in Figure 6.

3.1.2 Seeding Experiments. During the first year of the airborne seeding project a number of criteria were established to identify an operational period. These criteria were:

1. Cloud bases shall be no higher than 12,000 ft msl (4725 m).

2. Total cloud depth shall be at least 100 mb thick.

3. 700 mb temperature shall be -1°C or colder.

4. The cloud cover shall be not less than 8/10ths as viewed from Logan.

5. 700 mb wind direction shall be within the interval from 197 degrees to 317 degrees.

6. Conditions 1 through 5 shall be forecast to persist for not less than 8 consecutive hours.

The nearly 10,000 square mile area emcompassing the UWRL telemetering stations is too large for airborne seeding of winter storms by a single aircraft. Within this rather large area a fixed target area of 1,258 square miles was chosen. This smaller experimental target area allowed proper coordination between radar facilities, air-borne operations, ground personnel, as well as providing for a reasonable length of time between seeding passes. The coordinates of the four corners of the target area are:

Table 2. Seeding track designations for various combinations of wind speed and direction.

	Wind Direction at Seeding Altitude	Wind Speed at Seeding Altitude (Knots)				
		0-11	11-21	21-31	31-42	42-52
(mag)	180° - 220° (A)	A-1	A-2	A-3	A-4	A-5
(true)	197° - 237°					
(mag)	220° - 260° (B)	B-1	B-2	B-3	B-4	B-5
(true)	237° - 277°					
(mag)	260° - 300° (C)	C-1	C-2	C-3	C-4	C-5
(true)	277° - 317°					

1. 41°55'N, 112°08'W
2. 42°00'N, 111°25'W
3. 41°31'N, 111°19'W
4. 41°27'N, 112°02'W

This experimental target area had the highest density telemetry network within the overall area covered by the total network. Telemetering stations lying within the experimental target area included:

006 Tony Grove Ranger Station
008 Petersboro
012 Cinnamon Creek
015 Clarkston
017 Hell Canyon
020 Curtis Creek
025 Herd Hollow
026 Providence Traps
044 Hyrum Dam
046 Tony Grove Lake
066 Hardware Ranch
068 Paradise Canyon
070 Bug Lake
071 Deer Springs
113 Klondike Narrows
152 Trigara Springs
155 Utah Water Research Laboratory
164 Sinks

In order to obtain as many seeded periods as possible within a random design, the minimum length of storm period which would provide measureable precipitation in both the seeded and non-seeded time blocks was determined. Climatological records compiled by UWRL were examined for indications of precipitation periods. It followed that an 8-hour storm period could be expected to contain two 4-hourly precipitation amounts suitable for detection by the telemetry system, so that proposed seeding techniques might be evaluated. A 4-hour sampling unit was also within the capability of a single pilot and single aircraft to carry out.

It was decided to use a 4-hour sampling unit with randomization in blocks of two. When an 8-hour operational period was forecast to exist, a randomized decision whether to seed the first or second 4-hour time block was then made. The other 4-hour time block was left non-seeded. Within the designated 4-hour seeded block, actual seeding was conducted during the first two hours, the last two hours providing a "purge" time for seeding material.

Seeding was accomplished by AgI pyrotechnics (Olin R-15) mounted to the aircraft. According to manufacturing specifications this pyrotechnic was approximately 10^{14} effective nuclei per gram of AgI at -15°C. Seeding rates varied from about one to three grams per minute with most seeding accomplished at a rate of two grams per minute, or 120 grams per hour.

3.2 Ground Based Seeding

3.2.1 Description of Equipment. As part of the Bureau of Reclamation's project Skywater, a three year ground-based seeding experiment was conducted in the Northern Wasatch Mountains. In this experiment three mountaintop silver-iodide generators were used to seed on a random basis cold orographic clouds which meet certain meteorological criteria (Hill, 1974).

The design of the ground seeders was based upon Weather Measure ground generators. These generators were extensively modified to ensure their reliable operation and to permit remote control by use of the telemetry system. Each of the seeders had several monitoring devices which were read out at UWRL. A summary of the monitoring system is given in Table 3.

Each of the seeders emitted about 25 gm h^{-1} of AgI, or a total of 75 gm h^{-1}. The AgI was complexed with NaI in order to go into solution in acetone. The resulting fluid was sprayed into a propane flame to produce particles of AgI.

An automatic ignition system was designed and installed in the Willard seeder. This ignition system created a spark every 60 seconds at times when a temperature sensor indicated the propane flame should have been on but had been extinguished. The passage of vigorous cold fronts and other wind producing situations was the usual cause of flameouts. The Pisgah and Cache Peak seeders were not usually subject to these flameouts. The Willard Peak seeder, the highest of the stations, had frequent flameouts prior to installation of the automatic ignition system.

3.2.2 Seeding Experiments. During moist westerly flow conditions, a period of from four to eight

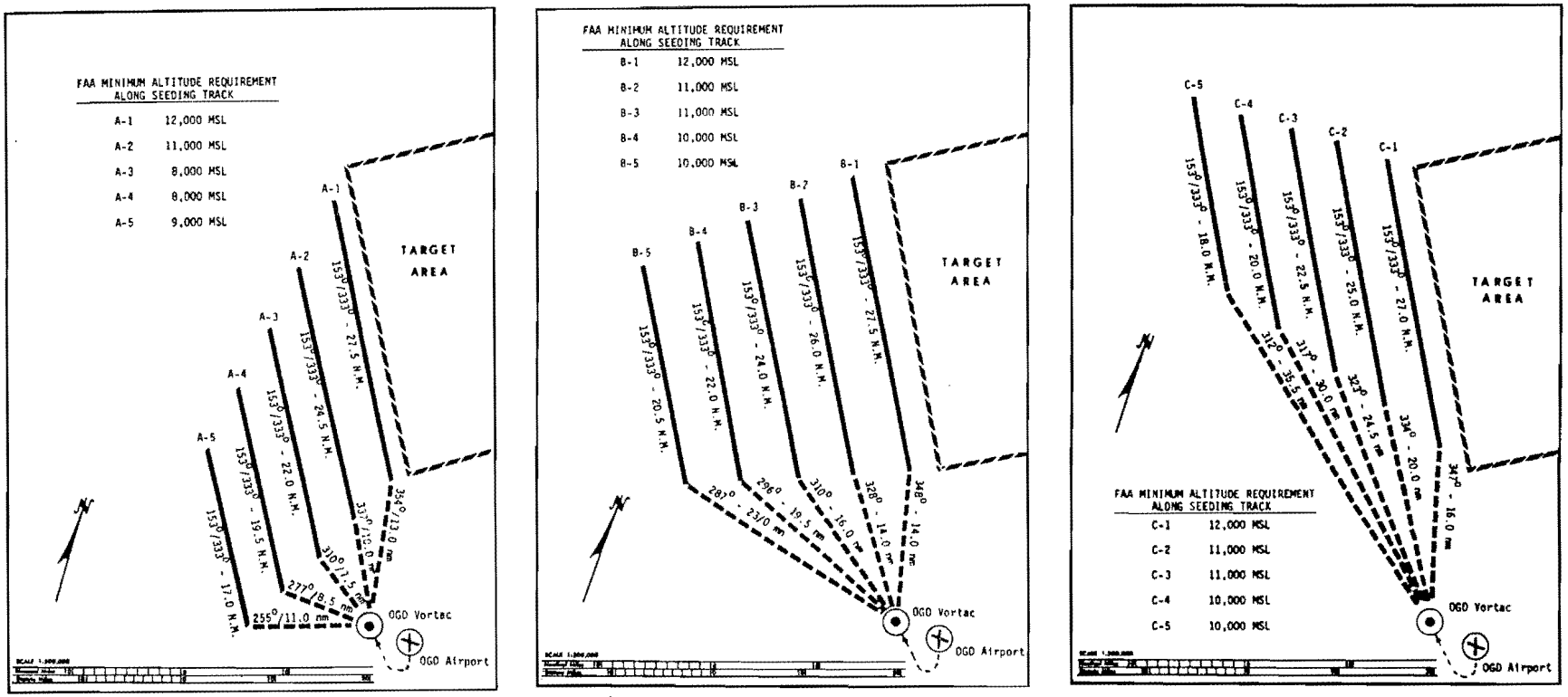

Figure 6. Seeding tracks for airborne seeding program.

Table 3. Summary of seeder monitoring system.

A	B	C	D	E	F	G	H	J	K	L
M	N	P	Q	R	S	T	U	V	W	X

ABC = Station Number
DE = Parameter Number
F = Error Code (0-4 data OK; 5-7 check data)
GHJ = Day of Year in 365 System
KL = Year (73)
MNPQ = Time in 2400 System
MN = Hours
PQ = Minutes
RS = Not Normally Used
TUVWX = Data Period in Microseconds

Seeder Site	Station Number	Parameter	Name	Expected Period Range
Willard	195 (on)	06	Temperature	
		05	Flow (Agl)	
		04	Main Burner	
		03	Flow (on-off)	
		02	Pilot	
	197 (off)	06	Temperature	
		05	Flow	
		04	Main Burner	
		03	Flow	
		02	Pilot	
Mt. Pisgah	196 (on)	03	Programmer	
		02	Main Burner	
	198 (off)	03	Programmer	
		02	Main Burner	
Cache Peak	191 (on)	05	N_2	
		04	Pilot	
		03	Main Burner	
		02	Latch	
	193 (off)	05	N_2	
		04	Pilot	
		03	Main Burner	
		02	Latch	

hours was declared seedable. Then, by random choice, it was decided whether or not to seed. If seeding was done, all three seeders were activated two hours prior to the designated starting time and continued until the end of the period. The first of two-hourly rawinsondes was released at the start of the period. Telemetered precipitation data were recorded at 20-minute intervals as soon as an event was declared, usually a minimum of four hours prior to the start. After four hours following the event data were collected once an hour for an additional 24 hours to check overall data quality.

The conditions required to declare an event were that precipitation be primarily orographically induced at least during the event, and that the surface to 500 mb relative humidity exceed 70 percent with the wind at both 700 and 500 mb between 220 and 320 degrees.

An event is considered orographic if no front, cyclone, or strong convective activity were nearby during the period. Because some such events inevitably were included in the data set, objective means to identify these events have been devised.

The physical layout of the second Wasatch experiment, consists of a base station at Logan, Utah, a rawinsonde site at Mendon, a vertical incidence cloud detection unit at Hill Air Force Base (data utilized, but not formally a part of the system), and eleven automatic telemetering precipitation gages. The eleven precipitation stations form two north-south lines of gages in high terrain. Analysis of data collected for this experiment will be given in Section 7.

4.0 THEORETICAL STUDIES

4.1 Physical Basis for Cloud Seeding

The physical basis for seeding cold orographic clouds may be examined and defined by investigating processes controlling the total water budget of these clouds. The following development is due to Chappell (1970).

The total water budget of a parcel of air may be written as

$$\frac{dq}{dt} + \frac{dl}{dt} + \frac{ds}{dt} = 0 \quad \ldots\ldots (1)$$

where q is the vapor mixing ratio, 1 the liquid mixing ratio and s the ice mixing ratio of the parcel.

The total water budget equation may be considered during various stages in the transit of a parcel over an orographic barrier as shown in Figure 7. For parcels moving in the sub-cloud layer, time variations of the parcel moisture quantities are given by

$$\frac{dq}{dt} = \frac{dl}{dt} = \frac{ds}{dt} = 0 \quad \ldots\ldots (2)$$

Equation 2 states that until saturation with respect to water is attained, the vapor mixing ratio is conserved and there is no formation of liquid water. Also growth of ice particles in the sub-cloud layer is negligible. For parcels with upward trajectories in the cloud system, the time variations of the parcel moisture quantities can be written as

$$\frac{dq}{dt} = \frac{dq_s}{dt} \quad \ldots\ldots (3)$$

$$\frac{dl}{dt} = -\frac{dq_s}{dt} - n_c \frac{dm}{dt} \quad \ldots\ldots (4)$$

and

$$\frac{ds}{dt} = n_c \frac{dm}{dt} \quad \ldots\ldots (5)$$

where q_s is the saturation vapor mixing ratio, n_c is the number of ice crystals per unit mass, and m is the ice crystal mass. Equations 3 and 4 apply best for zero supersaturation with respect to water.

Equation 3 shows that time variations of the vapor mixing ratio during the in-cloud stage are equivalent to changes in the saturation vapor mixing ratio of the parcel. Equation 4 gives the time variation of the liquid water content of the parcel as an imbalance between the vapor supply rate and the rate of ice growth in the parcel. Equation 5 gives the rate of ice growth in the parcel as the time change in crystal mass multiplied by the number of ice crystals per unit mass.

When parcels begin their downward trajectories in the cloud exit region, time variations of the parcel moisture quantities can be expressed by the following equations which apply until all liquid and solid condensates have evaporated. These equations are

$$\frac{dq}{dt} = \frac{de_w}{dt} + \frac{de_i}{dt} \quad \ldots\ldots (6)$$

$$\frac{dl}{dt} = -\frac{de_w}{dt} \quad \ldots\ldots (7)$$

and

$$\frac{ds}{dt} = -\frac{de_i}{dt} \quad \ldots\ldots (8)$$

In these equations de_w/dt and de_i/dt are the rates of evaporation of liquid water and ice form in the parcel, respectively.

If it is now assumed that precipitation fallout from the parcel is in ice form, the following conservation equations apply over a parcel trajectory that originates in the sub-cloud layer, extends upward in the cloud updraft and downward through the cloud exit region until all liquid and solid condensates have evaporated. These equations are

$$\frac{dq_s}{dt} + \frac{de_w}{dt} + \frac{de_i}{dt} + \frac{di}{dt} 0, \quad \ldots\ldots (9)$$

$$\frac{dl}{dt} = -\frac{dq_s}{dt} - n_c \frac{dm}{dt} - \frac{de_w}{dt} = 0, \quad \ldots\ldots (10)$$

and

$$n_c \frac{dm}{dt} - \frac{de_i}{dt} - \frac{di}{dt} = 0 \quad \ldots\ldots (11)$$

The net rate of ice growth over the parcel trajectory or equivalently, the snowfall intensity following the parcel is given by di/dt.

Both Equations 9 and 11 give expressions for this quantity, namely

$$\frac{di}{dt} = n_c \frac{dm}{dt} - \frac{de_i}{dt} = -\frac{dq_s}{dt} - \frac{de_w}{dt} - \frac{de_i}{dt} \quad \ldots\ldots (12)$$

From Equation 10, a relation designated the "rate" equation is given by

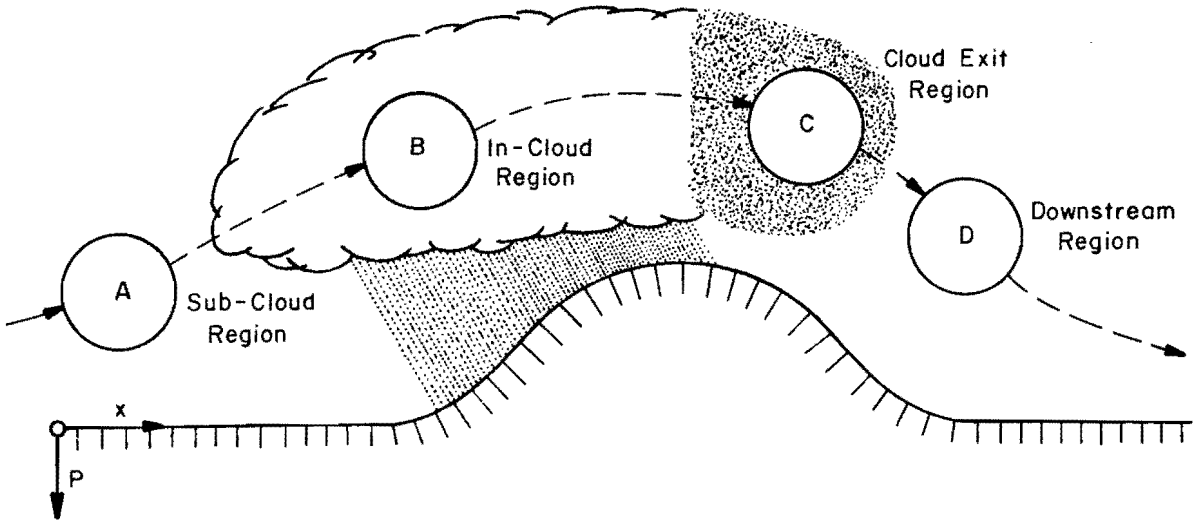

Figure 7. Total water budget in orographic flow with hypothetical air parcel trajectory.

$$\frac{de_w}{dt} = -\frac{dq_s}{dt} - n_c \frac{dm}{dt} \quad \ldots\ldots\ldots\ldots\ldots\ldots\ldots\ldots\ldots\ldots (13)$$

where

$$\frac{de_w}{dt} > 0 \text{ for } n_c \frac{dm}{dt} < -\frac{dq_s}{dt}$$

and

$$\frac{de_w}{dt} = 0 \text{ for } n_c \frac{dm}{dt} = \frac{dq_s}{dt}$$

Equation 13 shows that if the rate of vapor supplied to the ascending parcel is greater than the extraction rate due to ice crystal growth, there is an evaporation of liquid water in the cloud exit region. This evaporation loss arises due to accumulation of liquid water in the parcel through cloud droplet growth during its ascension. On the other hand, if the extraction rate of liquid cloud droplets by ice crystal growth is equal to the rate of liquid water formation in the ascending parcel, there is no net accumulation of liquid water and consequently, no evaporation of liquid droplets.

From Equation 13 it follows that a desirable condition, for minimizing losses and maximizing the cold cloud precipitation process, is for ice growth to occur at a rate equivalent to the vapor supply rate. Further, it is advantageous to have this conversion of cloud water to ice occur at water saturation, since this degree of cloud supersaturation provides for highest diffusional growth rates of crystals without a net growth of liquid water droplets. Thus, a process is envisioned wherein the vapor is converted to ice using liqiud droplets as a "buffer" or "catalyst" in the reaction.

The ultimate in cloud seeding operations would be to individually treat the various cloud parcels as they traverse through the orographic cloud system according to their immediate requirements. However, the technology to accomplish this does not exist, nor would it be economically feasible to attempt this, even if cloud requirements could be specified in such accurate detail. It would be more compatible with present technology to treat a cloud in its entirety. A mathematical formulation consistent with this approach may be developed if it is required that (1) steady state conditions apply, (2) temperature changes due to horizontal advection are small, (3) cloud base and top are nearly horizontal surfaces and (4) Equations 12 and 13 are satisfied when averaged over the cloud segment.

Converting Equations 12 and 13 into terms of unit volume, and averaging over the cloud segment, they may be written

$$\overline{\frac{dI}{dt}} = \overline{N}_c \overline{\frac{dm}{dt}} \quad \overline{\frac{dE_i}{dt}} = -\overline{\omega\rho}\,\overline{\frac{\partial q_s}{\partial p}} - \overline{\frac{dE_w}{dt}} - \overline{\frac{dE_i}{dt}} \quad \ldots\ldots (14)$$

and

$$\overline{\frac{dE_w}{dt}} = -\overline{\omega\rho}\,\overline{\frac{\partial q_s}{\partial p}} - \overline{N}_c \overline{\frac{dm}{dt}} \quad \ldots\ldots\ldots\ldots\ldots\ldots (15)$$

where the bar signifies an average over the cloud segment and the capitalized letters indicate quantities per unit volume.

Equations 14 and 15 demonstrate the possible effects of seeding supercooled orographic cloud systems. In Equation 14 it is seen that the precipitation rate can be augmented by increasing the rate of ice growth in the cloud system, or $N_c(dm/dt)$, providing that the loss due to ice crystal evaporation

does not increase correspondingly (this would happen in the case of overseeding). However, $N_c(dm/dt)$ cannot exceed the rate at which vapor is supplied to the cloud system, or $-\omega\rho(\partial q_s/\partial p)$. It is, therefore, possible, under a certain set of meteorological conditions, that the vapor supply is efficiently converted to ice growth, and snowfall augmentation is not possible. On the other hand, under those meteorological conditions where the rate of ice growth, $N_c(dm/dt)$ is less than the vapor supply rate $-\omega\rho(\partial q_s/\partial p)$, it is possible that a potential for snowfall augmentation exists.

Variation with temperature of the rate of ice growth in the cloud system $N_c(dm/dt)$, is mainly controlled by the ice crystal concentration term. Further, the effectiveness of primary ice nuclei in initiating ice crystal embryos controls the ice crystal concentrations in the cloud system in the absence of substantial ice crystal multiplication processes. Since the concentration of effective primary ice nuclei is crudely an inverse exponential function of temperature (tenfold increase for every 4°C or 5°C decrease in temperature), cloud system temperature appears to largely control the availability of weather modification potential. If artificial ice nuclei, more effective at warmer cloud temperatures than natural ice nuclei, are introduced into the cloud upwind of the mountain barrier, increased snowfall should result for these warmer cloud systems.

The modification potential associated with these microphysical processes is usually designated the "static modification potential" (SMP). However, it is possible under certain conditions that seeding may alter buoyancy effects within the cloud by changing the latent heat release in ascending parcels. In turn, this might warm the cloud system, increase cloud tops or alter the vertical motion field over the orographic barrier. The overall result could be to change the rate of vapor supply or cloud geometry during seeded conditions. The modification potential associated with these particular dynamic effects is called the "dynamic modification potential" (DMP).

A goal for seeding cold orographic clouds, therefore, is to introduce artificial ice nuclei into those cloud systems, whose natural supply of ice crystals is insufficient to convert the liquid water forming in the cloud system to ice form at the same rate. This equality can be expressed using only the mean terms arising from the average procedure by

$$\overline{N_c}\,\overline{\frac{dm}{dt}} = -\overline{\omega\rho}\,\overline{\frac{\partial q_s}{\partial p}} \qquad (16)$$

and solving for the ice crystal concentration,

$$\overline{N_c} = -\overline{\omega\rho}\,\overline{\frac{\partial q_s}{\partial p}} \Big/ \overline{\frac{dm}{dt}} \qquad (17)$$

Use of the mean terms only, that arise from the averaging procedure, has been shown by Chappell (1970) to describe the cloud processes adequately as a first approximation.

Assuming a one-to-one correspondence between ice nuclei and ice crystal concentrations, the concentrations of ice nuclei needed to make the ice process efficient within the cloud system can be computed from Equation 17.

The concepts and theory outlined in this section provide a physical foundation for supercooled orographic cloud seeding and numerous hypotheses to be tested by field experimentation.

4.2 Mixed Phase Clouds

Cloud supersaturation is a critical factor in defining the modification potential of cold orographic clouds. When a water-phase cloud is supersaturated with respect to water, water droplets will grow. Some of the liquid water accumulated in an updraft may evaporate in the subsiding air in the lee of the mountain barrier. This liquid water is therefore not converted to precipitation in the vicinity of the mountain. On the other hand when an ice-phase cloud is supersaturated with respect to ice, ice crystals will grow, and as with cloud droplets, may not reach the ground.

During the time interval when a water cloud is converted to an ice cloud, i.e., during the glaciation process, the saturation vapor pressure falls rapidly from a value close to the equilibrium vapor pressure over water to that of ice. It is during this period that a large amount of precipitation-size particles develop. Because water is deposited upon available ice particles the size of the resulting snowflakes will depend partially upon the number present. Furthermore, there is an additional supply of moisture available for precipitation in changing from a water phase to an ice phase cloud.

If in the natural atmosphere an insufficient number of ice particles are present to cause substantial glaciation, then the addition of artificial ice nuclei may induce both complete glaciation and enhance precipitation as described above.

In addition to recognizing situations wherein the introduction of artificial ice nuclei may lead to enhanced precipitation, it is also important to take into account the duration that the glaciation process requires. When artificial ice nuclei are placed into a completely water-phase cloud, a period between about five minutes to an hour is required for glaciation. The factor controlling this period is again the concentration of ice nuclei.

In the following work (Chappell and Johnson, 1974), cloud supersaturation is treated as a time dependent quantity, so that targeting of snowfall can be represented realistically. A time dependent equation for supersaturation with respect to ice in a mixed-phase cloud was presented by Juisto and Schmitt (1970), and Juisto (1971). Juisto developed a cold-cloud microphysical model that incorporated

cloud-supersaturation variations as a function of time. In this model, it was assumed that a single layered cloud was at a constant temperature, and ice-nuclei concentrations were arbitrarily chosen.

An equation expressing the time change of supersaturation with respect to ice was developed as follows:

$$\frac{dS_i}{dt} = \phi_1 \frac{dZ}{dt} - \phi_2 \frac{dW}{dt} - \phi_3 \frac{dI}{dt} \quad \ldots\ldots\ldots\ldots\ldots\ldots (18)$$

$$\phi_1 = \frac{eg\epsilon L_s}{e_{si} R_d T^2 C_p} - \frac{ge}{e_{si} R_d T} \quad \ldots\ldots\ldots\ldots\ldots\ldots (19)$$

$$\phi_2 = \frac{e\epsilon L_c L_s}{e_{si} C_p P T} + \frac{R_d T}{\epsilon e_{si}} \quad \ldots\ldots\ldots\ldots\ldots\ldots (20)$$

$$\phi_3 = \frac{e\epsilon L_s^2}{e_{si} C_p P T} + \frac{R_d T}{\epsilon e_{si}} \quad \ldots\ldots\ldots\ldots\ldots\ldots (21)$$

e = vapor pressure
e_{si} = saturation vapor pressure with respect to ice
C_p = specific heat of dry air at constant pressure
g = gravitational constant
L_s = latent heat of sublimation
L_c = latent heat of condensation
R_d = specific gas constant for dry air
T = temperature (^oK)
ϵ = ratio of molecular weight of water vapor to molecular weight of air
P = atmospheric pressure
$S_i = (e/e_{si}) - 1$

The three differentials in Equation 18 can be expressed as

$$\frac{dW}{dt} = N_d \left(\frac{dm}{dt}\right)_d = \text{time rate of change of water} \quad \ldots\ldots (22)$$

$$\frac{dI}{dt} = N_c \left(\frac{dm}{dt}\right)_c = \text{time rate of change of ice} \quad \ldots\ldots (23)$$

$$\frac{dZ}{dt} = U = \text{updraft speed} \quad \ldots\ldots\ldots\ldots\ldots\ldots (24)$$

in which

N_d = number of droplets
N_c = number of crystals
$\frac{dm}{dt}$ = time rate of change of mass

Numerical integrations of Equation 18 were applied to a parcel of air with a specified updraft speed over a particular time interval. Initial atmospheric parameters in all cases studied were:

$T = -20^oC$
$P = 800$ mb
$S_i = .215$
$N_d = 300$ cm^{-3}
$r_d = 7\ \mu$
$r_c = .1\ \mu$

The time steps used in the integration (Runga-Kutta scheme) were:

.01 sec for ice crystal mass $< 5 \times 10^{-8}$
.1 sec for ice crystal mass $< 5 \times 10^{-7}$
1 sec for ice crystal mass $> 5 \times 10^{-7}$

The results of these integrations are shown in Figure 8, wherein cloud supersaturation with respect to ice is given as a function of time for various ice-nuclei concentration with updraft speeds of 5 and 20 cm sec^{-1}. The most striking feature of these graphs is the rapid drop in supersaturation which occurs during glaciation. For ice-nuclei concentrations of around 500 to 1000 per liter glaciation occurs in about 5 minutes, whereas with 50 to 100 per liter glaciation is delayed until about 15 minutes. With 5 to 10 per liter glaciation is delayed until well over a half hour.

We may conclude from these calculations that when large amounts of ice nuclei are present, i.e., at relatively cold temperatures, the time required for glaciation should have little effect upon targeting. On the other hand for the same concentration of silver iodide at relatively warm temperatures, not only is the number of active ice nuclei much less than at cold temperatures, but the time required for growth to precipitation-size particles is greatly extended. Because it is at the warmer temperatures that we expect a potential augmentation of precipitation, we must be concerned with the time delay required for glaciation when answering questions regarding targeting.

4.3 Cloud Tops and Temperatures

In an analysis of cloud seeding effectiveness (Chappell et al., 1971) the criterion for determining cloud top height and the corresponding cloud top temperature is based upon the relative humidity profile. It was assumed that a cloud top is found at the height where the relative humidity decreases to 80 percent. This assumption has been reexamined.

The most obvious question relating to the 80 percent criterion is: Why not 100 percent? The only rational answer is that because the ice saturation vapor pressure at temperatures normally found in the mid- or upper troposphere during winter is about 80 percent of the saturation vapor pressure over water.

This criterion is not a valid one to use in establishing cloud top temperatures for use in the

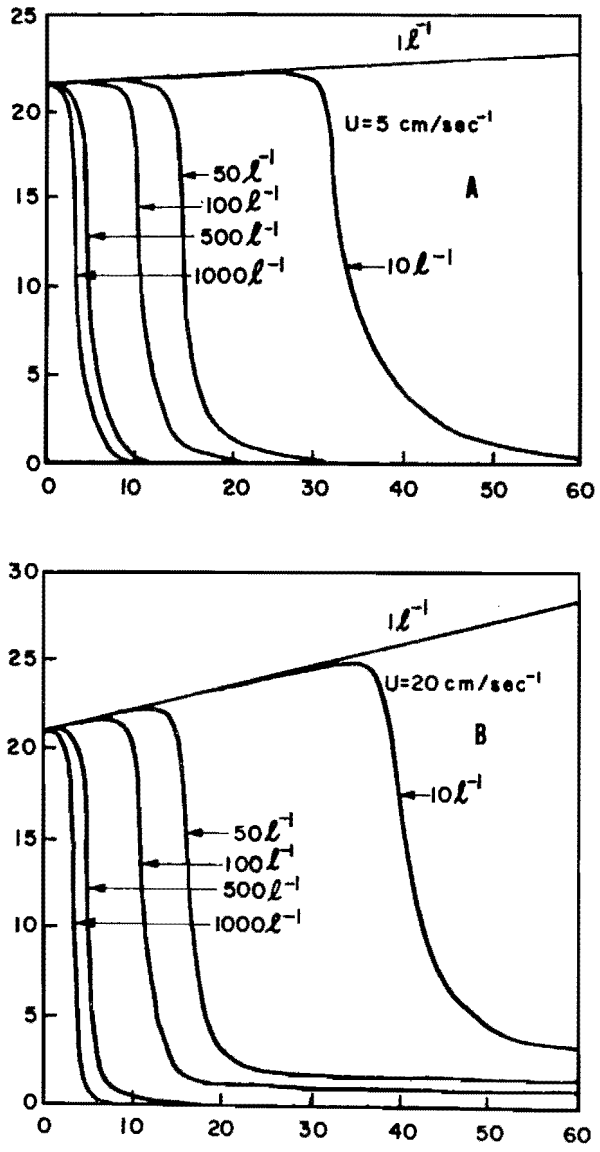

Figure 8. Cloud supersaturation with respect to ice versus time. Curves are shown for various ice crystal concentrations with an updraft speed of (A) 5 cm/sec and (B) 20 cm/sec.

analysis of seeding effectiveness. The reason is that the use of a constant value of 80 percent leads to large errors. To correct these difficulties a simple theoretical basis for determining the relative humidity for ice saturation is provided.

A theoretical development which expresses the dew point depression for ice saturation is as follows (Hill, 1974). The mathematical expression for ice saturation with respect to water, or the relative humidity at ice saturation, is well known. The formula is derived from an integration of the Clausius-Clapeyron equation. If the variation of latent heat with respect to temperature is neglected in the integration, the result is

$$r = \frac{e_{si}}{e_{sw}} = \frac{e_o \exp\left\{\frac{(T-T_o)\,L_i}{R_w T T_o}\right\}}{e_o \exp\left\{\frac{(T-T_o)\,L}{R_w T T_o}\right\}} \qquad \text{.....(25)}$$

where r is the relative humidity, e_{si} and e_{sw} are the ice and water saturation vapor pressures, respectively, at temperature T; T_o is a base temperature (273K), e_o is the vapor pressure at T_o, R_w is the gas constant for water, and L and L_i are the latent heat of condensation and sublimation, respectively.

This same relative humidity may be expressed in terms of vapor pressures over water at different temperatures, one at the dew point temperature T_D, the other at temperature T. This expression is

$$r = \frac{e_{swD}}{e_{sw}} = \frac{e_o \exp\left\{\frac{(T_D-T_o)L}{R_w T_D T_o}\right\}}{e_o \exp\left\{\frac{(T-T_D)\,L}{R_w T T_o}\right\}} \qquad \text{.....(26)}$$

If the two relative humidities are equated then we find

$$\frac{(T-T_o)L_i}{T} = \frac{(T_D T_o)L}{T_D} \qquad \text{.....(27)}$$

We now define $\Delta T = T-T_D$, where ΔT is the commonly known dew point depression. In particular ΔT_i is the dew point depression at ice saturation. After several algebraic manipulations, we obtain the formula

$$\Delta T_i = \frac{(T-T_o)\left(1-\frac{L}{L_i}\right)}{\frac{T_o}{T} + \left(1-\frac{L}{L_i}\right)} \qquad \text{.....(28)}$$

This equation expresses the dew point depression between water and ice saturation.

To show the relationship described by Equation 28, ΔT_i versus temperature is shown in Figure 9. This graph reveals the rather remarkable result that the dew point depression between water and ice saturation is nearly a **linear** function of temperature, and of course, independent of pressure. The chief virtue of Equation 28 is that a rawinsonde sounding may be inspected easily to check for appropriate observed ΔT_i's.

In evaluating effects from cloud seeding, we are interested in determining whether clouds are composed mainly of liquid supercooled drops or ice crystals, or perhaps a cloud layer of ice crystals above a cloud of liquid drops. In the application of Equation 28 there is no guarantee that a cloud is present even if the observed dew point depression is equal to or even less than ΔT_i. The reason is simply that there may be

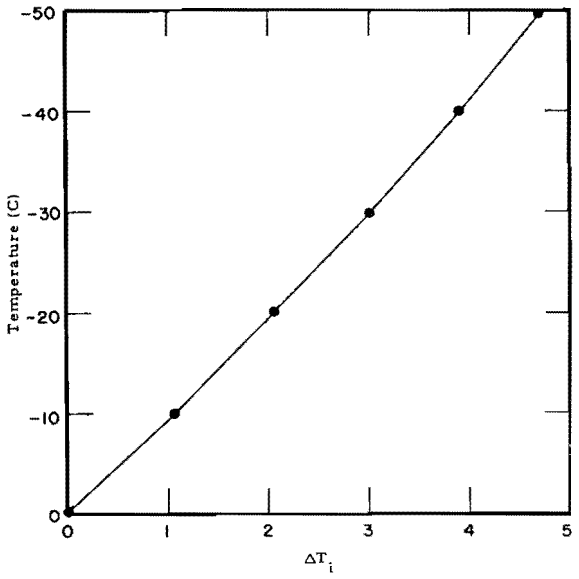

Figure 9. Dew point depression at ice saturation versus temperature.

no cloud present and the dew point depression happens to be ΔT_i. This ambiguity is, of course, present in the method using a fixed relative humidity criterion of 80 percent.

It is worthwhile to note that ΔT_i is equivalent to a relative humidity of 80 percent at a temperature of about -24°C. At warmer temperatures than -24°C the relative humidity is greater than 80 percent and at colder temperatures, less than 80 percent.

4.4 Diffusion

4.4.1 Diffusion from an Infinite Line Source. The development of a procedure for estimating downwind concentrations from an airborne, horizontal line source was developed. The basic equation provided by Turner (1969) for a continuous finite line source was selected and modified to include Gaussian variations in concentrations. It may be written as

$$C_L(x,o,z) = \frac{2q}{u\sigma_z\sqrt{2\pi}} * \exp\left[-0.5\left(\frac{T_A - S_A}{\sigma_z}\right)^2\right] * \int_{P_1}^{P_2} \frac{1}{2\pi} \exp(-0.5p^2)\, dp \quad \ldots\ldots\ldots\ldots\ldots\ldots (29)$$

where q is the source strength per unit distance (g $sec^{-1}m^{-1}$), C_L is concentration, TA and SA are target and seeder altitudes respectively, u is the mean horizontal wind speed, σ_z is the standard deviation of plume concentration distribution in the z direction, and $P_1 = y_1/\sigma_y$, and $P_2 = y_2/\sigma_y$.

The seeding path is taken in the y direction (crosswind). The equation applied for values of y between y_1 and y_2, where y_1 is less than y_2. When the seeding rate, aircraft speed, mean wind speed, effective particles per gram, target and seeding altitudes, and plume angle are specified, one may compute concentrations on a grid.

Calculations based upon computed diffusion constants were performed to describe the distribution of active ice nuclei resulting from aircraft seeding plumes. In these calculations mass diffusion from a unit length of a series of instantaneous, infinite line sources of silver iodide was found. The activation spectrum as a function of temperature was also included in the calculations. Values of active ice-nuclei concentrations were found for various elevations for particular vertical temperature profiles and values of vertical velocity. To transform the calculations from a Lagrangian to an Eulerian system, constant horizontal wind speeds were used. It was assumed that there are no losses of nuclei from any process. In addition, terrain influences have been ignored.

Detailed calculations of active ice-nuclei concentrations and their application are given in an example: example:

Seeding temperature	-10°C
Lapse rate	5C/km
Seeding altitude	3 km (10,000 ft)
Vertical velocity	25 cm/sec
Horizontal wind speed	15 m/s

The diffusion constants used are $K_x = 1000\ m^2\ sec^{-1}$ and $K_z = 200\ m^2\ sec^{-1}$. The temperature activation spectrum is that for the Olin R-15 pyrotechnic. All calculations are based on an aircraft speed of 100 kts and seeding rate of 120 gm hr^{-1}. The results are shown for a distribution of seeding material fifteen minutes after the completion of eight seeding passes each fifteen minutes in duration over a fixed ground track.

In Figure 10, the x-z cross-section of the mass distribution is shown by isopleths of 10^{-14} gm 1^{-1} along with the maximum concentration. Application of the temperature activation spectrum to this distribution produces the results labelled B. Isolines in this figure are drawn for concentrations of five and ten active nuclei per liter.

A rigorous description of the horizontal distribution of artificial ice-nuclei concentration is difficult to establish. In reality, aircraft seeding results in a zig-zag pattern of release with a subsequent complex mass distribution. The computations given herein are appropriate to the center of the tracks but are less realistic as the track ends are approached.

Another problem arises because the line sources are not infinite in length. Over the duration of time considered, approximately two hours, this problem is most serious at the track ends but not as serious near the middle. To treat this problem we assume that lateral diffusion at the track ends is limited in the cross-wind direction by a half-angle spread. The half-angle spread is defined as one-half the angle of

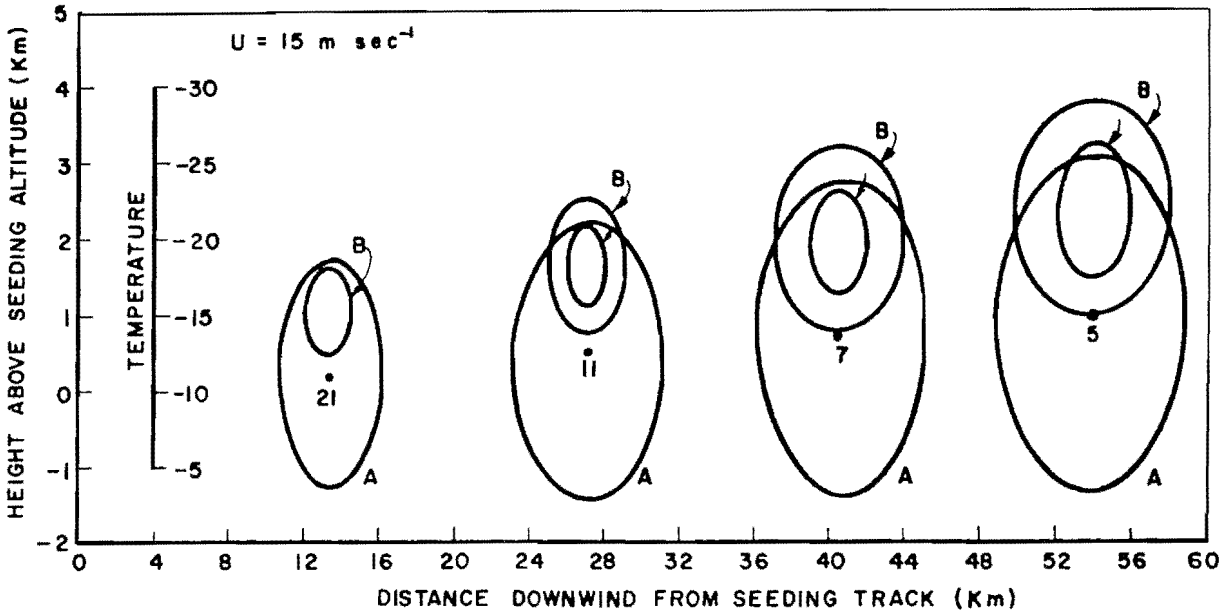

Figure 10. Artificial ice nuclei concentration as a function of downwind distance from airborne release. A: Mass of silver iodide (10^{-14} gm l^{-1}), dots are at center of mass; B: Active artificial ice nuclei (l^{-1}); outer, 5 l^{-1}, inner 10 l^{-1}. Data: seeding temperature, -10°C; mean vertical velocity, 25 cm/sec; horizontal velocity, 15 m/sec; time, 15 min after last of 8 seeding traverses.

spread of one standard deviation of effluent distribution either side of the maximum concentration from a point source. For a diffusion constant K_y=200m^2 sec^{-1}and wind speed of 15 m sec^{-1} this half angle is about 15 degrees. In Figure 11 the shaded areas show concentrations of artificial ice-nuclei greater than 5 per liter. Concentrations were first computed for the center of a seeding track and then extrapolated perpendicular to the wind until the half angles drawn from the ends of the seeding track were intersected.

While this model is highly idealized it can roughly approximate the geographical extent of a given concentration magnitude. Furthermore, by varying environmental conditions, an analysis of the relative importance of various meteorological factors concerning the placement of seeding material into critical parts of a cloud can be made. With the aid of such an analysis the approximate location of potential seeding effects can be determined.

4.4.2 Diffusion From a Point Source. As an aid in locating ground-based generator sites, and to evaluate these sites, a point source seeding model was developed.

The Pasquill-Gifford model (Gifford, 1968; Turner, 1969) was chosen for application to Project Snowman seeding problems. This model assumes 1) concial diffusion downwind with a Gaussian effluent concentration distribution in both the crosswind and vertical directions, 2) the emission is continuous for a period of time which is at least equal to the travel time from the source of a downwind point in question, 3) the diffusing material is a stable gas or aerosol (less than 20 microns diameter) which remains suspended in the air over long periods of time, 4) the equation of continuity is fulfilled, i.e., none of the material is removed from the plume as it moves downwind, 5) a mean wind speed representative of the diffusing layer can be specified, and 6) transport instead of diffusion is the dominant process in the downwind direction.

The sigma values (σ_y and σ_z) in the equation, as given in standard diagrams, are standard deviations of the effluent concentration distribution in the crosswind and vertical directions, respectively. These values were actually intended to apply to distances of a few hundred meters to about 10 km. However, Peterson (1968) reported that the lateral standard deviation of the plume fit reasonably well an extension of the Pasquill-Gifford neutral stability curve at distances up to 160 nautical miles downwind of the source.

The Pasquill-Gifford expression for a continuous point source, assuming the effective stack height is zero, can be written

$$C(x,y,z) = \frac{Q}{\pi \sigma_y \sigma_z u} \exp\left(-1/2 \frac{y}{\sigma_y}^2\right) \exp\left(-1/2 \frac{z}{\sigma_z}^2\right) \quad (30)$$

where

- C Concentration at a point (g m^{-3})
- x Downwind distance from the source to the point in question (m)
- y Crosswind distance from the source to the point in question (m)
- z Altitude of the point i question above the source (m)
- Q The source strength (g sec^{-1})

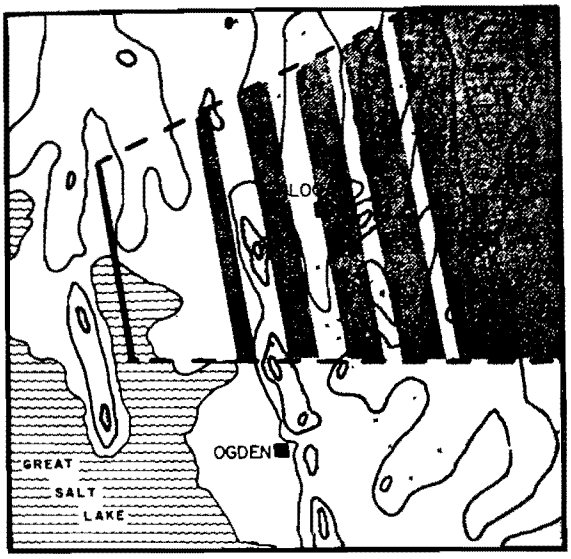

Figure 11. Areas with artificial ice nuclei concentration greater than 5 per liter. Seeding track (heavy solid line) and areas of ice nuclei (heavy shading) extrapolated to half angle boundaries (dashed lines).

σ_y Standard deviation of plume concentration distribution in the y direction (m)

σ_z Standard deviation of plume concentration distribution in the z direction (m)

u Representative mean wind speed affecting the plume (m sec^{-1})

Sigma values increase with increasing instability and σ_y is greater than σ_z. $y = \sigma_y$ defines the point at which the concentration is 0.6 of the concentration at the point $y = 0$ for the same altitude. $y = 2.14\,\sigma_y$ defines the 0.1 concentration point. In a similar manner, $z = \sigma_z$ and $z = 2.14\,\sigma_z$ define the 0.6 and 0.1 concentration points for locations at different altitudes in the respective x-z planes. Values for σ_y and σ_z can be taken from standard diagrams.

On the basis of plume tracking experiments conducted over mountainous terrain in Colorado and in the Wasatch Mountain area it appears advisable to compute sigma values from observed diffusion angles rather than those applicable near the ground over smooth terrain. The concept of a Gaussian distribution for the effluent concentration appears reasonable, however.

As a tool for assessing the effectiveness of seeding from selected sites, at selected rates, a computerized procedure was developed which applies the Pasquill-Gifford relationship to obtain seeding-agent concentrations at selected points. The points selected are the three seeder sites. Concentrations were computed for releases from each seeder site under various wind velocities.

A target grid composed of 10-minute intervals ranging from 41°N to 42°N and from 111°W to 112°W was used. All target grid stations were assumed to be on a level surface with separate calculations made for 3050 m msl, 3660 m msl, and 4270 m msl. Target minus source altitudes define the values of z in the equation.

Seeding rate was taken to be 25 g hr^{-1} with 10^{14} effective particles per gram assumed. Changes in either effluent output or particle production can be accounted for by multiplying the results of these calculations by appropriate ratios. Separate calculations were made for winds from the west, northwest, and southwest with a wind speed of 10 m sec^{-1}. Changes in the wind speed can be accounted for by multiplying the results of the calculations by appropriate ratios. σ_y and σ_z were calculated from assumed dispersion angles (Beta), which are the angles between the two 0.1 concentration points and the source.

5.0 DATA REDUCTION AND SYSTEM ANALYSIS

5.1 Telemetered Precipitation Data

5.1.1 Calibration and Conversion to Precipitation Values. Telemetered precipitation data were registered by the automatic readout console (ARC) in terms of electromagnetic periods. These were converted to precipitation values using a different calibration curve for each station and season. During the aircraft seeding program the calibration for an individual station was represented by a fifth order curve relating electronic period with the amount of water in the can. This procedure was changed for the ground seeding program, because it was found that equipment problems could be detected by the revised technique.

In the later calibration technique, the difference in electronic period versus the amount of water added was used. An example is shown in Figure 12 for a relatively well functioning gage. On the other hand, erratic behavior of the period differences was interpreted to mean mechanical or electronic difficulties, usually the former. When erratic changes in period were found, a station would be re-examined and rebuilt if necessary.

To be certain that a station would operate properly, not only was a calibration redone, but at several stages of loading, a finely tuned calibration was made. That is, the electronic period was recorded while small amounts of water were added, each addition being the equivalent of .006 inch of precipitation. If the response to this refined calibration at three stages of loading was not a smooth one, further work was performed. When telemetered data were computer processed both the calibration data and the telemetered precipitation data were printed out. In addition to the precipitation amount and electronic period, a number of other values were displayed on the printout. Among these were the hourly precipitation rate and the fraction of water accumulated in the can compared with the maximum amount. A winter recharge was necessary in cases when the fraction approached unity.

5.1.2 Data Quality Analysis. All telemetered precipitation data along with the recording-gage data from several stations were computer plotted on graphs so that editing and standardization between stations with widely differing seasonal totals could be accomplished. The graphical plots are of two types, one for gross editing and the other for detailed editing and measurements.

In the first type of graphical display a whole season's data is presented on one graph with 10 inches of precipitation shown by a 1-inch vertical spacing on the graph. Each eight hours is shown on the graphs by a one-tenth inch horizontal spacing. From such graphs the seasonal amount of precipitation is readily found. In addition spurious data and other gross anomalies in the data, such as a failure of the weighing device, are easily recognized.

In the second type of graphical display each month's data is plotted on a graph with one inch of precipitation shown by a 1-inch vertical spacing on the graph and an eightfold expanded time scale. From these graphs a detailed evaluation of data is facilitated. Four-hour amounts of precipitation can be read to a hundredth of an inch. In addition situations in which the accuracy of the data is questionable are easily recognized. These cases were either eliminated from the analysis or the data corrected when possible.

Two important sources of errors were encountered; one source of error is generated by snow sticking to the side of a can. The excess amount was determined in some cases by the amount of subsequent meltoff; otherwise that data were removed. Another problem arose when the weighing mechanism stuck and did not respond to the increased weight from incoming precipitation. If mechanical sticking resulted in a succession of short steps on the graphs the data were corrected, otherwise the data were removed. Whenever data were corrected, a coded notation was made on both the recording data sheets and on the areal displays of individual cases. In this way corrected data could be recognized and evaluated in terms of surrounding values.

5.1.3 Analysis of Precipitation Data. Edited precipitation data may not be linearly interpolated reliably between stations because of the large variations associated with elevation and slope. On the other hand, data which have been standardized according to the total seasonal amount can be interpolated between stations rather easily. Furthermore, the standardized values, when added together for statistical evaluation, each contribute more uniformly than do the unadjusted values.

Standardization of telemetered precipitation data is accomplished in the following way. For a particular station the amount of precipitation between each November 1 and March 31 is multiplied by a certain factor to obtain a 10 inch fall. For example, if a station

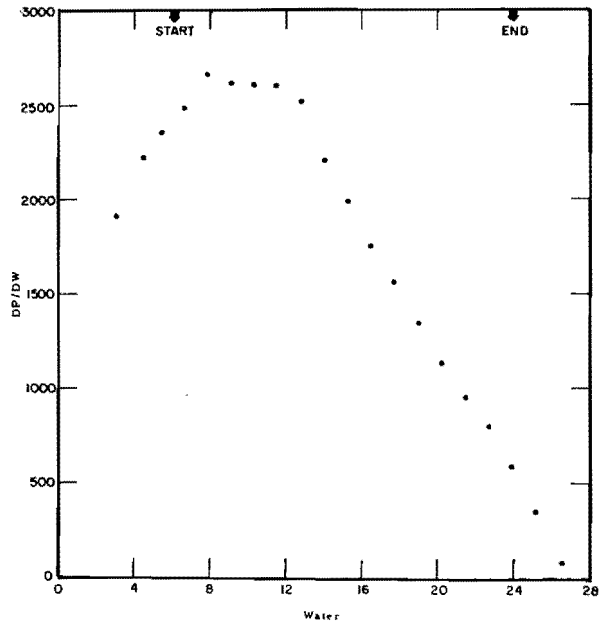

Figure 12. Sample calibration curve for telemetry data:differences in electronic period versus amount of water added.

received a 20 inch fall the factor would be .50. In the subsequent year the factor might be say .36. If in the second year a factor of 1.5 more precipitation fell over the whole target area than in the first year then the factor of .36 would be multiplied by 1.5 to give .54. Then the two factors .50 and .54 are averaged to give a final standardized value of .52.

In the standardization calculations carried out for the three years' data, fiscal year 1970 was chosen as the reference year. Either of the other years could have been used, and the results would differ only by a constant. The results show that if the scaling factor for FY 70 is 1.00 then it is 1.53 for FY 71 and 1.34 for FY 72. A list of final standardization factors is presented in Table 4; these factors are also presented in Figure 13.

To use these factors all four-hour amounts of precipitation are multiplied by the standardization factor appropriate to each station. Areal charts of actual and standardized values for a particular case are presented in Figures 14 and 15, respectively. The relatively irregular variation of the actual values compared to the standardized values found in this example is typical.

Table 4. Standardization factors by station.

Station	Standardization Factor (f^{-1})	Station	Standardization Factor (f^{-1})
2	0.988	65	0.652
6	0.840	66	1.260
8	1.649	68	0.509
12	0.824	70	0.618
15	0.698	71	0.533
16	0.418	78	0.807
17	0.475	80	0.486
20	0.484	113	1.015
21	0.638	124	0.644
25	0.714	132	0.487
26	0.440	146	2.995
29	0.599	147	0.489
44	1.292	152	0.527
45	0.535	164	0.499
46	0.310	188	1.244
49	0.342	189	1.626
50	0.580	190	1.405
63	1.028	572	2.005

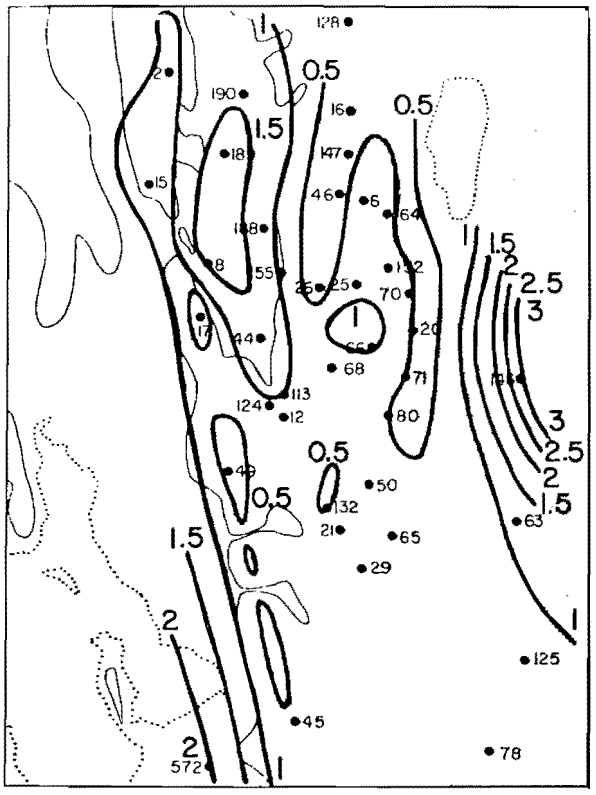

Figure 13. Geographical distribution of precipitation standardization factor.

5.2 Supporting Meteorological Data

5.2.1 Hill AFB Radar, Surface and Upper Level Observations. The most important meteorological parameters that affect the distribution of seeding material as well as possible seeding effects are the wind speed and direction at upper levels, the minimum cloud temperature, usually found at cloud top, and the amount of moisture available to the cloud. To determine cloud top temperatures and their time variation, both rawinsonde and vertical incidence radar data are used. Visual observations of cloud bases along with rawinsonde data are used to establish the cloud-base moisture content.

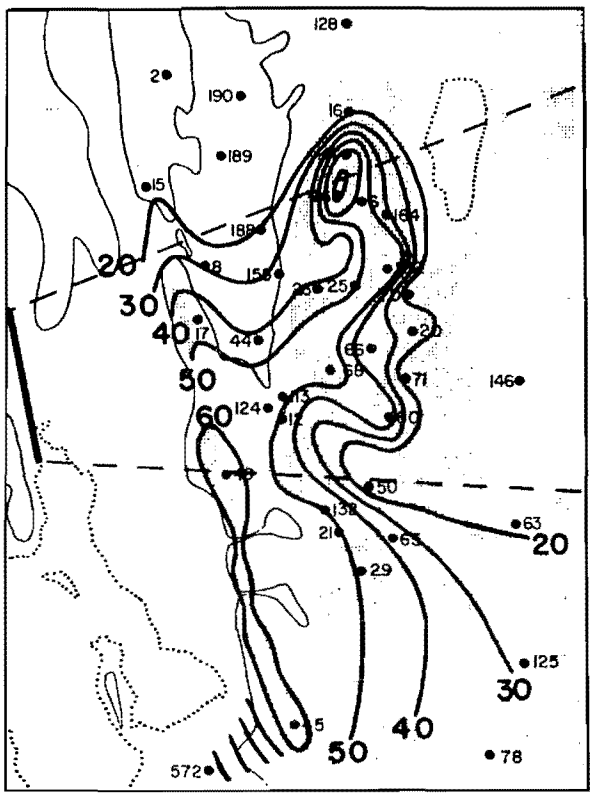

Figure 14. Areal distribution of measured precipitation for sample cases: four hour precipitation for case no. 4-1 FY 70 (Dec. 21, 1969, 2100-0100 MST).

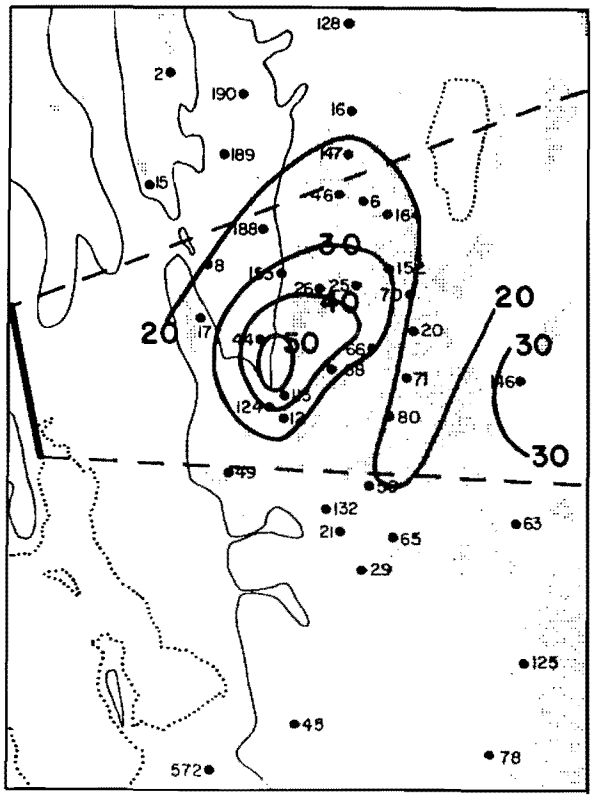

Figure 15. Areal distribution of standardization precipitation for sample case: four hour precipitation for case no. 4-1 FY 70 (Dec. 21, 1969, 2100-0100 MST).

It was found from radar data, measured at Hill Air Force Base, that the cloud tops sometimes varied by several thousand feet, or in terms of temperature by 10°C to 20°C in a period of four hours. In such cases this large variability must be taken into account in any evaluation.

To show how these meteorological parameters are determined a typical time plot is shown in Figure 16. Included in the figure is an eight-hour operational period and the hourly weather reported from Ogden. The heights of the observed cloud bases and radar tops for overcast conditions are outlined in solid. Broken clouds are similarly indicated but with dashed lines. From rawinsonde data several additional quantities are plotted. These are the temperature and saturation mixing ratio at two thousand-foot intervals and cloud tops estimated by the height where the relative humidity drops below ice saturation with further ascent.

In addition to the hourly surface observations at Hill AFB, similar observations were available from surrounding National Weather Service stations. Detailed surface observations were also taken at the rawinsonde site in Cache Valley.

Upper level wind, temperature, and humidity data from the National Weather Service network of rawinsonde stations were available regularly. Rawinsonde measurements were also made at times during operational events.

5.2.2 Cloud Structure and Its Variability. One of the objectives in analyzing rawinsonde and vertical incidence radar data is to obtain the temperature at cloud top. In one method rawinsonde data alone are used to find an ice cloud top temperature. In another method vertical incidence radar data are used to find the cloud top height, and the cloud top temperature may then easily be found by using rawinsonde temperature data.

In either approach, the dew point depression may be used as a basis for estimating whether the cloud is ice or supercooled water. If the dew point depression is equal to that appropriate for ice saturation and the level is within the cloud, then it is supposed that the cloud at that level is composed primarily of ice crystals. If the observed dew point depression is substantially less than the difference between the ambient temperature and the dew point at ice saturation, then it is supposed that a significant

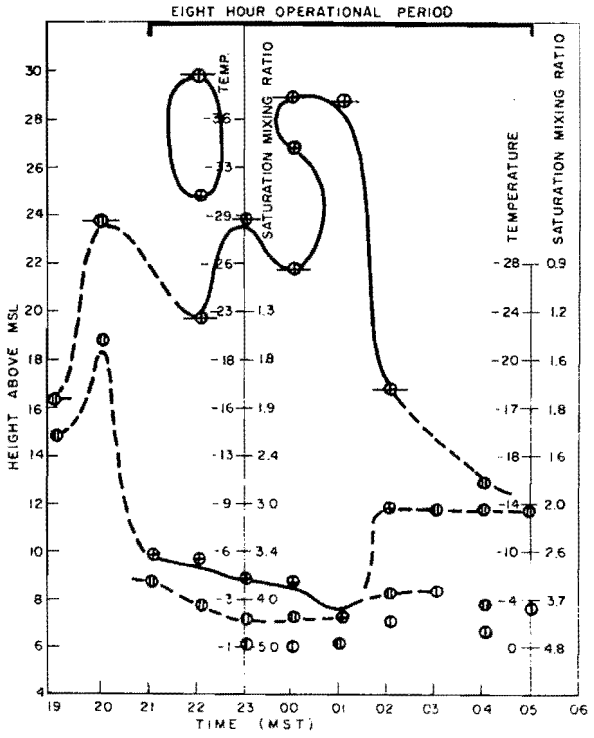

Figure 16. Cloud characteristics as a function of height and time reported by Hill Air Force Base radar: Case no. 4-1 FY70.

amount of water is present. Although the humidity element is probably affected by significant amounts of supercooled water, the very presence of the condition is probably sufficient to identify clouds containing significant amounts of water.

To illustrate the method of analysis case 14 of FY 74 is used as an example. In Figure 17 the time variation of cloud properties is shown as a function of elevation above sea level. The dashed line refers to cloud tops continuously measured by the Hill Air Force Base cloud detection unit. The thin solid lines indicate the temperature. The hatched area shows the region of zero dew point depression. The region with water vapor amounts between that of ice and water saturation is bounded by the solid curve and the edge of the hatched area. Thus the solid curve separates the regions below and above ice saturation.

In this example, the radar data indicate that the cloud top is made up primarily of ice and that toward the end of the event the whole cloud is composed primarily of ice. Thus, by such an analysis of each event, an estimation of cloud composition may be made. The same analysis actually may be made without the vertical incidence radar data. However, the radar data not only provides an independent source of cloud top heights, but also provides detailed information on cloud top climatology, including its variability on a time scale of minutes, hours, or other durations.

Thus, analysis of vertical incidence radar data shows that during operational events of the airborne experiment, the cloud top temperature varied by a standard deviation of 5°C during four-hour intervals and 8°C during eight-hour intervals. In a few instances the variation was greater than 20°C. Therefore, it is clearly evident that if moisture parameters are found from rawinsonde data frequent releases of the rawinsondes are required.

The internal characteristics of cloud systems may also undergo large changes over a period of several hours. A cloud composed almost wholly of supercooled water may become well supplied with ice crystals in an hour or two. Whether such an event could be appropriately classified according to a single temperature is questionable.

5.2.3 Analysis of Meteorological Events. An important aspect of an evaluation of a cloud seeding program is related to the type of storm. For cold cloud systems in mountainous regions there are essentially four types: orographic, frontal, convective, and cyclonic. More than one type may exist simultaneously. The significance of identifying cloud systems according to types is both their respective ability to produce precipitation and the representativeness of

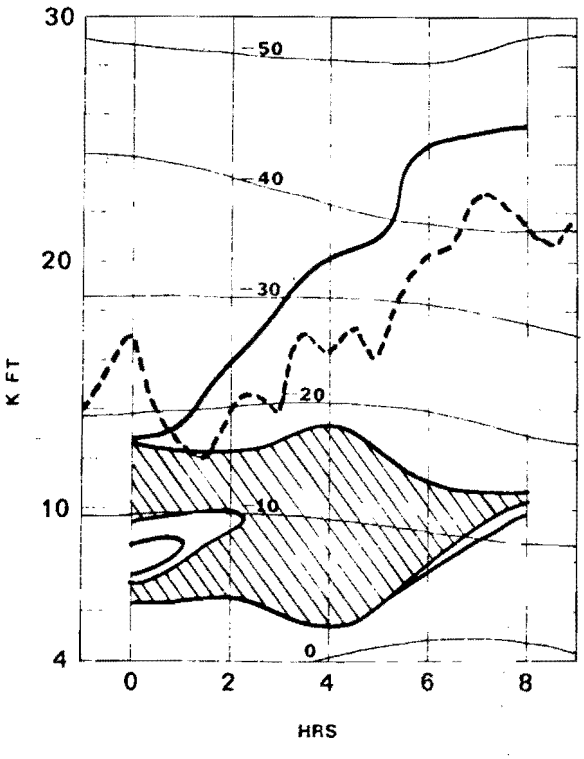

Figure 17. Cloud moisture properties as a function of height and time: Case no. 14 FY 74. Radar cloud tops (dashed curve) temperature (thin solid curves), supercooled water (hatched area), ice saturation (heavy solid curve).

supporting meteorological data. In the former, a mixed set of data could be dominated by a very strong cyclonic storm which showed only weak precipitation potential according to predictions based upon meteorological factors relating to moist orographic flow. In the latter, a convective situation could produce heavy precipitation, yet little potential might be evident from a series of rawinsonde observations. In general, there is a need to seek relative uniform sets of events, amenable to both diagnosis (by modeling) and representation by discrete measurements.

To classify operational events, several definitions were established. For the airborne experiment an event was called convective if either cumulonimbus or thunderstorms were reported in the target area, or thunderstorms reported by radar. With the ground seeding program, convection was defined objectively from the rawinsonde data. This method will be described in Section 7.0. An event was called cyclonic if a frontal system existed near or south of the target area and a low pressure system was approaching or within the target area. Only a few such cases were found. Also, in events classed as cyclonic, the wind criteria for an orographic case were not usually satisfied; that is, the wind at low levels was from the south or southeast. But the main concern with cyclonic cases is that the large-scale vertical motion and moisture fields would result in anomalously high precipitation compared to what would occur in the absence of cyclonic effects.

Frontal cases were identified first by inspection of the hourly wind velocity at Hill Air Force Base. In cold frontal cases the wind characteristically shifted abruptly in a veering direction, e.g., from southwest to northwest. The wind shift criterion was verified by inspection of surface synoptic charts. A frontal intensity was assigned by first finding the cross product of the surface wind just after passage and the wind at 11,000 ft. This product is indicative of the amount of cold air advection. Then, the mixing ratio difference between cloud base and top in the three hours following frontal passage was used as a measure of the cloud depth associated with the front. The frontal intensity was found by taking the product of the wind cross product and the mixing ratio difference.

6.0 ANALYSIS OF SEEDING EFFECTIVENESS— AIRBORNE SEEDING EVENTS

6.1 Data for Airborne Seeding Analysis

6.1.1 Telemetered Precipitation Data. The telemetered precipitation data were standardized as previously described so that spatial variations of precipitation other than the dominant one of orographically controlled precipitation could be emphasized. In other words, by reducing the large spatial variations due to orographic effects, any modification of precipitation due to cloud seeding would be more readily distinguished than otherwise.

Areal charts of standardized precipitation for the three years' airborne seeding experiment were analyzed. That is, isopleths of 4-hour standardized precipitation were drawn, the limits of downwind lateral spread from the seeding track were marked on the charts, and the average value of standardized precipitation was found based upon reporting stations with acceptable data within the downwind region. For the unseeded cases, the upwind areal limit was the seeding track used in the seeded half of the 8-hour period; this choice of upwind limit for the unseeded half was intended to make the downwind seeded and unseeded areas comparable to each other. It should be noted that because the wind direction at seeding altitude and above varied significantly from case to case, the "target area" was in fact variable from case to case.

All acceptable precipitation data downwind from the seeding track were used in the calculation of the standardized precipitation average. Previously, an attempt was made to pinpoint the specific area where seeding effects were expected. However, the precipitation trajectories of seeded clouds would be subject to a relatively large uncertainty compared to the overall size of the target area. Slight or moderate differences in horizontal wind speed, vertical diffusion, or minimum value of the required artificial ice-nuclei concentration would result in a significantly different precipitation target area.

As a result of the above considerations, the upwind limit was taken to be the seeding track rather than a variable limit based upon diffusion calculations. With this procedure any seeding effects would be included within the area, even if the magnitude were reduced by the use of a larger area than theoretically required.

6.1.2 Supporting Meteorological Data. As described in Section 5.2 both radar cloud data from Hill Air Force Base and rawinsonde data from Cache Peak and Salt Lake City were plotted on graphs to show the time-height evolution of various meteorological parameters during operational events. From these graphs meteorological data were measured, such as cloud top temperature (radar tops), cloud-base and cloud-top mixing ratio, and wind velocity at various altitudes. In Section 6.2 the method of classification of events into meteorological types will be discussed.

The basic meteorological classes of events, which undoubtedly have different precipitation statistics from each other, are orographic, cold frontal, convective and cyclonic. The primary aim is to investigate orographic effects of seeding. This objective is not only a matter of following the original purpose of the study, but is dictated by the fact that there are relatively few frontal, convective, or cyclonic events. However, when taken together about half of the events fall into at least one of the classes besides orographic.

6.1.3 Analysis of Silver Samples. Isopleths of silver based upon snow samples following airborne seeding events are shown in Figure 18. The amount of silver is highest along the Wasatch Mountains and mostly confined to the target area, except for a north-south band to the north. Isopleths of silver following seeding from Willard Mountain only are shown in Figure 19. The amounts of seeding material from this generator are similar but evidently greater than that from the airborne generators. It is noted that in the ground seeding program, three generators were used simultaneously, so the silver amounts would be even greater than in the case of only one generator.

For unseeded storms the isopleth analysis, as shown in Figure 20, reveals much lower amounts of silver compared to the amounts following seeding. It is clear from these figures that seeding material, released from either the airborne or mountaintop generators, covers most of the target area, at least on the average.

6.2 Classification of Events and Tabulation of Data

A complete tabulation of airborne seeding events carried out during fiscal years 1970 through 1972 is provided in Table 5. These events lasted eight hours with one-half considered seeded and the other half unseeded. Which half was seeded was determined by random choice. Actually the seeding by aircraft lasted

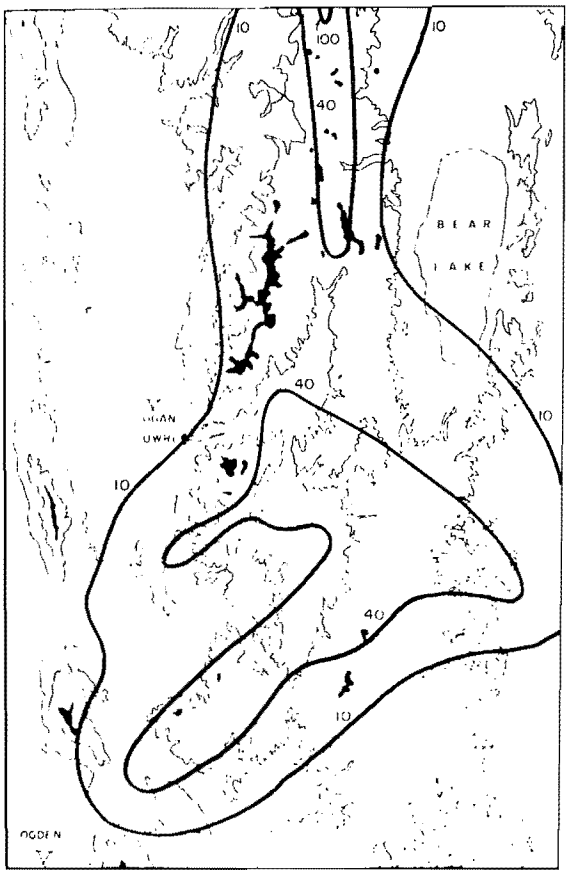

Figure 18a. Isopleths of silver concentration (gm/ml times 10-12) for snow samples taken following airborne seeding: FY 70.

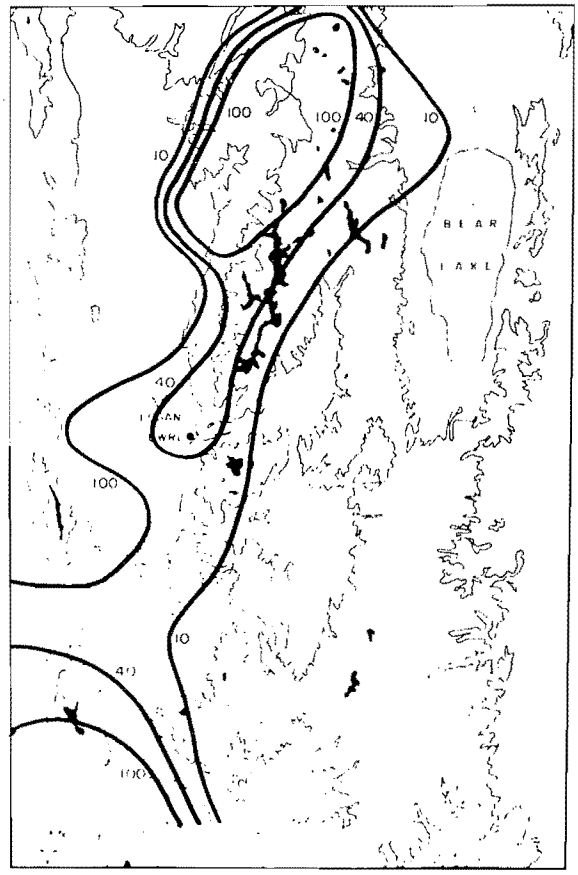

Figure 18b. Isopleths of silver concentration (gm/ml times 10-12) for snow samples taken following airborne seeding: FY 71.

two hours, but this material covered portions of the target for periods of around two hours after seeding was stopped. Thus the period during which at least some seeding material remained over the target was about four hours. In each seeding event approximately 240 gm of silver iodide were released. Whether an unseeded portion could have become contaminated by seeding material depended first upon whether seeding preceded, and second, whether the wind conditions permitted seeding material to remain over the target during the unseeded half.

For each of the 8-hour events, compilations of telemetered precipitation data, upper level winds, heights of cloud bases and tops, along with humidity and temperature were made. In addition, each event was analyzed separately. Areal maps of precipitation and locations of expected seeding effects were prepared.

In Table 5 the column headings identify the entries. For the case type the following definitions apply: OROG means orographic; FR means frontal; THSTM means thunderstorm or cumulonimbus present; and CYCL means a low pressure center with frontal system in Utah or Nevada. The standardized precipitation is given in inches averaged over the reporting stations downstream of the seeding track. Parameters derived from radar and rawinsonde data are RCTT, CTMR, and CBMR; these are the radar cloud top temperature, the cloud-top mixing ratio, and cloud-base mixing ratio, respectively. The rawinsonde location is indicated by SL for Salt Lake City and CP for Cache Peak. The rawinsonde-sounding time is indicated by a number in parentheses. This number is the time of the sounding in hours after the middle of a 4-hour event; a plus means the sounding was made after the middle of the 4-hour period and a minus means before. In the next column the wind direction and speed in knots at 9,000 ft is given. In the next column to the right, the rawinsonde cloud top temperature as found by using the ice top criterion is given. No evaluation was made for cloud top temperatures from the Salt Lake City soundings. In the last column the radar cloud top temperature at the time of the rawinsonde measurement is shown.

6.3 Analysis of Seeded and Unseeded Events

6.3.1 Previous Analyses. Because of findings to be discussed later, it is useful to review previous project analyses of seeding effects. Following the first two years of the project, it was found, as shown in Figure 21, that ratios of seeded to unseeded

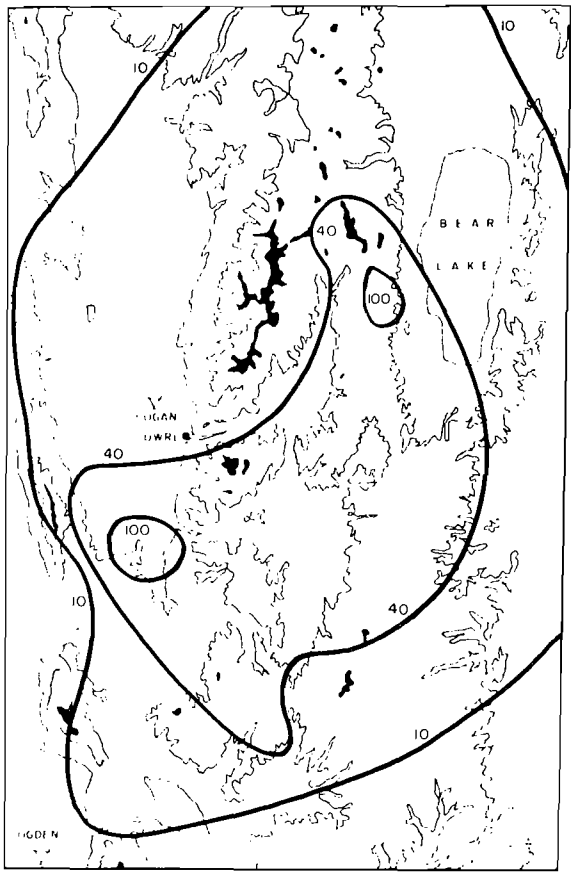

Figure 19a. Isopleths of silver concentration (gm/ml times 10-12) for snow samples taken following seeding from the Willard Mountain generator during selected storms: FY 70.

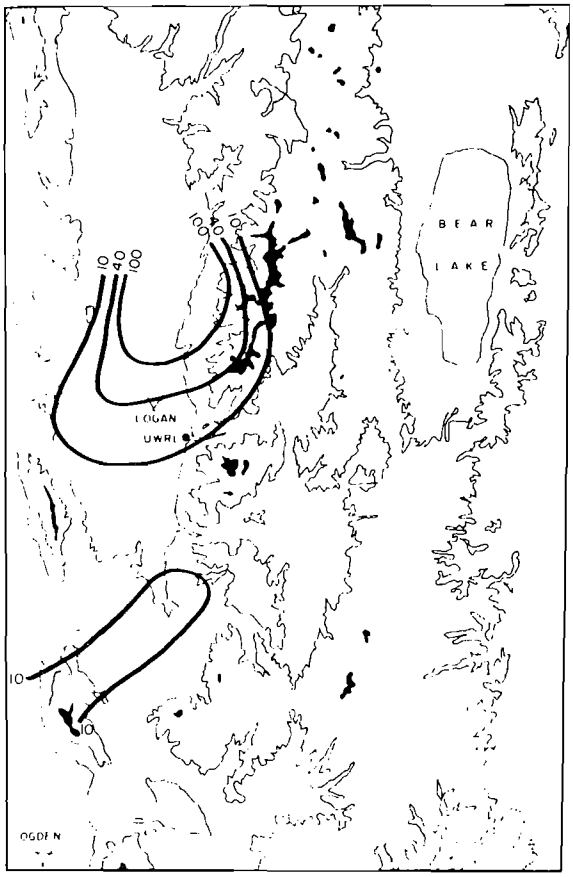

Figure 19b. Isopleths of silver concentration (gm/ml times 10-12) for snow samples taken following seeding from the Willard Mountain generator during selected storms: FY 71.

precipitation far exceed unity over most of the target area when the cloud top temperature was between -13°C and -23°C (Chappell et al., 1972). Otherwise the ratios were generally close to or less than unity. The cloud top temperatures were based upon rawinsonde observations, with cloud tops deduced from the 80 percent criterion.

Later an analysis of precipitation data from five key stations in the high Wasatch[1] showed increases due to seeding in the cloud top temperature range between -16°C and -24°C as shown in Figure 22; with other temperatures the ratios were generally less than unity (McNeill et al., 1972).

More recently, another analysis utilized the radar cloud top temperatures. In orographic and weak frontal events precipitation in seeded storms was found to be higher than in unseeded events in the temperature range of about -25°C to -35°C. However, this finding was attributed mainly to chance variation rather than any seeding effect. In fact, an empirical predictor method showed that this result could be accounted for by the occurrence of stronger storms in seeded periods compared to unseeded ones (Hill, 1973).

6.3.2 Review of Cloud Top Temperatures. Cloud top temperatures may be found by direct observation of the temperature at the visual cloud top, or by indirect methods. The indirect methods usually employ rawinsonde data to find where the humidity falls below a particular percent, or below ice saturation upon further ascent. Another indirect method utilizes vertical incidence radar from which cloud top heights are found. Rawinsonde temperature data, which is a uniformly varying quantity in space, is used to find the temperature at cloud top. During the course of this experiment visual cloud top observations were not generally available. Thus, the cloud top temperatures were found indirectly. Because such temperatures have been used to evaluate this project and others as well, it is worthwhile to critically examine the method. Based upon physical arguments

[1]Tony Grove Lake, Trigara Springs, Bug Lake, Paradise Canyon, and Monte Cristo.

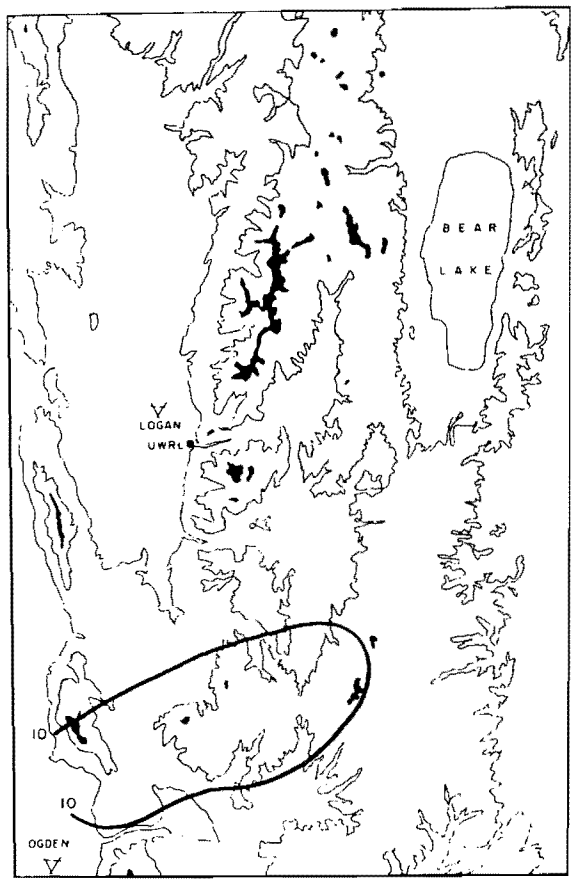

Figure 20a. Isopleths of silver concentration (gm/ml times 10-12) for snow samples taken following unseeded storms: FY 70.

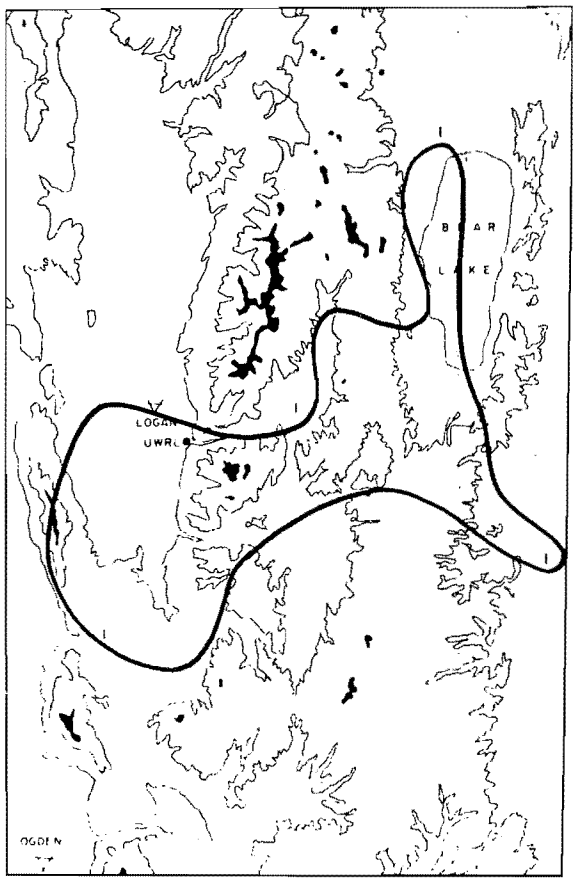

Figure 20b. Isopleths of silver concentration (gm/ml times 10-12) for snow samples taken following unseeded storms: FY 71.

there is little question that the ice top temperature is preferred over the temperature found from applying the 80 percent relative humidity criterion. However, large differences in cloud top temperature between these methods occur only when the humidity remains just at ice saturation at very cold temperatures.

On the other hand measurements of cloud top temperatures made several years ago may be greatly affected by whether the rawinsonde was illuminated by the sun. To demonstrate this effect use is made of the radar cloud top temperatures. In Figure 23 a graph of the radar cloud top temperature versus the rawinsonde cloud top temperature is shown for all available FY 70 data. At each point the letter D for daytime rawinsonde release, or N for nighttime release is shown. In two cases both letters are given because the releases were made when the sun was near the horizon, but the precise release times are not known. Arrows indicate the temperature is colder by an unknown amount; the cause of the limit is that the soundings were taken only to 400 mb. A similar graph for the FY 71 data is shown in Figure 24. It is immediately obvious that the daytime rawinsonde cloud top temperatures are grossly in error. When only the nighttime temperatures are considered we find that the rawinsonde temperatures are systematically colder than the radar temperatures by about 4°C to 5°C at the coldest temperatures. This difference is attributed to the fact that the vertical incidence radar is located at Hill AFB, which is upwind of the Wasatch range by a few miles. On the other hand, the rawinsonde releases were made from Cache Peak, and by the time the package reached cloud tops of -25°C to -35°C, it would be over the Wasatch range. An orographic lift of about 600 m (2000 ft) would account for the difference, at least on the average.

There are a few cases when the rawinsonde temperature was much colder than the radar temperature. In these cases convection tended to occur; there might be a difference due to the representativeness of data on convective conditions, but it appears that the orographic-convective effect is amplified by the mountains, so the difference in the two temperatures tends to be exaggerated with convection.

A further manifestation of the differences between day and night rawinsondes may be found from Table 5. In six events a definite radar cloud top was evident, but the rawinsonde data indicated no clouds were present. All six of these soundings were taken during the daytime. (In one other event the

Table 5. Airborne seeding events. A: Fiscal Year 1970

Case	Half	S/U	Start Date	Period MST	Case Type	Stand. Precip.	Radar			Rawinsonde			
							RCTT	CTMR	CBMR	Stn/Time	Wind 9K	SCTT	RCTT/S
1	1	S	Dec. 10	2300-	OROG	0.01	-17	1.6	2.3	CP(-2.0)	250/25	-33	-17
	2	U		0700	OROG	0.01	-15	1.9	2.6	SL(0.0)	260/10	M	M
2	1	S	Dec. 19	2330-	OROG	0.05	-22	1.4	3.7	CP(+3.5)	285/32	M	M
	2	U		0730	OROG	0.01	-30	0.7	1.3	CP(-0.5)	290/35	- 7	M
3	1	U	Dec. 20	2300-	OROG	0.04	-24	1.3	4.2	SL(+4.0)	240/20	M	M
	2	S		0700	OROG	0.00	-35	0.6	2.7	SL(0.0)	255/22	M	M
4	1	S	Dec. 21	2100-	FR	0.28	-37	0.4	3.8	CP(0.0)	300/25	-25*	-23*
	2	U		0500	OROG	0.05	-16	1.6	2.6	SL(+2.0)	305/32	M	M
5	1	U	Jan. 9	1700-	OROG	0.03	-44	0.2	3.8	CP(-2.0)	230/15	-20	-31*
	2	S		0100	OROG	0.03	-43	0.2	3.7	CP(0.0)	230/25	-30	-30*
6	1	S	Jan. 10	1100-	OROG	0.04	-22	1.3	3.7	CP(-2.0)	260/25	-12	-30*
	2	U		1900	OROG	0.03	-19	1.5	3.1	CP(0.0)	270/20	-20	-22
7	1	M	M	M	M	M	-42	0.3	4.8	SL(-1.0)	M	M	M
	2	M				M	-41	0.3	5.0	SL(-5.0)	M	M	M
8	1	U	Jan. 16	1400-	OROG	0.14	-43	0.3	4.5	CP(+1.0)	250/25	-18	-29*
	2	S		2200	OROG	0.22	-36	0.5	4.0	CP(+3.0)	265/28	-33*	-26
9	1	S	Jan. 21	1230-	OROG	0.08	-25	1.2	4.8	CP(+2.5)	290/25	-19	-30*
	2	U		2030	OROG	0.06	-44	0.2	4.0	CP(-1.5)	305/23		
10	1	S	Jan. 21	2030-	OROG	0.14	-41	0.4	4.7	CP(+0.5)	260/25	-30*	-26*
	2	U		0430	FR	0.18	-28	1.0	5.2	CP(+2.5)	265/25	-25	-21
11	1	U	Jan. 22	0430-	FR	0.20	-18	1.9	5.5	CP(-1.5)	270/23	-25	-19
	2	S		1230	OROG	0.14	-29	0.9	5.1	CP(+0.5)	270/20	-15	-15
12	1	S	Jan. 27	1030-	FR	M	-39	0.4	3.3	CP(-3.5)	290/20	-18	-30*
	2	U		1830	THSTM	0.11	-25	1.0	3.9	CP(+0.5)	330/25	-15	-26
13	1	S	Feb. 12	2300-	FR	0.21	-19	1.7	4.3	CP(-1.0)	310/28	-35*	-17
	2	U		0700	THSTM	0.05	-25	1.0	4.2	SL(0.0)	340/20	M	M
14	1	S	Feb. 14	0100-	OROG	0.01	-18	1.6	1.6	SL(+2.0)	330/15	M	M
	2	U		0900	OROG	0.00	-17	1.7	1.9	SL(-2.0)	330/15	M	M
15	1	M	M	M	OROG	M	-42	0.3	2.1	M	M	M	M
	2	M			FR	M	-42	0.3	3.5	M	M	M	M
16	1	S	Mar. 14	2000-	FR	0.19	-45	0.2	3.3	CP(+1.0)	310/25	-37*	-33*
	2	U		0400	THSTM	0.05	-33	0.6	2.7	CP(-3.0)	300/20		
17	1	U	Mar. 16	2300-	FR	0.19	-36	0.4	3.5	CP(-2.0)	230/22	-38*	-23
	2	S		0700	FR	0.08	-26	0.9	1.9	SL(0.0)	300/30	M	M
18	1	S	Mar. 28	1000-	THSTM	M	-22	1.2	2.2	CP(-1.0)	M	-10	-23
	2	U		1800	FR	M	-29	0.7	2.0	CP(+1.0)	M	None	-30

Table 5. Continued. B: Fiscal Year 1971

Case	Half	S/U	Start Date	Period MST	Case Type	Stand. Precip.	Radar			Rawinsonde			
							RCTT	CTMR	CBMR	Stn/Time	Wind 9K	SCTT	RCTT/S
1	1	U	Dec. 8	2300-	FR	0.03	-40	0.3	4.1	SL(+4.0)	188/18	M	M
	2	S		0700	FR	0.06	-44	0.2	4.7	SL(0.0)	190/22	M	M
2	1	S	Dec. 9	0800-	FR	0.13	-30	0.8	4.5	SL(-5.0)	250/21	M	M
	2	U		1600	FR	0.09	-24	1.1	4.6	SL(+3.0)	280/20	M	M
3	1	U	Dec. 14	2330-	FR	0.05	-31	0.6	3.3	SL(+3.5)	285/20	M	M
	2	S		0730	FR	0.06	-22	1.1	2.5	SL(-0.5)	310/20	M	M
4	1	U	Dec. 16	0930-	FR	0.10	-19	1.6	4.0	SL(+5.5)	250/27	M	M
	2	S		1730	OROG	0.03	-27	0.9	3.9	SL(+1.5)	285/22	M	M
5	1	S	Dec. 18	0900-	OROG	0.06	-41	0.2	3.3	SL(+6.0)	290/10	M	M
	2	U		1700	OROG	0.03	-31	0.5	1.7	SL(+2.0)	265/13	M	M
6	1	U	Dec. 21	1100-	CYCL	0.07	-30	0.7	2.2	CP(+1.0)	210/25	- 9	-28
	2	S		1900	CYCL	0.03	-38	0.3	3.0	CP(-3.0)	217/27		

Table 5. Continued. B: Fiscal Year 1971.

Case	Half	S/U	Start Date	Period MST	Case Type	Stand. Precip.	Radar			Rawinsonde			
							RCTT	CTMR	CBMR	Stn/Time	Wind9K	SCTT	RCTT/S
7	1	S	Jan. 10	1430-	THSTM	0.26	-26	1.0	2.8	CP(+1.5)	310/25	-24	-27
	2	U		2230	THSTM	0.20	-23	1.2	3.9	CP(-2.5)	245/25		
8	1	U	Jan. 10	2230-	FR	0.10	-23	1.2	3.3	CP(+0.5)	250/40	-33*	-27
	2	S		0630	FR	0.09	-27	1.0	3.9	SL(+0.5)	245/25	M	M
9	1	U	Jan. 11	1500-	FR	0.02	-45	0.1	2.8	CP(+1.0)	200/20	-38*	-37*
	2	S		2300	FR	0.03	-36	0.4	2.8	CP(-3.0)	M		
10	1	S	Jan. 11	2300-	FR	M	-26	0.9	2.7	CP(0.0)	210/20	-33*	-33
	2	U		0700	FR	M	-48	0.2	3.2	SL(0.0)	210/20	M	M
11	1	U	Jan. 12	1500-	THSTM	0.22	-30	0.6	3.1	CP(+1.0)	250/20	-44*	-36
	2	S		2300	THSTM	0.20	-40	0.3	3.7	CP(-3.0)	247/20		
12	1	S	Jan. 13	1500-	OROG	0.05	-43	0.2	1.1	SL(0.0)	270/30	M	M
	2	U		2300	OROG	0.00	-36	0.4	0.6	SL(-4.0)	263/32	M	M
13	1	U	Jan. 15	1130-	OROG	0.03	-26	1.2	3.2	CP(+1.5)	230/15	-17	-18*
	2	S		1930	OROG	0.01	-32	0.6	2.6	SL(-0.5)	210/20	M	M
14	1	U	Jan. 25	1100-	OROG	0.00	-15	2.0	2.1	CP(+1.0)	270/15	-13	-12
	2	S		1900	OROG	0.00	-10	2.9	3.0	CP(-3.0)	270/15		
15	1	U	Feb. 4	1400-	OROG	0.02	-19	1.4	2.2	CP(+1.0)	250/25	-22	-18
	2	S		2200	OROG	M	-21	1.3	2.2	CP(-3.0)	270/26	M	M
16	1	S	Feb. 10	1200-	OROG	0.00	-22	1.7	3.3	CP(+2.0)	300/35	- 8	-11
	2	U		2000	OROG	0.01	- 9	3.6	4.2	CP(-2.0)	300/35		
17	1	U	Feb. 15	0930-	FR	0.18	-45	0.1	2.9	CP(+1.5)	270/20	-10	-33*
	2	S		1730	THSTM	0.07	-42	0.2	1.3	CP(-2.5)	270/20		
18	1	S	Feb. 19	0830-	CYCL	0.22	-40	0.2	4.1	CP(+3.5)	200/15	M	M
	2	U		1630	CYCL	0.00	-19	1.5	4.1	CP(-0.5)	175/15	None	-17
19	1		Feb. 25	0030-	FR	0.16	-20	1.4	2.3	SL(+2.5)	300/35	M	M
	2	S		0830	FR	M	-37	0.4	4.7	SL(-1.5)	300/35	M	M
20	1	S	Mar. 8	0530-	FR	0.02	-48	0.1	3.4	CP(+1.5)	305/08	None	-37*
	2			1330	OROG	0.03	-27	1.2	2.5	CP(-2.5)	295/10		
21	1		Mar. 10	0700-	M	0.01	M	M	3.1	CP(+1.0)	270/10	None	-12
	2	S			M	0 01	M	M	2.4	CP(-3.0)	280/10		
22	1		Mar. 11	0430-	OROG	0.02	-36	0.4	3.7	CP(+0.5)	260/10	-24	-27
	2	S		1230	OROG	0.01	-44	0.2	2.2	CP(-2.5)	250/10	M	M
23	1	S	Mar. 12	0130-	OROG	0.03	-35	0.4	2.7	CP(+2.5)	210/35	-10	-26
	2			0930	OROG	0.01	-33	0.5	2.8	CP(-1 5)	210/35		
24	1		Mar. 12	2030-	FR	0.08	-19	1.7	3.3	SL(+6.5)	210/25	M	M
	2	S		0430	FR	0.24	-28	0.9	2.9	SL(+2.5)	270/25	M	M
25	1	S	Mar. 13	0500-	FR	0.06	-30	0.7	3.8	CP(+2.0)	302/22	None	-28
	2			1300	OROG	0.03	-36	0.4	2.4	CP(-2.0)	300/13		
26	1	S	Mar. 15	0310-	FR	0.02	-36	0.4	2.1	CP(+2.5)	300/12	-38	-24
	2			0930	OROG	0.03	-28	0.8	3.2	CP(-1.5)	300/12		
27	1	S	Mar. 17	0030-	CYCL	0.13	-41	0.2	1.0	CP(+2.5)	185/10	-41*	-39*
	2			0830	CYCL	0.14	-30	0.7	3.2	CP(-1.5)	185/10		
28	1	S	Mar. 17	0900-	OROG	0.05	-24	1.1	3.0	SL(+6.0)	330/20	M	M
	2			1700	OROG	0.03	M	M	2.1	SL(+2.0)	330/20	M	M
29	1		Mar. 22	2330-	OROG	0.03	-34	0.7	4.2	CP(+1.5)	262/25	-29*	-28
	2	S		0730	OROG	0.04	-28	1.0	5.8	CP(-2.5)	195/20		
30	1		Mar. 23	0730-	FR	0.03	-33	0.7	4.8	CP(+1.5)	250/16	None	-34
	2	S		1530	FR	0.04	-44	0.2	3.7	CP(-2.5)	250/14		
31	1	S	Mar. 23	1630-	CYCL	0.07	-42	0.2	3.3	CP(-0.5)	230/20	-32*	-32*
	2			0030	CYCL	0.19	-36	0.5	5.0	CP(-4.5)	260/18	M	M
32	1		Mar. 25	1830-	OROG	0.02	-31	1.2	3.2	CP(+1.5)	200/25	-23	-21
	2	S		0230	OROG	0.02	-27	1.0	4.7	CP(-2.5)	210/27		
33	1	S	Mar. 26	0230-	OROG	0.01	-32	0.7	5.5	CP(+1.5)	200/35	-13	-24*
	2			1030	OROG	0.01	-34	M	4.2	CP(-2.5)	205/35		
34	1		Mar. 26	1600-	THSTM	0.35	-24	1.2	5.7	SL(-1.0)	230/35	M	M
	2	S		0000	THSTM	0.03	-35	M	2.5	CP(0.0)	240/15	-14	None

Table 5. Continued. C: Fiscal Year 1972.

Case	Half	S/U	Start Date	Period MST	Case Type	Stand. Precip.	Rawinsonde[a]			Rawinsonde	
							SCTT	CTMR	CBMR	Stn/Time	Wind 9K
1	1	U	Dec. 2	2330-	M	0.06	-23	1.0	4.2	CP(+0.5)	255/20
	2	S		0730	M	0.04	-37	0.3	4.0	CP(+0.5)	290/15
2	1	S	Dec. 3	1900-	M	M	M	M	M	M	M
	2	U				M	M	M	M	M	M
3	1	U	Dec. 5	1230-		M	M	M	M	M	M
	2	S		2030		M	M	M	M	M	M
4	1	S	Dec. 10	1730-	OROG	0.02	-19	1.2	2.6	CP(+0.5)	280/25
	2	U		0130	OROG	0.02	-10	2.3	2.7	CP(-0.5)	295/12
5	1	S	Dec. 12	1330-	CYCL	0.05	-43	0.1	1.4	CP(+2.5)	245/25
	2	U		2130	CYCL	0.08	-38	0.2	2.8	CP(+1.5)	262/22
6	1	S	Dec. 14	1200-	OROG	0.04	-16	M	M	CP(+1.0)	240/35
	2	U		2000	FR	0.03	-44	0.2	2.5	CP(0.0)	290/20
7	1	U	Dec. 22	0900-	OROG	0.02	- 9	M	M	CP(0.0)	210/40
	2	S		1700	FR	0.11	- 2	M	M	CP(0.0)	220/40
8	1	U	Dec. 28	1030-	OROG	0.04	- 7	M	M	CP(+1.5)	205/25
	2	S		1830	OROG	0.02	-10	M	M	CP(+0.5)	225/20
9	1	U	Dec. 29	1100-	OROG	0.05	M	M	M	CP(+1.0)	240/24
	2	S		1900	OROG	0.02	-13	M	M	CP(0.0)	275/15
10	1	S	Dec. 29	1900-	OROG	0.03	-42	0.2	2.6	CP(0.0)	270/20
	2	U		0300	OROG	0.03	-16	1.6	2.6	CP(-1.0)	280/20
11	1	M	M	M	M	M	M	M	M	M	M
	2	M				M	M	M	M	M	M
12	1	U	Jan. 5	2130-	OROG	0.00	-11	2.6	2.6	CP(+0.5)	240/12
	2	S		0530	OROG	0.01	-11	2.6	2.6	CP(+0.5)	275/25
13	1	M	M	M	M	M	M	M	M	M	M
	2	M				M	M	M	M	M	M
14	1	U	Jan. 10	1200-	OROG	0.02	M	M	M	SL(+3.0)	295/25
	2	S		2000	OROG	0.05	M	M	M	SL(-1.0)	295/25
15	1	U	Jan. 11	1200-	OROG	0.07	M	M	M	SL(+3.0)	250/30
	2	S		2000	OROG	0.07	M	M	M	SL(-1.0)	250/30
16	1	S	Jan. 11	2000-	FR	0.09	M	M	M	SL(+7.0)	255/35
	2	U		0400	FR	0.11	M	M	M	SL(+3.0)	255/35
17	1	U	Jan. 12	1330-	OROG	0.04	M	M	M	SL(+1.5)	310/45
	2	S		2130	OROG	0.01	M	M	M	SL(-2.5)	310/45
18	1	S	Jan. 17	2200-	OROG	0.02	-32	0.6	4.8	CP(+2.0)	M
	2	U		0600	OROG	0.03	M	M	M	SL(+1.0)	265/20
19	1	S	Jan. 18	0600-	OROG	0.07	M	M	M	SL(-3.0)	265/20
	2	U		1106	FR	M	M	M	M	M	265/20
20	1	S	Jan. 20	1200-	OROG	M	-12	M	M	CP(+2.0)	M
	2	U		2000	OROG	M	-12	M	M	CP(-2.0)	M
21	1	U	Jan. 21	0930-	OROG	0.16	- 6	M	M	CP(+0.5)	280/40
	2	S		1730	OROG	0.07	-31	M	M	CP(+0.5)	270/25
22	1	S	Jan. 21	1730-	OROG	0.03	-33	0.5	4.6	CP(+0.5)	290/30
	2	U		0130	OROG	0.06	-32	0.6	4.5	CP(-0.5)	255/25
23	1	U	Jan. 22	0900-	OROG	0.20	- 4	M	M	CP(0.0)	275/35
	2	S		1700	FR	0.06	-30	M	M	CP(0.0)	275/35
24	1	U	Jan. 26	2300-	FR	0.04	-40	0.3	2.9	CP(+1.0)	255/05
	2	S		0700	FR	0.15	-39	0.2	2.6	CP(0.0)	335/05
25	1	U	Jan. 27	1900-	CYCL	0.02	-40	0.3	0.8	CP(+1.0)	215/25
	2	S		0300	CYCL	M	-40	M	M	CP(-3.0)	215/25
26	1	S	Mar. 18	2330-	THSTM	0.06	-17	1.6	2.3	CP(+0.5)	295/30
	2	U		0730	THSTM	0.12	-35	0.7	4.0	CP(-0.5)	315/20
27	1	S	Mar. 23	0830-	THSTM	0.05	M	M	M	CP(+0.5)	305/10
	2	U		1630	THSTM	0.02	M	M	M	CP(-0.5)	295/20

[a]Hill AFB cloud detection unit was inoperative; rawinsonde cloud parameters are substituted (day-night differences in sounding data discussed in text).

*An asterisk indicates the cloud top temperature is colder than the value shown. (The reason for the limitation is that the rawinsonde data were normally terminated at around the 400 mb level.)

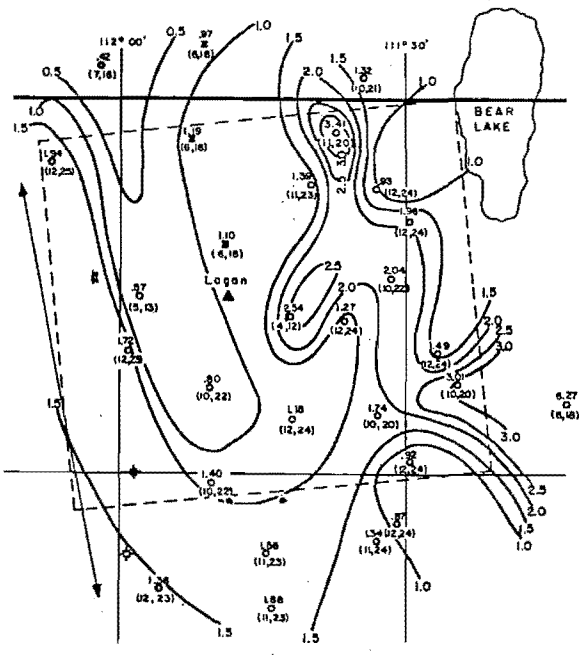

Figure 21. Ratios of two year mean precipitation during seeded periods to mean precipitation during unseeded periods when cloud top temperatures were considered to be in the range -15° to -25°. Number of events are shown as (S, U).

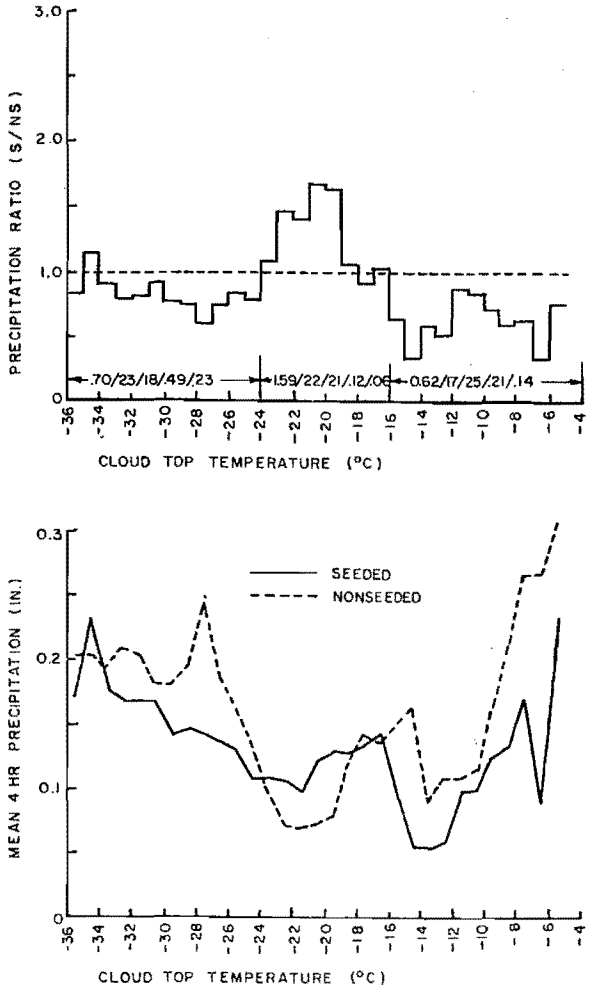

Figure 22. Three year mean seeded and unseeded precipitation and their ratio as a function of cloud top temperature. Data for the three ranges are: precipitation ratio/number of seeded events/number of unseeded events/significance level from Wilcoxon test/significance level from Sum of Squared Ranks test.

reverse situation occurred, i.e., there was no cloud according to radar, but rawinsonde data indicated one was present. This sounding was at night, and as previously mentioned there tends to be more cloudiness near the rawinsonde site compared to the radar site.)

It is clear from the foregoing analysis that the most realistic cloud top temperatures are those based upon the radar data. These data can be used at either time, day or night. (An analysis to be discussed in the next section, in connection with the ground seeding program, shows that the rawinsondes which have improved ventilation for the humidity element give cloud top temperatures in good agreement with the radar data, day or night; thus, either method may be used for more recent observations.)

During FY 72 the Hill AFB radar was inoperative. Thus, in order to utilize FY 72 data, it must first be found out whether ventilated or unventilated rawinsondes were used; no records of this sort are available, and has already been mentioned, practically no radar observations were made for these storms. Therefore, only a simple comparison between day and night values of the sounding ice top temperature could be made. In Figure 25, these temperatures are shown according to whether the release was made in daylight or at night. It is evident from this information, that the unventilated rawinsondes were still being used, because the median cloud top temperature was -10°C during the day and -32°C at night. This very large difference is as might be expected from the instrumentation, rather than any natural variation. At best we can use the nighttime data; but there are still some differences between radar and rawinsonde cloud top temperatures, as previously discussed.

Thus, we find that in the analysis of cloud seeding effects during the airborne seeding program several factors relating to the accuracy of cloud top temperatures must be considered; these are (1) errors due to the use of rawinsonde humidity elements which are subject to solar illumination, (2) uncertainties of cloud top temperatures due to natural space-time variations, (3) errors in cloud top temperature due to marginal situations in which a slight change or correction of humidity readings results in a large

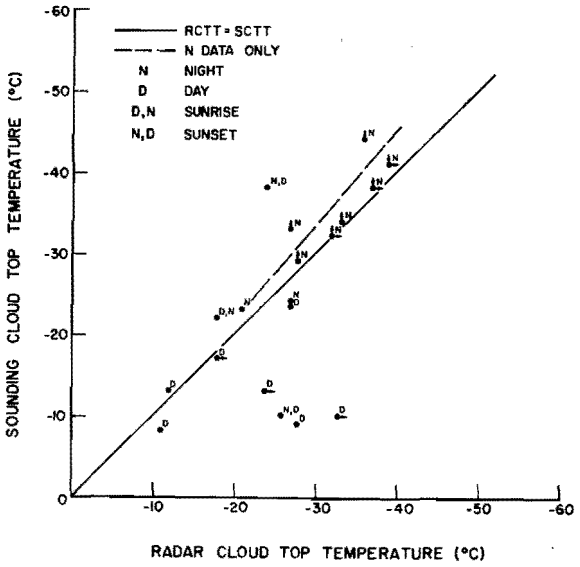

Figure 23. Radar versus rawinsonde cloud top temperatures for FY 70. Arrows indicate temperature may be lower than that shown.

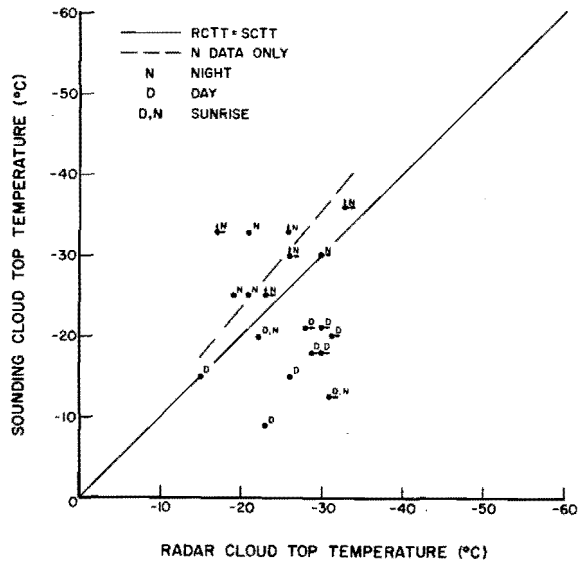

Figure 24. Radar versus rawinsonde cloud top temperatures for FY 71. Arrows indicate temperature may be lower than that shown.

change in cloud top height and temperature, and (4) other sources of errors such as the use of an ice cloud top temperature, when in fact the cloud is composed entirely of supercooled water.

6.3.3 Analysis of Cloud Seeding Effects. In previous sections we have found that the cloud top temperatures used to assess seeding effects are in error by large amounts. For the daytime events the error is often as much as 20°C; natural variability accounts for another several degrees discrepancy

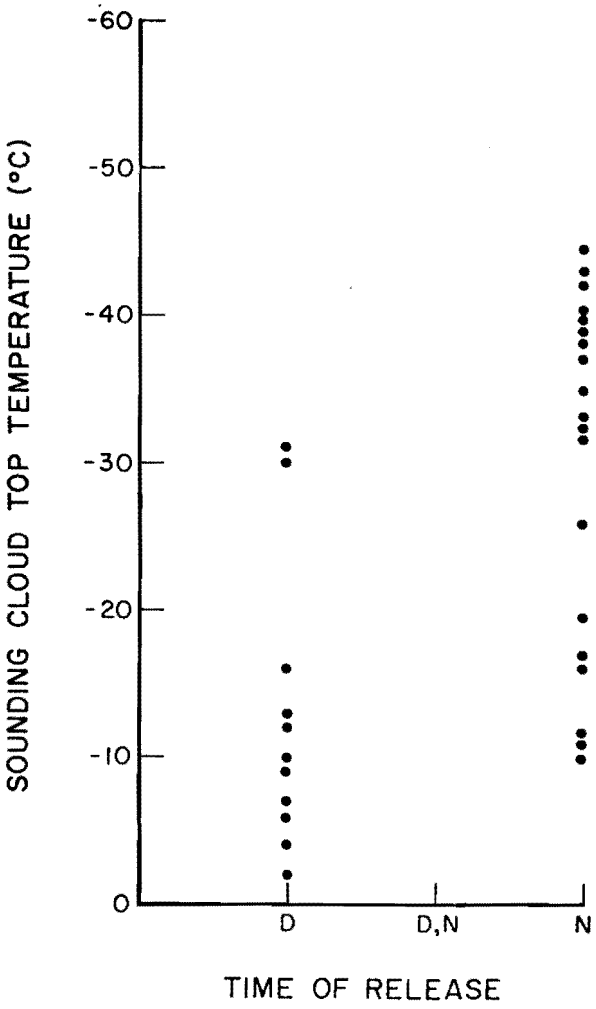

Figure 25. Rawinsonde cloud top temperatures for FY 72 according to whether a day or night release.

between readings averaged over a four-hour period and a single reading within the period; use of an 80 percent relative humidity criterion also adds several degrees error. Thus it is abundantly clear that for both of the analyses described earlier in this section, the increases in precipitation in seeded cases within certain temperature ranges cannot be substantiated. Corrections to these analyses would involve large but irregular shifts in cloud top temperature. Of course, analysis of these events can be made using the radar cloud top temperatures, as will be discussed later.

The question may be raised, how does one arrive at an apparent increase in precipitation within a particular cloud top temperature range, when in fact the result must be regarded as fortuitous. Yet statistics are used to show the results are significant.

The reason suggested here is that when one is free to choose the temperature limits within which an effect is supposed to occur, an otherwise not statistically significant variation becomes apparently

significant. It is the exclusion of apparently adverse seeding effects by the precise specification of temperature limits that augments the variation to a more favorable amount.

For example, in the first analysis described, the temperature limits of the "seeding window" were between -13°C and -23°C. In the second analysis the limits were -16°C and -24°C. Now if the original limits had been retained in the second analysis, the apparent seeding effect would have been much less, as may be noted from Figure 22, and with little statistical significance. Therefore, even though apparent seeding effects may be found in temperature regions wherein a physical basis is present, it is not appropriate to choose limits after an analysis of precipitation ratios is completed. Of course, one does choose limits for the various quantities, presumably with a physical basis, but these limits should at least be chosen in advance of the analysis.

This situation described above applies to other projects as well. In fact in some projects more than one pair of limits is used. For example, in the evaluation of the San Juan Pilot Project, Elliott et al. (1976) used several parameters each of which contributed to the seeding effect, apparently. For example, we note sections 5.8 through 5.10 of their report. Yet the very same problem may exist. That is, even though there may be a physical basis for a seeding effect, it is augmented and perhaps made apparently significant by the detailed choice of limits.

It is recognized that as the number of cases becomes very large, even the free choice of limits-of-effect becomes relatively less important. Another way to reduce the problem is to utilize covariates to account for natural variability of precipitation. Neither of these approaches negates the previous discussion. It is merely pointed out now, that these approaches do reduce the magnitude of the problem.

6.3.4 Analysis of Airborne Seeding Program with Cloud Top Temperature Stratification. An analysis of the airborne seeding program is carried out using both radar cloud top temperatures and covariate techniques. Discussion of cloud top temperatures has been already given; additional comments on the use of precipitation estimators are appropriate. Because a variety of storm types occurs in winter in Northern Utah, no single estimator is likely to be successful. Inasmuch as the basic physical processes in each storm type are sufficiently different, it is likely that entirely different estimators would be needed for each type.

However, one estimator which is probably common to each cloud type is the amount of moisture available for precipitation. A crude measure of this is the difference between the cloud base and top mixing ratios.[2] These are listed in Table 5; note that the values of FY 72 are derived from rawinsonde ice tops.

[2]Ratio of grams of water vapor to kilograms of air.

Orographic cloud types are separated into warm and cold cloud tops, i.e., CTT $\geq$ -29°C and CTT $\leq$ -30°C, respectively. Precipitation is plotted against the mixing-ratio parameter for seeded and unseeded cases in the warm category as shown in Figure 26. At each data point the cloud top temperature is plotted; FY 72 data are shown as crosses. The ratio of seeded to unseeded precipitation is found to be 1.66. This apparent seeding effect is clearly due to the fact that in the seeded storms the cloud depth was much greater than in the unseeded storms. Regression lines, which are forced through the origin, actually show less precipitation in the seeded storms compared to the unseeded, but the difference is small and has little significance.

For the cold category, shown in Figure 27, the precipitation ratio is 1.48, which again is primarily due to a difference of cloud depths. For a given cloud depth the ratio is reduced to 1.22. However, without the exceptionally strong precipitation in one seeded event the ratio would be close to unity.

A similar analysis is made for events classified as frontal or cyclonic. In the warm category there are only 5 seeded storms, whereas there are 9 unseeded storms. As shown in Figure 28 there is a large scatter of precipitation amounts, but on the average, much greater amounts than in the orographic category. It is highly doubtful that significance can be given to differences between seeded and unseeded storms with this limited amount of data. It is also evident that combining orographic events with the frontal and cyclonic events would permit the latter, with the larger precipitation amounts and greater variability, to dominate and perhaps to yield apparent significant differences in seeded and unseeded precipitation, because of the relatively large total number of events. In other words only a portion of the events have both high amounts and high variability.

For the cold category of the frontal and cyclonic storms, there are 15 seeded and 13 unseeded events; these data are plotted in Figure 29. The precipitation ratio for a fixed cloud depth is 1.12. Again with the very high variability, this ratio is primarily due to chance. (It is interesting to note that in the warm category, the 9 unseeded cases have a similar relationship between precipitation and cloud depth as in the cold category, but not the 5 seeded cases, which evidently are too few in number.)

Cases with thunderstorms reported in the vicinity are treated as a separate category, regardless of the cloud top temperature. Only 4 such cases were seeded and 7 were left unseeded. As shown in Figure 30 there is a large scatter of data and higher amounts on the average than the frontal-cyclonic category. It should be recognized that the mixing-ratio parameter as measured is the least representative in this category, because with convection, there is high variability in cloud tops both in time and space. No special significance is given to differences between seeded and unseeded precipitation with this amount of data. However, we stress again the importance of storm

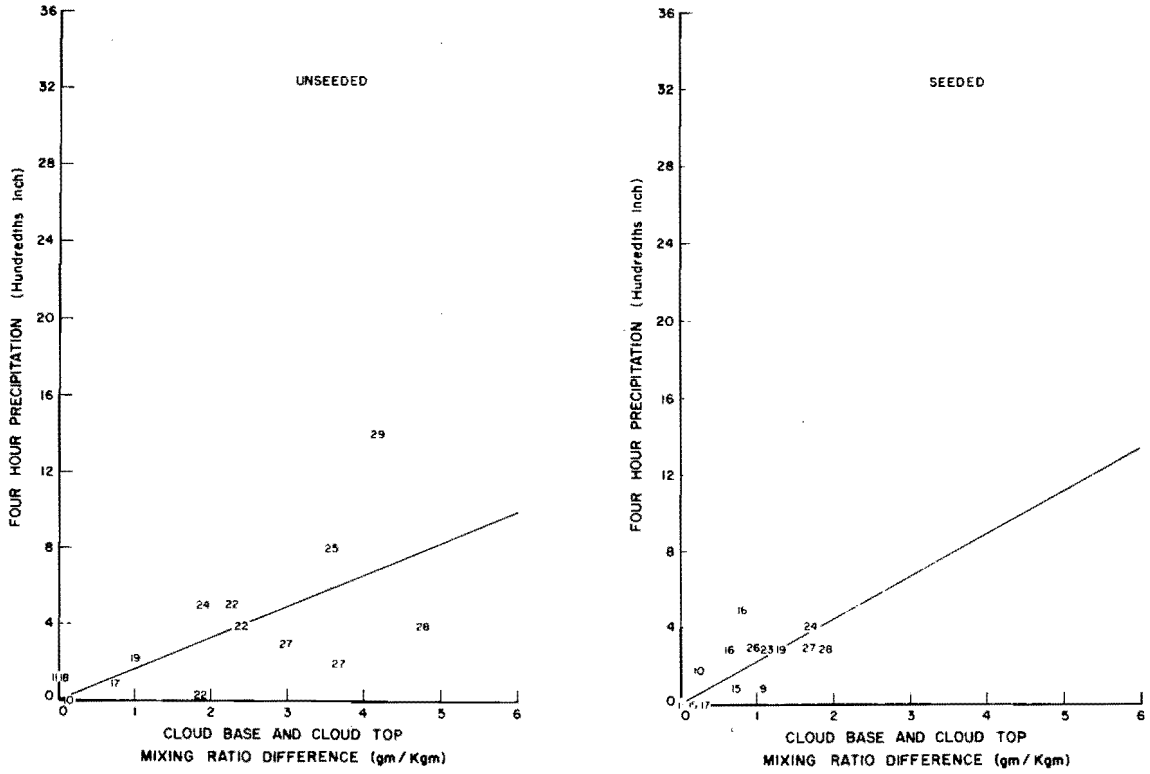

Figure 26. Precipitation versus mixing-ratio parameter for unseeded and seeded orographic events in the **warm** *Cloud top temperature category. Numbers on the graph are (negative degrees Celsius) cloud top temperatures; italicized values refer to FY 72 nighttime data.*

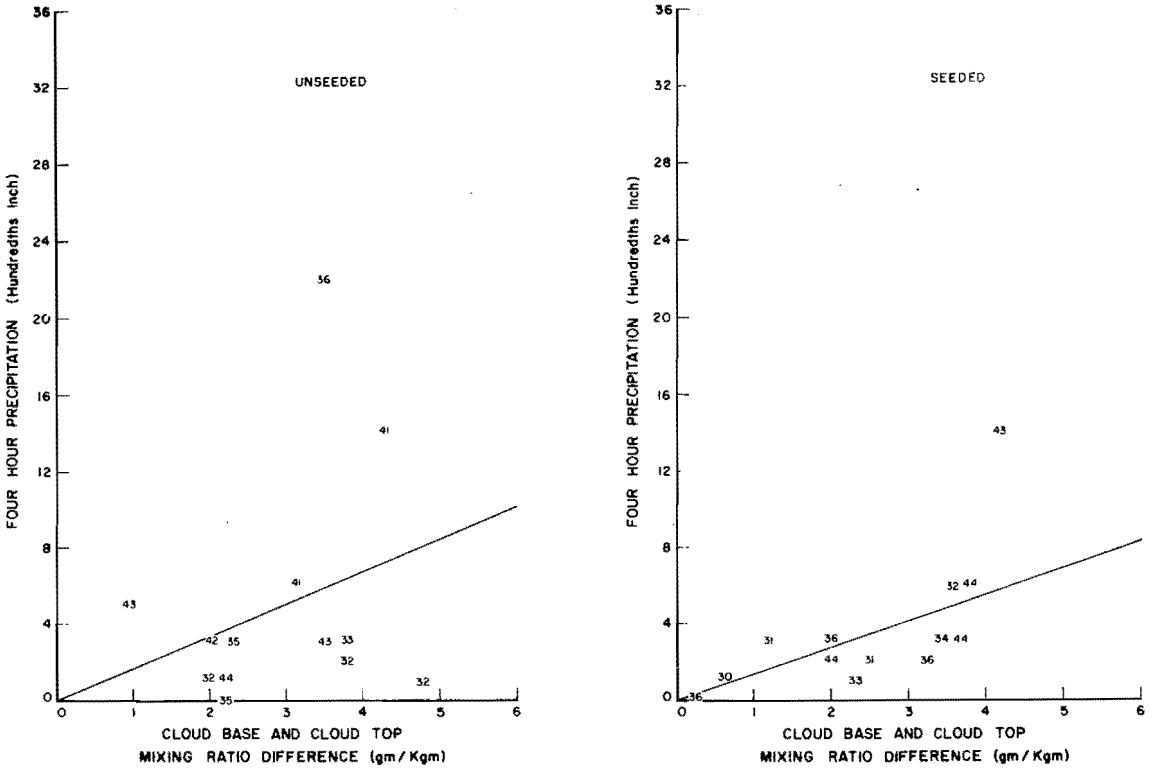

Figure 27. Precipitation versus mixing-ratio parameter for unseeded and seeded orographic events in the **cold** *cloud top temperature category. Numbers on the graph are (negative degrees Celsius) cloud top temperatures; italicized values refer to FY 72 nighttime data.*

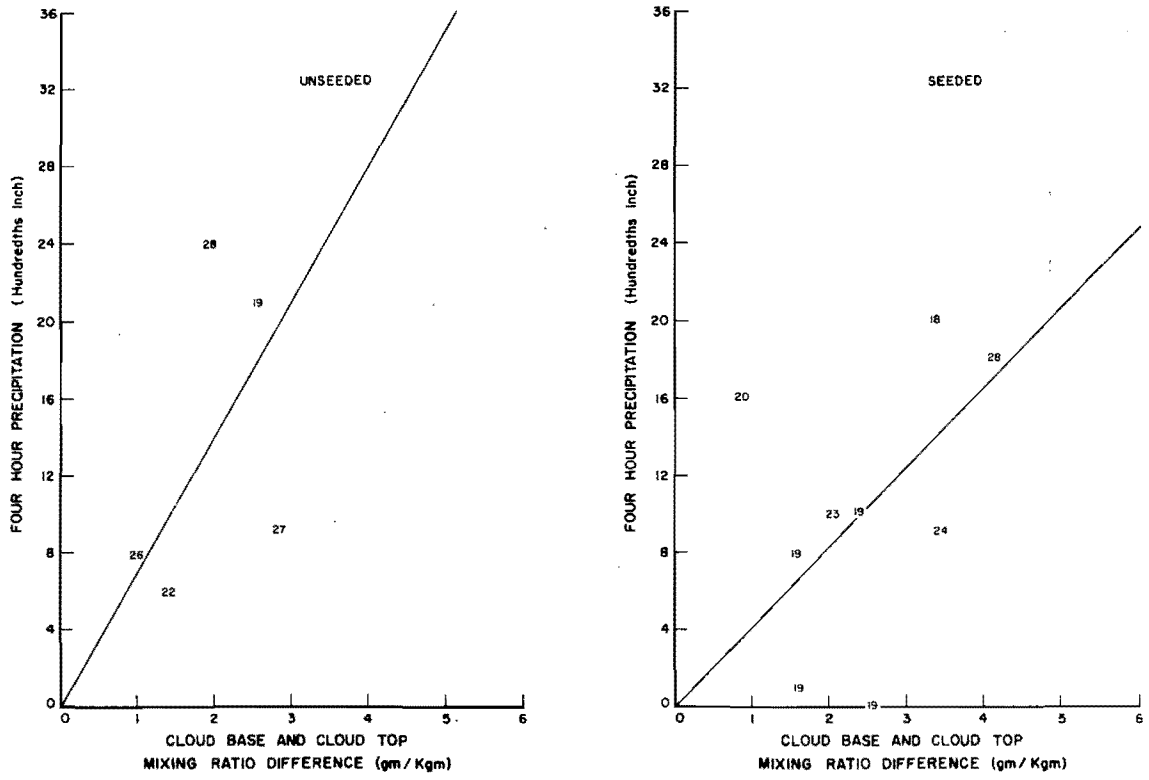

*Figure 28. Precipitation versus mixing-ratio parameter for unseeded and seeded frontal and cyclonic events in the **warm** cloud top temperature category. Numbers on the graph are (negative degrees Celsius) cloud top temperatures; italicized values refer to FY 72 nighttime data.*

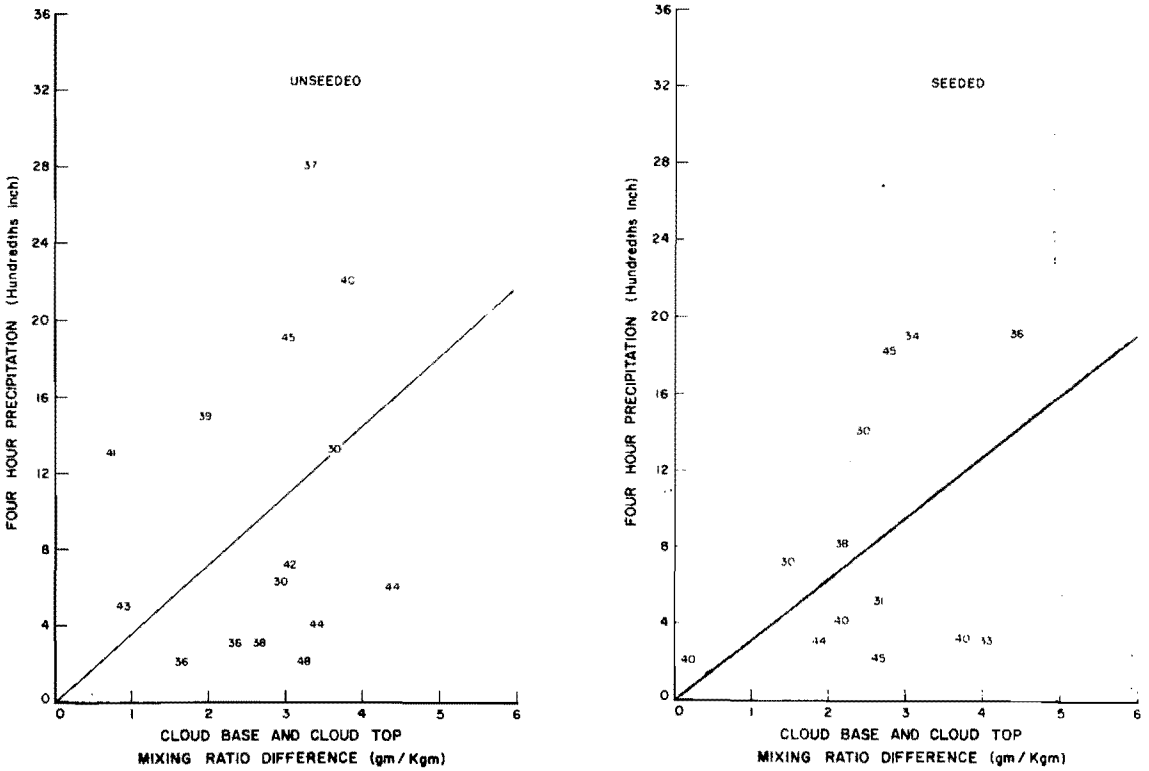

*Figure 29. Precipitation versus mixing-ratio parameter for unseeded and seeded frontal and cyclonic events in the **cold** cloud top temperature category. Numbers on the graph are (negative degrees Celsius) cloud top temperatures; italicized values refer to FY 72 nighttime data.*

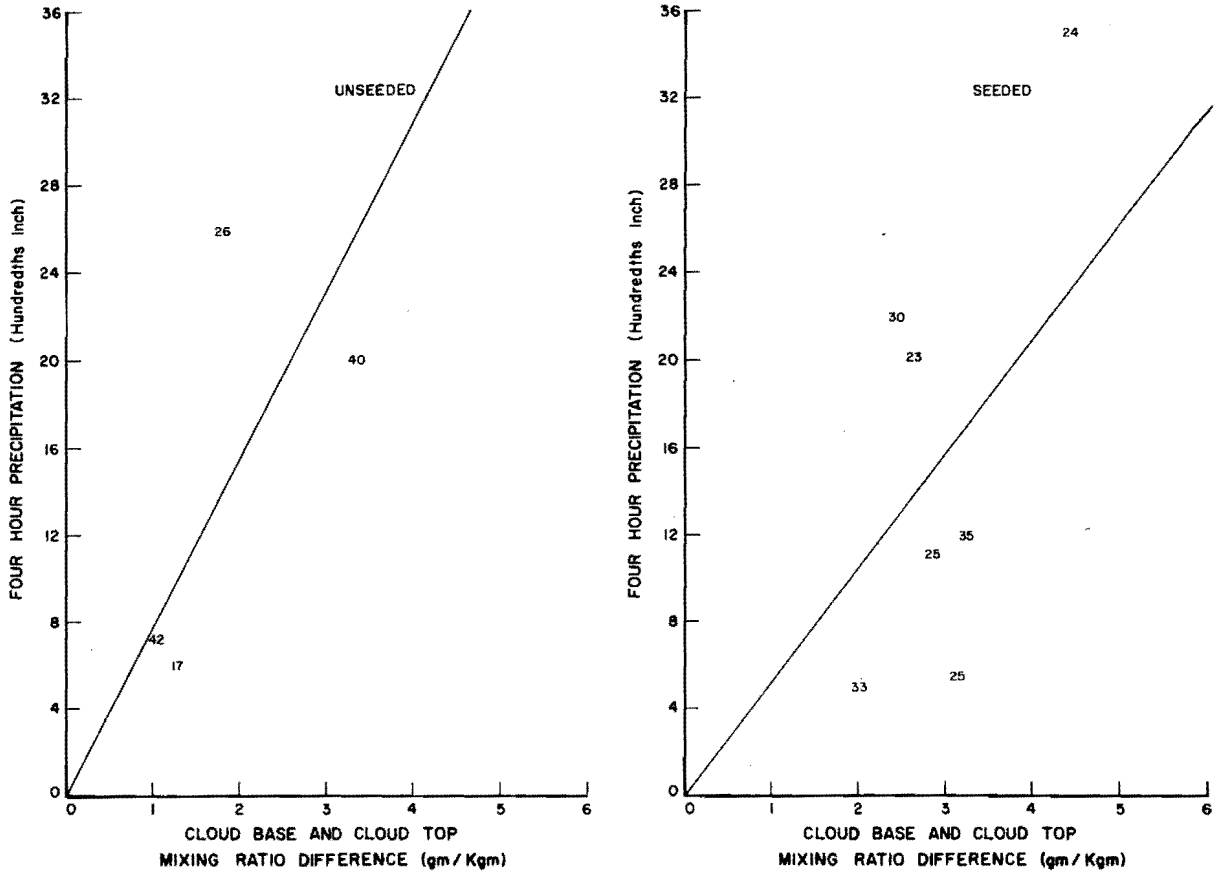

Figure 30. Precipitation versus mixing-ratio parameter for unseeded and seeded thunderstorm events in combined **warm** *and* **cold** *cloud top temperature categories. Numbers on the graph are (negative degrees Celsius) cloud top temperatures; italicized values refer to FY 72 nighttime data.*

type in the evaluation of seeding effectiveness. Here, the presence of thunderstorms increases both the precipitation and its variability over other categories and may tend to dominate the results if combined with other categories.

Because the orographic events may lend themselves to analysis by use of improved precipitation estimators, the mixing ratio difference is multiplied by the 2750 m (9000 ft) wind normal to the mountain-barrier axis to form a new estimator. It is written

$$\epsilon = (\text{CBMR} - \text{CTMR}) * \text{V} \quad \ldots\ldots\ldots\ldots\ldots\ldots\ldots\ldots (31)$$

where ϵ the precipitation estimator, CBMR and CTMR are the cloud base and cloud top mixing ratios, respectively, and V is the normal wind component. Values of the estimator for each event are included in Table 6. Again, the events are separated into a warm and a cold category. In the warm category the unseeded events have little potential for precipitation compared to the seeded events, as shown in Figure 31. Thus, the higher precipitation in the seeded events is accounted for by natural variability. In fact the unseeded precipitation appears to be higher than the seeded for a given estimator value, but this difference could well be due to the lack of data in the unseeded events at high values of the estimator. In the cold category, in which a similar distribution of estimator values is found in both the unseeded and seeded events, there is only a small difference in precipitation for a given estimator as shown in Figure 32. Thus the use of physically based improved estimators leads to an inconclusive seeding effect when cloud top temperature is used as a basis of stratification.

In summary of this subsection, we have found that in the analysis of the airborne seeding program, rawinsonde cloud top temperatures were greatly affected by the type of instrumentation. However, with the use of radar data from Hill AFB, a meaningful analysis could be conducted. By separating experimental events into storm types, it was found that when the use of a simple precipitation estimator was employed there was little difference between seeded and unseeded storms of the purely orographic type in either a warm or a cold cloud-top temperature category. Without the use of an estimator an apparent seeding effect occurred in the warm category, and to a lesser extent in the cold category.

Table 6. Aircraft orographic events.

Year	Case	S/U	CBMR	CTMR	ΔMR	V[a]	Estimator	Precip.[b]	RCTT
70	1-1	S	2.3	1.6	0.7	23	16	1	-17
	1-2	U	2.6	1.9	0.9	10	7	1	-15
	2-1	S	3.7	1.4	2.3	31	71	5	-22
	2-2	U	1.3	0.7	0.6	33	20	1	-30
	3-1	U	3.1	1.4	1.7	17	29	4	-24
	3-2	S	2.7	0.6	2.1	21	44	0	-35
	4-2	U	2.6	1.8	0.8	26	21	5	-16
	5-1	U	3.8	0.2	3.6	11	40	3	-44
	5-2	S	3.7	0.2	3.5	19	67	3	-43
	6-1	S	3.7	1.3	2.4	25	60	4	-22
	6-2	U	2.8	1.5	1.3	20	26	3	-19
	8-1	U	4.5	0.3	4.2	23	97	14	-43
	8-2	S	4.0	0.5	3.5	28	98	22	-36
	9-1	S	4.8	1.2	3.6	23	83	8	-25
	9-2	U	4.0	0.2	3.8	19	72	6	-44
	10-1	S	4.7	0.4	4.3	25	108	14	-41
	11-2	S	5.1	0.9	4.2	20	84	14	-29
	14-1	S	1.6	1.6	0.0	7	0	1	-18
	14-2	U	1.9	1.7	0.2	7	1	0	-17
71	4-2	S	3.9	0.9	3.0	21	63	3	-27
	5-1	S	3.3	0.2	3.1	9	28	6	-41
	5-2	U	1.7	0.5	1.2	13	16	3	-31
	12-1	S	1.1	0.2	0.9	30	27	5	-43
	12-2	U	0.6	0.4	0.2	32	6	0	-36
	13-1	U	2.2	1.2	1.0	11	11	3	-26
	13-2	S	2.6	0.6	2.0	10	20	1	-32
	14-1	U	2.1	2.0	0.1	15	2	0	-15
	14-2	S	3.0	2.9	0.1	15	2	0	-10
	15-1	U	2.2	0.2	2.0	23	46	2	-44
	16-1	S	3.3	1.4	1.9	30	57	0	-22
	16-2	U	4.2	3.1	1.1	30	33	1	- 9
	20-2	U	2.5	0.8	1.7	9	15	3	-27
	22-1	U	3.7	0.4	3.3	10	33	2	-36
	22-2	S	2.2	0.2	2.0	9	18	1	-44
	23-1	S	2.7	0.4	2.3	17	39	3	-35
	23-2	U	2.8	0.5	2.3	17	39	1	-33
	25-2	U	2.4	0.4	2.0	11	22	3	-36
	26-2	U	2.7	0.8	1.9	4	8	3	-28
	28-1	S	3.0	1.1	1.9	10	19	5	-24
	28-2	U	2.1	1.0	1.1	10	11	3	-23
	29-1	U	4.2	0.7	3.5	25	88	3	-34
	29-2	S	5.8	1.0	4.8	5	24	4	-28
	32-1	U	3.2	0.7	2.5	9	23	2	-31
	32-2	S	4.7	1.0	3.7	13	48	2	-27
	33-1	S	5.5	0.7	4.8	12	58	1	-32
72[c]	4-1	S	2.6	1.2	1.4	25	34	2	-19
	4-2	U	2.7	2.3	0.4	11	4	2	-10
	10-1	S	2.6	0.2	2.4	20	48	3	-44
	10-2	U	2.6	1.6	1.0	20	20	3	-16
	12-1	U	2.6	2.6	0.0	10	0	0	-11
	12-2	S	2.6	2.6	0.0	25	0	1	-11
	22-1	S	4.6	0.5	4.1	28	116	3	-33
	22-2	U	4.5	0.6	3.9	24	94	6	-32

[a]Night events only.
[b]Knots.
[c]Hundredths inch.

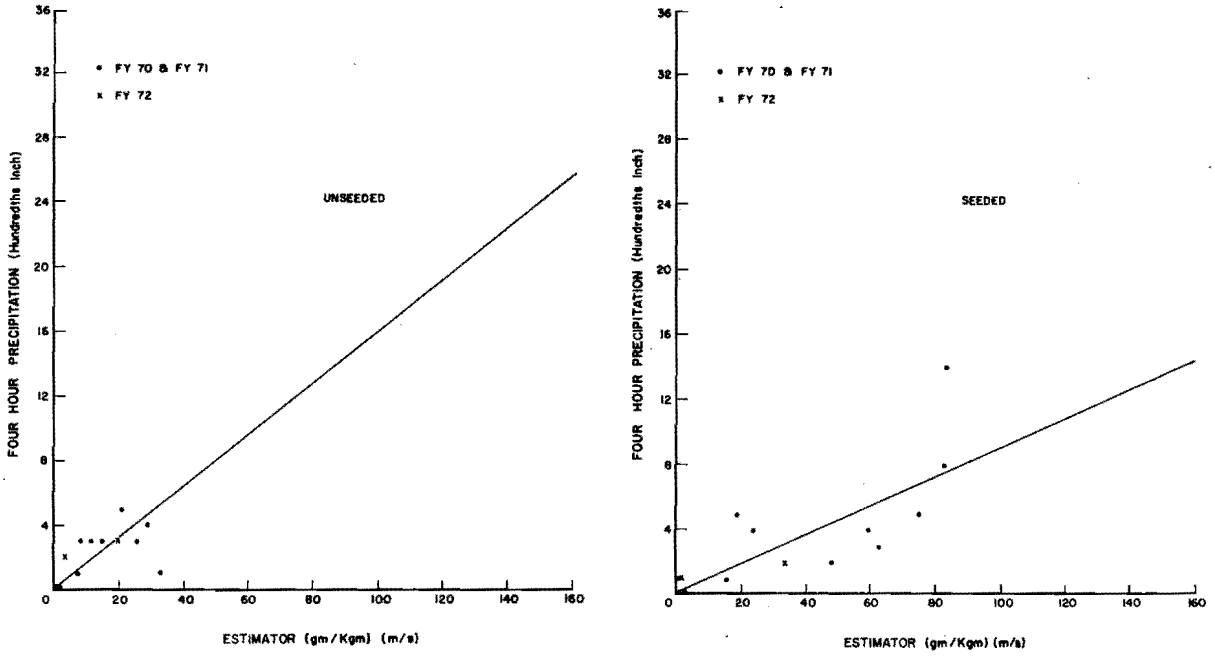

Figure 31. Precipitation versus orographic precipitation estimator for unseeded and seeded orographic events in the warm cloud top temperature category.

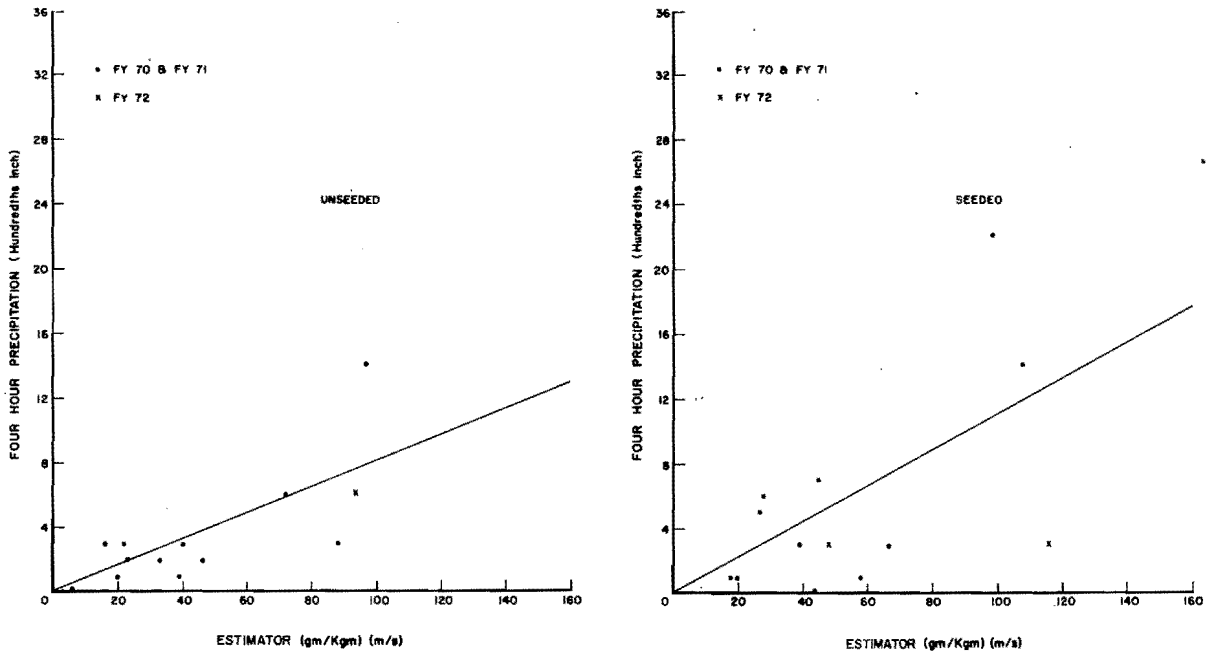

Figure 32. Precipitation versus orographic precipitation estimator for unseeded and seeded orographic events in the cold cloud top temperature category.

With events characterized by fronts, cyclonic systems, or thunderstorms, much greater amounts of precipitation fell compared to orographic storms. The variability of precipitation was far greater in the non-orographic storms compared to the orographic. These facts, along with the limited number of cases available, preclude any definitive statements about seeding effectiveness.

6.3.5 Analysis of Airborne Seeding Program with Supercooled Water Stratification. The use of a cloud-top temperature, as a means of identifying whether or not a seeding opportunity exists, has its basis in the number of active ice-nuclei present. With cold temperatures and large amounts of ice nuclei, the precipitation process would not be inefficient because of a lack of nuclei. Conversely, we would expect the warmer clouds to have supercooled water present and offer a possibility for seeding, so that the supercooled water could be converted to precipitation-size ice particles rather than evaporate on the other side of a mountain barrier.

One measure of the presence of supercooled water is the rate of aircraft icing in subfreezing temperatures. In the airborne seeding project records of flying conditions during seeding missions were kept. It is noted that this measure applies to the locality of the seeding tracks and not necessarily to the region of the mountain barrier. However, when significant amounts of supercooled water are present it is probable that insufficient numbers of ice crystals are present in comparison to the rate at which visible water is being formed. This condition is likely to be augmented by air forced to rise over the barrier.

The seeding aircraft was flown usually at around 11,000 ft (msl). At this altitude light to moderate or greater icing was reported during 14 events, listed in Table 7; in several events precipitation and/or other data were not available. (See Appendix A1 for a detailed list of icing reports.)

The cloud top temperatures associated with these events are given in Figure 33. The median cloud top temperature is -28°C. From these events it appears that large amounts of supercooled water occur with both warm and cold cloud-top temperatures. There is little doubt that with the cold cloud tops there are very large numbers of ice crystals present. But how

Table 7. Aircraft icing events: airborne seeding.

Year	Event	S/U	CTT	CBMR	CTMR	ΔMR	V	Estimator	Stand. Precip.	Non-Orog	Orographic Events With Full Data
FY 70[a]	8-1	U	-43	4.5	0.3	4.2	24	101	0.14		●
	8-2	S	-36	4.0	0.5	3.5	28	98	0.22		●
	11-1	U	-18	5.5	1.9	3.6	23	83	0.20	x	
	11-2	S	-29	5.1	0.9	4.2	20	84	0.14		●
	16-1	S	-45	3.3	0.2	3.1	19	59	0.19	x	
	16-2	U	-33	2.7	0.6	2.1	17	36	0.05	x	
FY 71[a]	2-1	S	-30	4.5	0.8	3.7	20	74	0.13	x	
	2-2	U	-24	4.6	1.1	3.5	20	70	0.09	x	
	14-1	U	-15	2.1	2.0	0.1	15	2	0.00		●
	14-2	S	-10	3.0	2.9	0.1	15	2	0.00		●
	15-1	U	-19	2.2	1.4	0.8	23	18	0.02		●
	15-2	S	-21	2.2	1.3	0.9	23	21	M		
	21-1	U	M	M	M	M	M	M	0.01	M	
	21-2	S	M	M	M	M	M	M	0.01	M	
	24-1	U	-19	3.3	1.7	1.6	13	21	0.08	x	
	24-2	S	-28	2.9	0.9	2.0	25	50	0.24	x	
FY 72[b]	3-1	U	M	M	M	M	M	M	M	M	
	3-2	S	M	M	M	M	M	M	M	M	
	15-1	U	M	M	M	M	M	M	0.07		
	15-2	S	M	M	M	M	M	M	0.07		
	16-1	S	M	M	M	M	M	M	0.09	x	
	16-2	U	M	M	M	M	M	M	0.11	x	
	18-1	S	-32	3.7[a]	0.6	3.1	20	62	0.02		
	18-2	U	-32	4.1[a]	0.6	3.5	20	70	0.03		●
	19-1	S	M	M	M	M	M	M	0.07		●
	19-2	U	M	M	M	M	M	M	M	x	
	26-1	S	-17	2.3	1.6	0.7	27	19	0.06	x	
	26-2	U	-35	4.0	0.7	3.3	14	46	0.12	x	

[a]Radar cloud data.

[b]Rawinsonde cloud data.

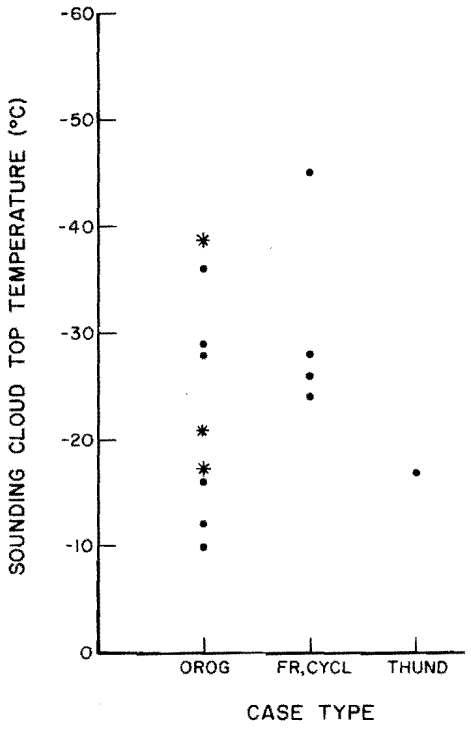

Figure 33. Cloud top temperatures and storm type for events with reports of at least moderate icing on the seeding aircraft.

many of these enter the lower levels in some instances is not known, especially during orographic uplift.

A comparison of precipitation during seeded events with light to moderate or greater aircraft icing conditions is made with the unseeded counterpart. There are no direct observations of icing during unseeded events. In Figure 34 the unseeded and seeded precipitation are plotted against a simple estimator, which is the product of the difference between the cloud base and cloud top mixture ratios and the 2750 m (9000 ft) wind normal to the mountain-barrier axis. Best fit lines for the orographic cases and for all cases are shown in the figure; the lines are forced through the origin.

For a given value of the estimator there is about 24 percent more precipitation in the seeded events than in the unseeded, when all events are considered. When only the orographic events are considered, the increase of precipitation in the seeded events is 40 percent. These results are not significant at the 10 percent level. While there yet may be a seeding effect present, there are only a relatively small number of events in the unseeded and seeded categories. However, analysis of ground seeding events will be found to support these results. Furthermore, the development of an improved estimator will be shown to yield results statistically significant at the 0.03 level when the ground and airborne seeding programs are combined.

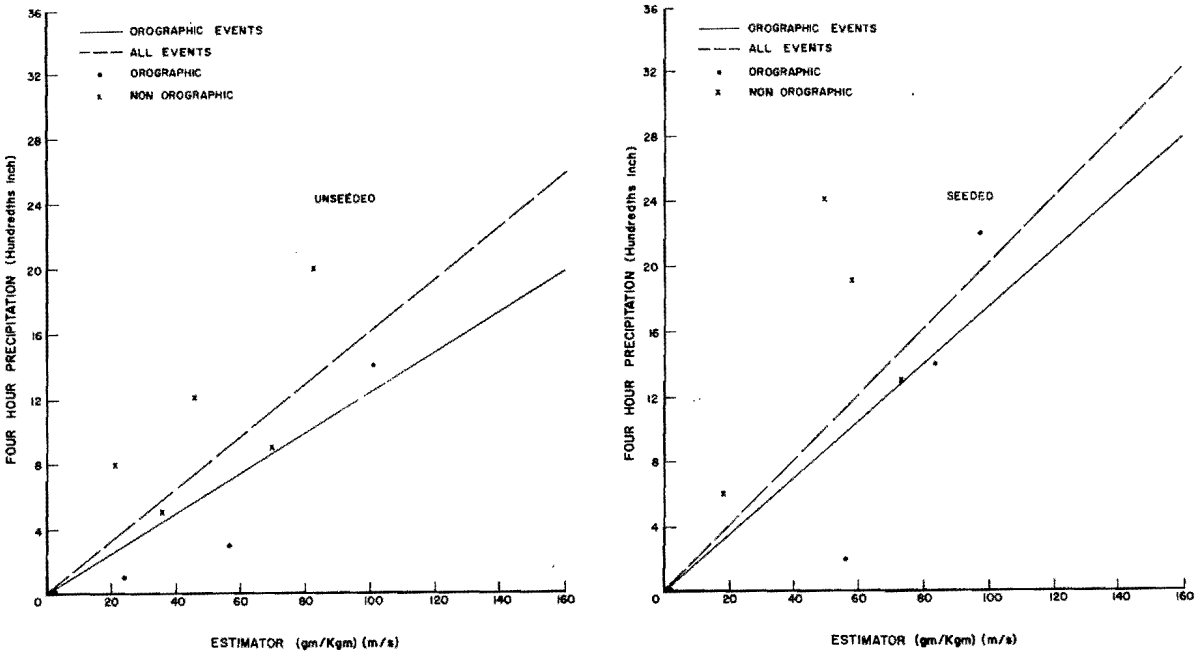

Figure 34. Precipitation versus orographic precipitation estimator for unseeded and seeded events for aircraft icing cases.

7.0 ANALYSIS OF SEEDING EFFECTIVENESS— GROUND SEEDING EVENTS

7.1 Experimental Design

7.1.1 Experimental Framework. Based upon a number of factors, most of which were derived from the experience gained from the aircraft seeding experiment, a new program using three mountaintop seeders was established (Hill, 1973). Seeding was to be carried out on a randomized basis, as before, but each event was either seeded or left unseeded for the entire period of the event. This change was necessary because the purge time of seeding material is presumed much longer with ground seeding than with airborne seeding.

In this experiment it was postulated that increased precipitation from seeding would be found in orographic clouds if the cloud ice top temperature were warmer than -28°C. This simple specification of the hypothesis implies several requirements. The term orographic was taken seriously; that is, frontal, cyclonic, and convective type storms were to be eliminated from consideration. Therefore, whenever any of these storm types were forecast, no event was called. Only when a period free of these storm types was forecast, was an event possible. Should a front or convective activity then occur during an event, the event was appropriately classified by objective means, which will be discussed later.

Another implied requirement was that rawinsondes would be released frequently, because the variability of cloud tops, and the humidity field in general, had been found previously to be rather high. Therefore, the releases were made at two hour intervals.

7.1.2 Measuring System. The measuring system for this project consisted for a network of telemetering precipitation gages and the automatic readout console, three remotely controlled mountaintop AgI generators, a rawinsonde tracking and recording unit, and meteorological data made available by outside agencies (Hill AFB radar, NAFAX weather charts and Service A teletype).

a) Precipitation Measuring System. Precipitation measurements for this experiment were taken from eleven stations out of the original larger network. These stations, shown in Figure 35, form two north south lines, approximately. The stations are mainly those at the highest elevations in the area. All of these stations were provided with protective sleeves, made from sewer liners. These liners were placed over the outside of the precipitation can so that ice and snow would not stick to it and be weighed in as precipitation, but fall off at a later time. In addition, at three stations, specially designed precipitation cans were developed and installed, so that additional checks on the quality of data could be made. In this design the whole outside portion of the can was separated from the can in which the precipitation actually accumulated and was weighed. Any precipitation sticking to the outside would not be weighed. The fully shielded gages had no cases with negative trends in the amount of catch, a problem symptomatic of weighed snow melting on the outside of a can. Comparisons between the fully shielded gages and those protected with sleeves showed that the sleeved gages performed well except in a very few instances.

In previous precipitation records it was evident that the weighing mechanism itself could be affected by a very slight bend in the internal support for the can, and a smooth increase in the weight of the can during precipitation was not found. Instead, a stepwise precipitation trace was obtained. The revised calibration procedures detected the presence of this difficulty. When it was found repairs were made. As a result of these two modifications, the sleeves and the surveillance and repair of the weighing mechanisms, a relatively good set of precipitation data was obtained.

b) Seeding Delivery System. To place seeding material into the clouds three mountaintop generators were operated. The seeder locations are also shown in Figure 35. The most northerly is Cache Peak, elevation 1738 m, then Pisgah, 2134 m, and Willard Mt., 2805 m. Numerous modifications to these seeders were made to improve reliability of operation.

In carrying out the experiment the three ground seeders were operated and monitored by remote control. Seeding events were chosen by first establishing whether a period was suitable for seeding and then it was decided randomly whether to seed or not. No restriction on the number of sequentially seeded or unseeded cases was made.

In cases where seeding was to be performed, the seeders were ignited 2 hours prior to the precipitation event. This procedure allowed seeding material to diffuse over a large portion of the network by the time precipitation was to be measured. Otherwise, the first 2 hours might have remained essentially unseeded over most of the network. The seeders remained on

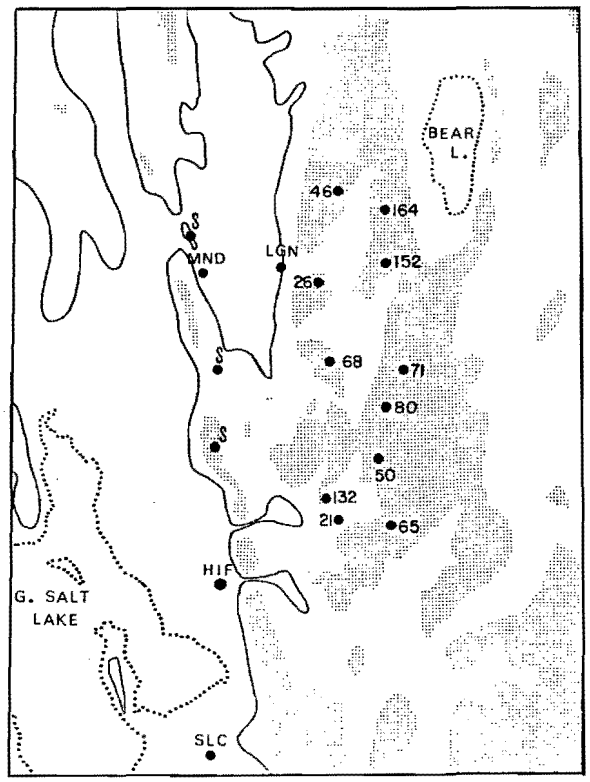

Figure 35. Network of precipitation stations and mountain top seeding generators for ground-based seeding experiment.

until the end of the precipitation event. No event was started until at least 24 hours had elapsed since seeding was last performed.

c) Upper-level Data Collection. An RD-65 rawinsonde unit was placed at Mendon. Two-hourly releases were made to obtain upper level data during storms. The first release was made at the start of an event and the last at the end of the event. Thus each two hour increment was bracketed by rawinsonde releases.

In addition to providing information on cloud tops, the rawinsonde data were used to form estimators of precipitation. Also, the data were used as an objective basis for identifying events with substantial convection.

d) Other Data. The Hill AFB TPQ-11 cloud detection unit operated during most of the events of this experiment. Additional information on the variability of cloud top temperatures was obtained. Further comparisons with rawinsonde cloud top temperatures were also made. These aspects of the project will be discussed in Section 7.2.

National Weather Service facsimile charts and Service A teletype data were obtained on a continuous basis. This information was used in forecasting suitable events. The criteria for declaring an event were that the forecast precipitation be primarily orographic, the surface to 500 mb relative humidity exceed 70 percent, and the wind direction at both 700 mb and 500 mb be between 220 and 320 degrees.

7.1.3 Classification of Events. Precipitation was considered orographic unless either a front, a cyclonic system, or convection was present. A front was considered present if it was within 40 miles of any of the precipitation gages or the rawinsonde site. The position of fronts, nearly always cold fronts, was well marked by the rapid wind shift accompanying its passage. Hourly and special observations at Pocatello, Malad, Hill AFB, and at the Mendon or Logan sites along with the facsimile charts were used to track the fronts.

The occurrence of convection could have been noted from visual reports, at least during the daytime. However, at night only the presence of thunderstorms was evident. The occurrence of cumulonimbus might not have been detected by visual means. In fact, on occasion observations of cumulus congestus or cumulonimbus were made in the field but were not reported on any of the National Weather Service data sources. For these reasons, an objective technique was developed to exclude cellular convection.

The method for excluding convective cases utilizes the rawinsonde data. Because in the presence of cellular convection the rawinsonde humidity data are likely not to be representative of the surrounding moisture field, it is first assumed that all soundings are at saturation. Then a parcel of air is lifted moist adiabatically until the parcel's temperature is not greater than the temperature of the sounding. In some cases no lifting is required, because immediately the lifted parcel is colder than the temperature of the sounding. In this case no convection is present, according to stability arguments. When the lifted parcel is warmer than the sounding value, the area on the thermodynamic diagram is measured. The greater the area the more intense the convection should be. This method, of course, assumes saturation, an assumption which may not always hold. In that situation an event, in which no convection existed, might be excluded. This exclusion presents no special problem, other than a loss of data. The important point is that the method detects convection even if the sounding is taken in between large cells, a condition which is often the case.

In finding the area on the thermodynamic chart, parcels are lifted from two different levels, 800 mb and 750 mb. The parcel with the maximum area is selected to represent the potential for convection. This index of convection potential for each case is given in Table 8, along with other information such as with the airborne experiment. In the ground seeding experiment, about 750 gms of silver iodide were released for each event through March 10, 1975. Subsequently, about 450 gms were released for each event.

Table 8. Ground seeding events. A: Fiscal Year 1974.

Case	2 Hour Periods	S/U	Start Date	Period MST	Case Type / Conv. Index	Precip West	Precip East	Radar RCTT	Rawinsonde CTT	CBH	CTH	Wind 9K
1	1	S	Nov. 27	1400	OROG	0.2	1.0	M	-13*	8	12*	290/30
	2			:	8	0.0	1.0	M	-13*	8	11*	289/28
	3			:		0.0	0.2	M	-11*	8	10*	299/26
	4			2200		0.0	0.4	M	-10*	9	10*	276/25
2	1	U	Dec. 12	0100	OROG	5.0	6.2	M	-15	8	12	282/28
	2			:	60	0.4	1.2	M	-16	9	11	287/22
	3			:		0.0	0.2	M	-16	10	11	280/14
	4			0900		0.0	0.0	M	-13	10	10	264/19
3	1	S	Dec. 13	0000	OROG	0.2	0.2	M	V	V	V	233/33
	2			:	3	0.0	0.0	M	-45	14,20	32+	228/32
	3			:		0.4	0.0	M	-47	14	32+	235/37
	4			0800		0.2	0.2	M	-48	13	32+	241/44
4	1	U	Dec. 22	0000	OROG	0.0	0.0	-29	- 9	8	12	214/25
	2			:	34	0.0	0.2	-44	-11	8	14	213/22
	3			:		1.4	1.7	-54	-15	8**	16	211/18
	4			0800		0.0	0.3	-18V	-15	8	15	212/18
5	1	U	Dec. 22	1830	OROG	6.8	2.3	-25	-29	7	19	307/33
	2			:	66	2.2	2.3	M	V	8	V	316/24
	3			:		0.6	1.3	M	-14	8	11	318/23
	4			0230		1.4	1.0	M	-18	8	12	316/25
6	1	S	Dec. 28	1430	OROG	0.4	0.7	M	V	V	V	301/44
	2			:	88	0.2	0.2	-41	-13,-31	8,21	10,23	296/36
	3			:		0.0	0.2	-44	-12,-31	8,18	9,22	286/29
	4			2230		0.0	0.3	-38	-16,-33	8,16	11,23	272/17
7	1	S	Dec. 29	1500	FR/C	14.0	12.3	M	V	V	V	294/58
	2			:	133	4.0	4.7	M	V	V	V	305/50
	3			:		4.8	8.0	M	V	V	V	303/41
	4			2300		7.2	11.7	M	V	V	V	299/41
8	1	S	Jan. 7	0900	OROG	6.8	4.0	-19	-31	5	18	250/26
	2			:	7	4.8	14.0	-19	-30	5	17	261/29
	3			:		6.5	9.7	-25	-25	5	15	264/27
	4			1700		3.8	4.7	-25	-25	5	15	266/27
9	1	S	Jan. 12	0500	OROG	1.8	1.0	-31	-46	7	32	253/30
	2			:	0	1.3	1.2	-24	-18*	5	16*	261/33
	3			:		2.8	1.8	-18	-16	5	15	270/35
	4			1300		5.3	2.5	-12	-15	5	15	268/33
10	1	S	Jan. 13	1230	OROG	22.8	14.7	-37	-48	7	30	270/39
	2			:	15	13.5	15.3	M	-10	9	12	279/29
	3			:		4.8	5.7	-15	- 9	9	11	277/25
	4			2030		1.3	1.3	-12	- 8	10	11	M
11	1	U	Jan. 17	0330	FR	8.0	4.8	-30V	-31	6	23	238/15
	2			:	6	7.3	9.0	-31V	-26	6	21	287/16
	3			:		2.3	3.8	-29V	- 8	6	12	312/17
	4			1630		0.5	0.5	-19V	- 7	7	10	311/18
12	1	S	Jan. 19	0930	OROG	8.0	5.5	-28	-11	5,10	13	286/18
	2			:	19	4.8	3.8	M	-12	11	13	280/16
	3			:		1.3	1.3	M	-13	7	14	267/14
	4			1730		2.3	0.8	M	-23	8	18	264/14
13	1	U	Jan. 20	1600	OROG	2.3	2.0	M	V	V	V	336/12
	2			:	2	2.5	1.0	M	V	V	V	345/13
	3			:		2.5	2.5	M	-48	6	28	341/13
	4			0000		3.5	3.0	M	-50	6	28	325/15
14	1	S	Jan. 25	1700	OROG	0.3	1.5	-20	-21	6	14	272/19
	2			:	43	1.3	2.2	-19	-29	6	18	283/20
	3			:		15.5	9.0	-29	-36	6	21	292/20
	4			0100		13.0	11.2	-38	-47	9	25	289/21
15	1	U	Jan. 27	1530	OROG	0.6	0.7	-12	-12	7	12	279/25
	2			:	4	2.4	2.8	-19	-25	7	19	272/28
	3			:		2.6	4.7	-38	-54	7	30	281/27
	4			2330		1.8	3.0	-35	-55	8	30	286/25

Table 8. Continued. A: Fiscal Year 1974.

Case	2 Hour Periods	S/U	Start Date	Period MST	Case Type Conv. Index	Precip West	Precip East	Radar RCTT	Rawinsonde CTT	CBH	CTH	Wind 9K
16	1	U	Jan. 31	1430	OROG	10.8	7.0	-28	-28	7	24	259/41
	2			:	3	12.4	8.6	-27	-44	7	30	254/37
	3			:		19.4	13.0	-31	-45	7	33	257/32
	4			2230		24.0	18.0	-39	-36	7	25	262/37
17	1	U	Feb. 17	0930	OROG	1.2	0.5	-23	S	S	S	320/12
	2			:	43	0.8	0.7	M	S	S	S	322/8
	3			:		0.6	1.5	M	-14	9	10	323/9
	4			1730		0.6	0.2	M	S	S	S	328/13
18	1	U	Feb. 19	0600	FR	21.2	16.8	M	-45	5	31	263/37
	2			:	38	24.6	14.8	M	-15*	5	14*	274/28
	3			:		20.8	18.0	M	S	S	S	299/24
	4			1400		15.6	12.7	M	S	S	S	313/28
19	1	S	Feb. 22	1100	C	10.0	9.2	-38	V	V	V	298/25
	2			:	183	7.6	7.8	-36	V	V	V	299/25
	3			:		3.2	6.5	-37	-43	14	20	299/28
	4			1900		2.0	3.2	-26	-42	16	19	304/29

Table 8. Continued. B: Fiscal Year 1975.

Case	2 Hour Periods	S/U	Start Date	Period MST	Case Type Conv. Index	Precip West	Precip East	Radar RCTT	Rawinsonde CTT	CBH	CTH	Wind 9K
1	1	U	Feb. 7	1000	OROG	1.4	3.3	-17	-35	8	25	274/27
	2			:	27	3.2	2.0	-17	-14,-38	8	14,25	270/25
	3			:		1.6	0.5	-17,-38	-12	8	12	272/24
	4			1800		0.6	0.5	-20	-14	9	13	271/24
2	1	U	Feb. 9	1730	C	0.2	0.8	-32	S	S	S	265/22
	2			:	457	2.4	3.3	-41	-30	17	20	264/24
	3			:		5.0	4.3	-29	-29	16	20	259/23
	4			0130		4.6	4.8	M	V	6	V	240/27
3	1	U	Feb. 12	0900	OROG	0.0	0.0	V	-47	12	32	239/27
	2			:	76	0.2	0.2	-47	V	12	V	227/27
	3			:		0.0	0.2	-41	S	S	S	224/28
	4			1700		0.0	0.0	-42	V	15	V	235/27
4	1	S	Feb. 19	1700	OROG	2.4	1.2	-43	-53	S	32	241/26
	2			:	52	8.6	5.3	-45	-50	6	32	239/28
	3			:		7.2	6.2	-47	-52	5	32	248/30
	4			0100		14.2	12.7	V	-51	6	28	250/31
5	1	U	Feb. 27	0830	OROG	0.2	0.0	-10	- 9	5	11	290/12
	2			:	9	0.8	0.3	-10	- 9	5	11	290/12
	3			:		1.2	0.2	-10	-10	7	12	290/13
	4			1630		1.6	0.2	-11	- 9	8	11	293/16
6	1	U	Feb. 28	1000	OROG	5.2	3.2	-16	- 7	7	13	280/22
	2			:	47	1.2	1.5	-19	-20	8	19	287/19
	3			:		0.0	0.8	-18	-18	17	18	299/14
	4			1800		0.4	0.2	S	-17	17	18	306/12
7	1	S	Mar. 6	1100	C	7.6	6.5	-17	-13,-22	11	13,17	259/23
	2			:	390	5.4	3.8	-12	-22	12	17	250/21
	3			:		3.0	3.8	V	V	V	V	234/16
	4			1900		4.4	2.7	V	V	7	V	234/16
8	1	U	Mar. 10	0500	C	5.6	1.5	-13	-10*	6	10*	252/7
	2			:	121	7.6	1.0	M	- 8*	6	9*	269/6
	3			:		4.6	4.2	M	- 4*	6	7*	272/4
	4			1300		0.8	2.2	-18	S	S	S	248/3

Table 8. Continued. B: Fiscal Year 1975.

Case	2 Hour Periods	S/U	Start Date	Period MST	Case Type	Precip West	Precip East	Radar	Rawinsonde			
					Conv. Index			RCTT	CTT	CBH	CTH	Wind 9K
9	1	S	Mar. 16	1600-	OROG	6.5	5.0	M	S	S	S	309/19
	2			2000	33	4.8	1.3	M	-40	10	22	312/20
10	1	U	Mar. 17	2030-	OROG	0.6	0.3	V	-12	10	13	259/23
	2			0030	32	1.6	1.0	V	-27	9	20	265/23
11	1	S	Mar. 20	1045-	C	1.5	2.2	-17	-17	14	15	252/17
	2			1445	223	1.5	0.8	M	-21	14	17	257/15
12	1	S	Mar. 21	1815-	C[a]	1.0	2.5	-42	-45	V	29	218/29
	2			2215	1196	2.0	0.8	-48	-50	V	31	207/31
13	1	S	Mar. 22	0915-	C	18.2	12.4	V	S	S	S	292/19
	2			1315	190	5.8	7.4	V	S	S	S	282/19
14	1	S	Mar. 24	0845-	OROG	1.4	0.8	-15V	-11	7	11	291/21
	2			1245	42	1.6	0.7	-15V	-14	7	12	294/20
15	1	S	Mar. 25	0545-	CYCL	20.4	13.2	-45	-48	6	31	230/28
	2			0945	15	26.6	17.5	-45	-13*	7	15*	220/21

[a]No convection observed; this is the only case excluded by the index of potential convection, wherein no convection was observed.

Table 8. Continued. C: Fiscal Year 1976.

Case	2 Hour Periods	S/U	Start Date	Period MST	Case Type	Precip West	Precip East	Radar	Rawinsonde			
					Conv. Index			RCTT	CTT	CBH	CTH	Wind 9K
1	1	S	Feb. 8	2000-	OROG	15.0	12.2	M	-48	5	32	238/24
	2			0000	23	10.8	9.8	M	-49	8	32	236/24
2	1	U	Feb. 14	1300-	OROG	6.3	4.0	V	-13	9	12	253/34
	2			1700	17	1.5	1.6	V	-15	8	13	257/28
3	1	S	Feb. 15	1230-	C	8.5	6.8	-28	-25	13	17	289/25
	2			1630	107	3.3	1.6	-21V	-20	12	14	289/17
4	1	U	Feb. 16	1400-	OROG	8.3	9.4	-39	-48,-12	7	32,13	258/34
	2			1800	1	7.3	2.8	-32,-13	-16	8	14	267/35
5	1	S	Feb. 19	2000-	OROG	3.3	2.6	-25	-16	9	10	294/11
	2			0000	51	1.3	0.6	S	-18	7	11	326/13
6	1	S	feb. 28	2230-	FR,CYCL	7.3	5.3	-25	-51	5	32	255/33
	2			0230	1	7.0	7.8	-24	V	5	V	255/35
7	1	U	Mar. 1	1445-	OROG	10.3	10.7	-47	-47	6	27	278/22
	2			1845	2	4.8	7.3	-47	V	5	V	279/22
8	1	U	Mar. 14	1200-	FR/C	16.0	17.3	-26	S	S	S	297/24
	2			1600	115	6.3	5.5	M	-15	9	12	303/23
9	1	S	Mar. 19	0700-	C	6.3	6.5	-21*	-40	11	21	293/21
	2			1100	233	2.0	0.0	-20*	-21*	10	12*	295/21
10	1	U	Mar. 27	1315-	OROG	2.7	3.7	-28	-19	11	14	291/13
	2			1715	35	2.3	0.0	-35	-20	12	14	296/18

M Data missing.
S No cloud layer detected.
V Highly variable.
* Cloud layer above.
** Thin cloud layer below.

During the course of the program, it became evident that events of about four hours would be more appropriate for analysis. The typically strong variations over an eight hour interval preclude the characterization of an event by a single value of a parameter such as cloud top temperature. In many instances the second half of an event was greatly different from the first half. Therefore, it was decided to split the eight hour events into two parts and proceed to collect subsequent data in four hour units.

7.2 Analysis of Seeded and Unseeded Events

7.2.1 Radar Versus Rawinsonde Cloud Heights and Temperatures. The Hill AFB vertical incidence radar unit and the Mendon rawinsondes provide independent sources of cloud top heights and temperatures. A comparison of data obtained by the two methods, therefore, is desirable. In this comparison both data sets consist of four hour averages.

Values of cloud top temperature for the two methods for all four hour periods with available data are shown in Figure 36. There is an apparent relationship between the cloud top temperatures determined by the different methods, but there is a large scatter of data. Presumably, the scatter could be due to differences in the method or to natural variability of the cloud top distribution. For example, the convective events, which are circled in the figure, are widely scattered. Furthermore, an inspection of Table 8 reveals that there is a large time variation of cloud top temperatures within each event for both methods.

To reduce this natural variability only the cloud top temperatures are compared for orographic events with single layer structure, and relatively low time variation of cloud tops as determined by either method. These cloud top heights are shown in Figure 37 and the cloud top temperatures in Figure 38. It is clear from these figures that there is a well defined relationship between the radar and rawinsonde cloud top heights and temperatures. In general the rawinsonde temperatures are about 10°C colder for the very coldest clouds; there is about a one to one for the very coldest clouds; there is about a one to one correspondence for the warmest clouds. One notable exception to the relationship is case 74-4a; further inspection of related data indicates that the clouds were deeper over Hill AFB than in the vicinity of the rawinsonde site.

The main systematic difference between the two cloud top temperature determinations may be explained by at least two reasons. One is that radar signals are attenuated roughly in proportion to the depth of the cloud. Thus, the radar cloud top temperatures would be warmer than the rawinsonde temperatures. Another reason is that whereas the Hill AFB soundings are upwind of the mountains, the rawinsondes are closer or even over the mountains by the time the package reaches cloud top heights. With lifting occurring in the vicinity of the mountains the rawinsonde cloud top temperatures would be colder than the radar temperatures. The vertical motion required for this change in cloud top can be easily estimated. For example, with a humidity of 75 percent of ice saturation at a temperature of -45°C, a vertical velocity of around 15 cm sec^{-1} over a half hour period is needed to produce ice saturation.

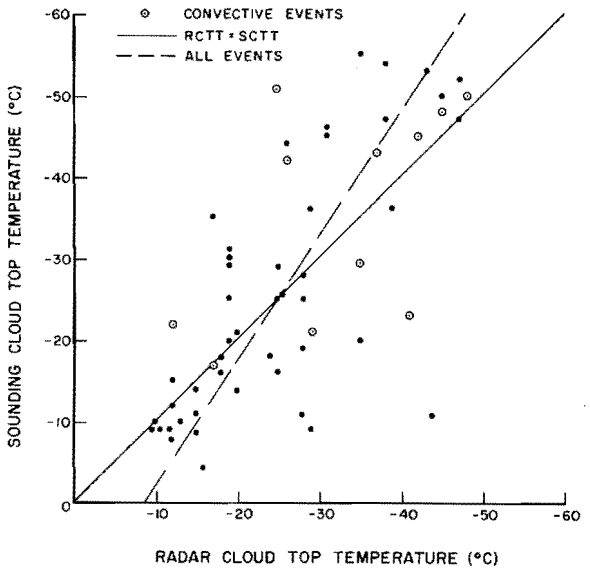

Figure 36. Radar and rawinsonde cloud top temperatures.

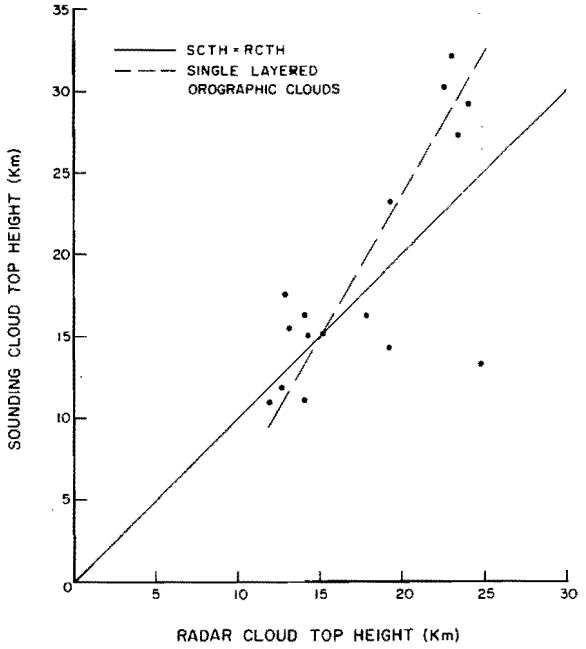

Figure 37. Cloud top heights in orographic, single-layered clouds from radar and rawinsondes.

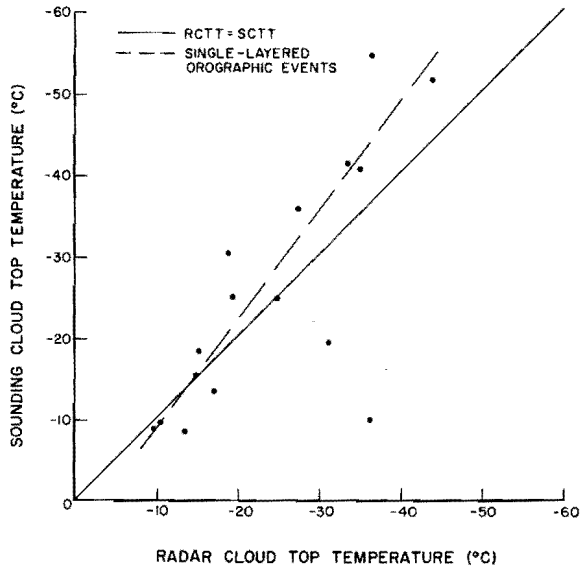

Figure 38. Cloud top temperatures in orographic, single-layered clouds from radar and rawinsondes.

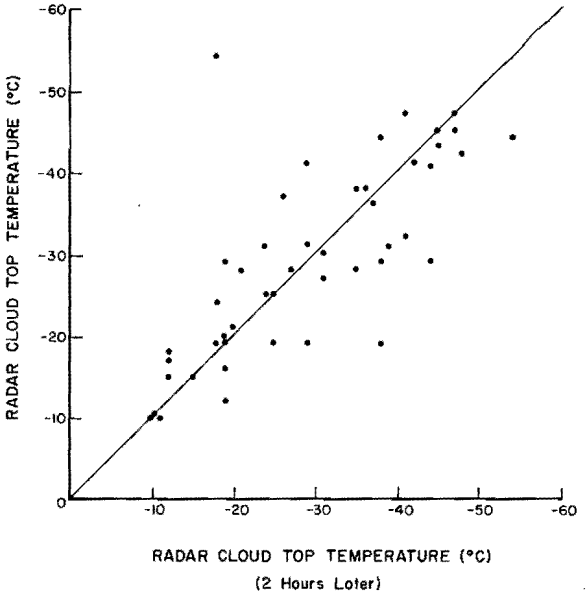

Figure 39. Radar cloud top temperatures at successive two hour intervals.

Of the two reasons for the differences, the latter is likely to be the responsible one. Higher cloud tops over the mountains compared to those over locations just upwind of the mountains are commonly observed. Furthermore, attenuation of signals from the TPQ-11 radar over the distances involved is probably of little consequence.

7.2.2 Cloud Top Temperature Variability. If it is indeed the cloud top temperature that identifies suitable clouds for seeding, an analysis of the space-time variability is desired. It has already been found that when rawinsonde and radar cloud top temperatures are compared from measurements at stations about 70 km apart and in a variety of meteorlogical cloud types, the correspondence is poor. But when only single layer orographic clouds are considered the relationship is greatly improved. Thus, the wide scatter of the full data set indicates strong natural variability over the distance between stations. To eliminate differences in cloud top temperature due to location and method, a comparison of radar cloud top temperatures at successive two-hour periods is made. These data are shown in Figure 39. The standard deviation of the two-hour average cloud top temperature from the two previous hours for the locations of Hill AFB is 6°C. These two-hourly values are average values, so some smoothing of the natural variability has already been made. Furthermore, pairs of two-hourly periods in which no radar cloud top temperature was reported in either period, due to scattered cloud conditions, are not included in the analysis. Therefore, whatever variability is found represents an underestimate of cloud top temperature variability.

A similar comparison may be made for the rawinsonde cloud top temperatures; these data are shown in Figure 40. Here the standard deviation of the two-hour change is about 5°C. However, the overall scatter is larger for the rawinsonde data than the radar data. The difference in scatter is probably due to the reporting procedures; with scattered or broken cloud cover the radar cloud tops are often not reported. Thus, instances with large changes in cloud top heights, such as during clearing conditions, may

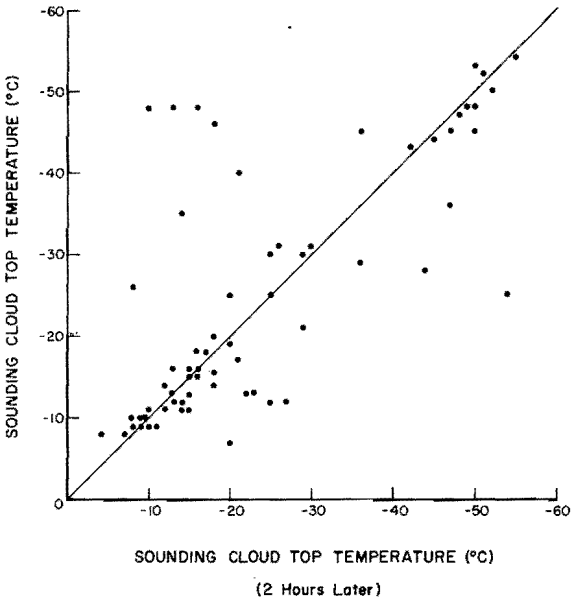

Figure 40. Rawinsonde cloud top temperatures at successive two hour intervals.

not be reported in the radar data. In any case the standard deviation of cloud top temperatures for well defined clouds is around 5°C or 6°C for two-hourly changes. For longer periods than two hours the change in cloud top temperature is much larger. For four-hour changes of the two-hour averages of rawinsonde cloud top temperatures, the standard deviation is about 13°C. Data for these cases, derived from Table 8, are shown in Figure 41. For a six-hour change the standard deviation increases to about 22°C, although this deviation is based upon a relatively small sample, as shown in Figure 42. A graph of these standard deviations of two-hourly averages of cloud top temperatures for the various time periods is shown in Figure 43. It is clear that as the time span increases, the cloud top temperature undergoes increasingly large variations. We may conclude that substantial changes in cloud top temperature occur over relatively short periods of time; in other words cloud top temperatures used as a guide for cloud seeding potential should be determined at intervals no greater than about two hours.

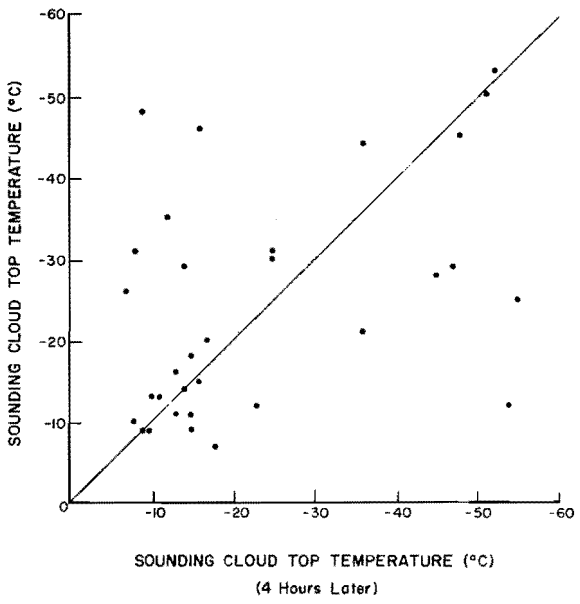

Figure 41. Rawinsonde cloud top temperatures at successive four hour intervals.

7.2.3 Cloud Seeding Potential. The use of cloud top temperature for identifying cloud seeding potential is, of course, related to the concentration of ice particles, which grow at the expense of supercooled water. The presence of supercooled water may indicate a deficiency in the concentration of ice particles. With cold cloud tops there is likely to be an abundance of ice particles, and consequently, very little supercooled water. Conversely, with relatively warm cloud tops, in excess of -25°C for example, there may be a deficiency in the ice particle concentration and supercooled cloud droplets could be sustained. Thus, the cloud top temperature is used as an index of

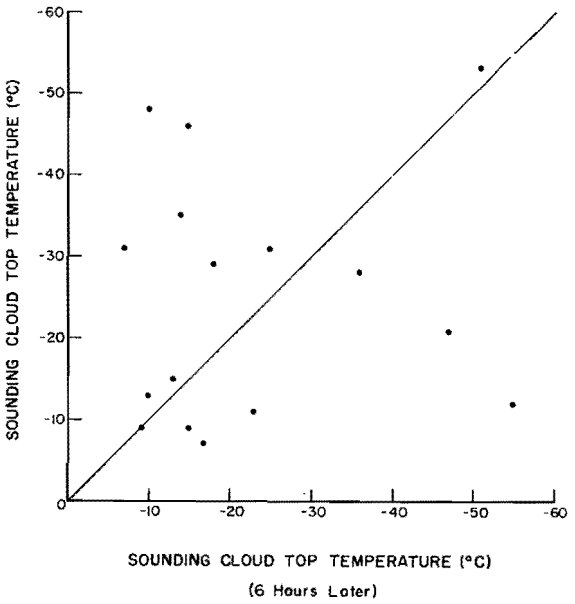

Figure 42. Rawinsondes cloud top temperatures at successive six hour intervals.

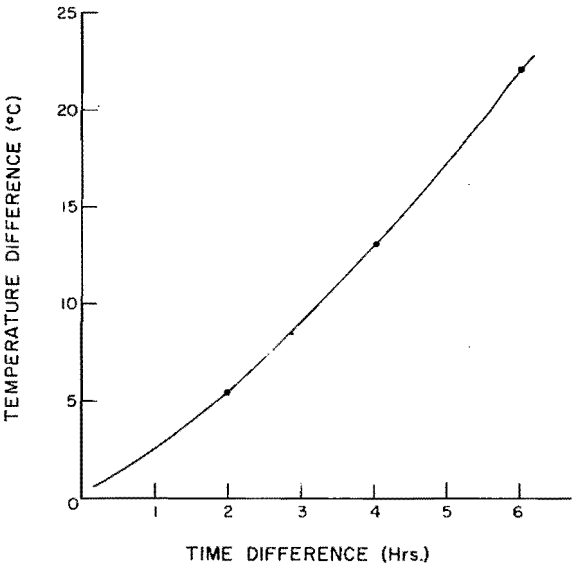

Figure 43. Standard deviation of two hourly averages of cloud top temperatures versus time.

the ice crystal concentration, which in turn affects the amount of supercooled water.

Direct measurements of the ice crystal and supercooled water concentrations would be preferable. There are various quasi-direct measurements of supercooled water available. One such is based upon reports of aircraft icing. These reports give qualitative measurements of the icing rate, which is a crude measure of the concentration of supercooled water.

To estimate the concentration of ice crystals, precipitation amounts over specified intervals may be used. That is, high precipitation rates would correspond to high amounts of ice within a cloud system and low precipitation rates would correspond to low amounts.

In this analysis, four-hour periods were used, two from eight-hour events and one from four-hour events. Aircraft icing reports were plotted on time-height charts and each four-hour period classified into categories of icing varying from none, very light, light, light to moderate, moderate, moderate to heavy, and heavy; a corresponding numerical value ranging from 0 to 6 was assigned to each period. These icing rates are shown as a function of rawinsonde cloud top temperature in Figure 44. Cases with scattered clouds, or thicknesses of 600 m (2000 ft) or less were omitted, because aircraft could easily fly outside of such clouds. There appears to be a very slight trend toward increased icing for the warmer cloud tops. This trend is in spite of the generally thinner clouds sometimes found with the warmer, or lower, clouds.

To obtain an overall measure of seedability the aircraft icing rate is divided by the four-hour precipitation amount. This ratio is an index of the ratio of supercooled water concentration to the concentration of ice particles. The seedability indices for four-hour periods with available data are shown in Figure 45 as a function of the rawinsonde cloud top temperature for unseeded and seeded cases. The trend toward increased seedability at warmer cloud top temperatures is evident. Out of all the unseeded events, about 15 percent of the precipitation fell when the seedability index was equal to 0.5 or greater. If by seeding in these cases the amount of precipitation were doubled, the overall increase in precipitation would be 15 percent. Of course, the actual increase in precipitation for these events is not known, but a doubling for particular individual events is not unreasonable.

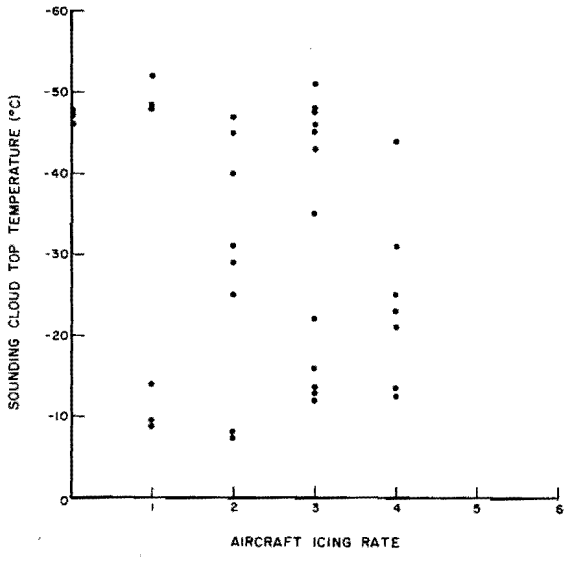

Figure 44. Aircraft icing rate versus rawinsonde cloud top temperature.

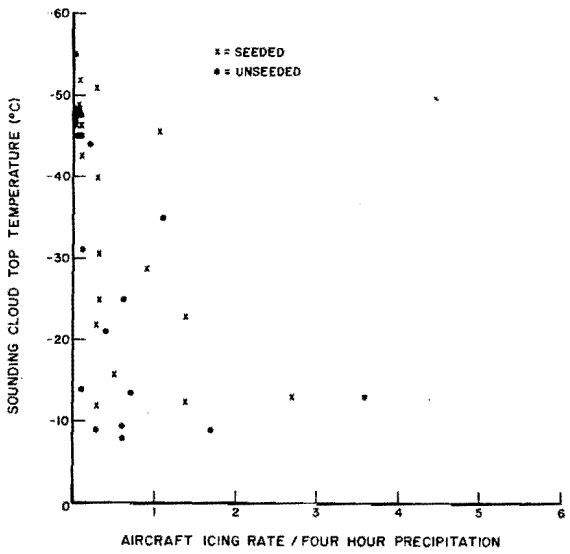

Figure 45. Aircraft icing rate divided by four hour precipitation versus rawinsonde cloud top temperature.

7.2.4 Use of Precipitation Estimators and the Analysis of Seeding Effects. To reduce the uncertainty of precipitation due to natural variations, use of precipitation estimators is made. Available meteorological parameters are those derived from rawinsonde data. As before, the difference in cloud base and cloud top mixing ratio is multiplied by the 2750 m (9000 ft) wind normal to the mountain-barrier axis.

A tabulation of data for four-hour periods is given in Table 9 for events designated as orographic but with single cloud layers and not highly variable. All unseeded orographic events listed in Table 8 in which two consecutive entries appear with numerical values of the required parameters were used to develop the predictor. In Table 9 four-hour averages of cloud-base and cloud-top mixing ratios, the cloud top temperature, wind, and precipitation are given.

An improved relationship between the precipitation estimator and precipitation is obtained if the linear estimator is squared. Or, another equivalent relationship is found by using the fourth root of the precipitation and the square root of the linear estimator. This approach is preferable because the distribution of the fourth root of precipitation is nearly normal (Lopez and Nason, 1967). For this reason, results are given with precipitation to the fourth root along with the square root of the precipitation estimator; that is $p^{.25}$ is compared with $\epsilon^{.5}$.

Table 9. Single layered orographic clouds (with available data).

Year	Case	S/U	CBMR	CTMR	ΔMR	V	Estimator	Precip.	SCTT
74	2a	U	2.5	1.3	1.2	24	29	6.4	-16
	2b	U	1.9	1.8	0.1	16	2	0.1	-15
	3b	S	2.8	0.2	2.6	34	88	0.4	-48
	4a	U	4.0	3.0	1.0	13	13	0.1	-10
	5b	U	3.1	1.9	1.2	16	19	2.1	-16
	8a	S	2.8	0.6	2.2	26	57	14.8	-31
	8b	S	3.2	0.9	2.3	27	62	12.3	-25
	9b	S	3.6	1.8	1.8	34	61	6.2	-16
	10a	S	4.0	0.8	3.2	34	108	33.1	-48
	10b	S	3.4	2.8	0.6	25	15	6.5	- 9
	12b	S	4.2	1.2	3.0	14	42	2.8	-18
	13b	U	3.3	0.2	3.1	6	19	5.7	-49
	14a	S	4.1	1.1	3.0	19	57	2.6	-25
	14b	S	3.2	0.3	2.9	19	55	24.3	-42
	15a	U	2.8	1.7	1.1	26	29	3.2	-19
	15b	U	2.8	0.1	2.7	25	68	6.0	-55
	16a	U	4.4	0.2	4.2	38	160	19.4	-36
	16b	U	4.7	0.2	4.5	33	149	37.2	-41
75	4a	S	3.4	0.1	3.3	23	76	8.7	-52
	4b	S	4.0	0.1	3.9	28	109	20.1	-52
	5a	U	3.7	2.9	0.8	11	9	0.6	- 9
	5b	U	4.6	2.9	1.7	13	22	1.6	-10
	6a	U	5.4	1.6	3.8	19	72	5.5	-14
	6b	U	2.1	1.8	0.3	11	3	0.7	-18
	10	U	2.7	1.6	1.1	23	25	1.7	-20
	14	S	3.5	2.0	1.5	19	29	2.2	-13
76	1	S	4.6	0.2	4.4	20	88	23.9	-49
	2	U	3.2	2.0	1.2	30	36	6.7	-14
	5	S	2.4	1.6	0.8	9	7	3.9	-17
	10	U	1.7	1.2	0.5	14	7	4.3	-20

The first comparison using the improved estimator is made between unseeded and seeded events from Table 9 for warm and cold cloud top temperature categories. For the unseeded events both the warm and cold categories are used together because there are relatively few events. Precipitation data versus the precipitation estimator for the unseeded events and the seeded events in the warm category are shown in Figure 46. The difference between unseeded and seeded precipitation is not statistically significant at the 0.10 level, based upon a one tailed Student's t test. Similarly, precipitation data versus the precipitation estimator for unseeded events and seeded events in the cold category are shown in Figure 47; no significant difference is found at the 0.10 level.

7.2.5 Analysis of Ground Seeding Program with Supercooled Water Stratification. An analysis of ground seeding events classified according to aircraft reports of icing conditions is made in a similar way as was done in the aircraft seeding program. For this purpose Pilot Reports (PIREPS) were analyzed for each event. All reports were noted on the height-time graphs of cloud structure; these reports are listed in Appendix A. Then each four-hour period was classified according to categories as described in Section 7.2.3. Events classified as light to moderate icing or greater are considered in this analysis; these events and related data are listed in Table 10. To obtain a result that would be comparable to the airborne seeding program, the (linear) estimator used is the same as that in the earlier program, namely, the product of the difference between the cloud base and cloud top mixing ratios and the 2750 m (9000 ft) wind normal to the mountain-barrier axis. Results for events with available data are shown in Figure 48; compare with Figure 34 for the airborne seeding program.

For a given value of the estimator there is about 20 percent more precipitation in the seeded events than in the unseeded, when all events are considered. When only the orographic events are considered, an increase of precipitation in the seeded events is 42 percent. Again, as in the airborne seeding program, the small number of events in the unseeded and seeded categories makes the results uncertain and not statistically significant at the 0.10 level. However, these differences in precipitation between the unseeded and seeded events are similar in both programs. Thus, in a sense, the two programs are both additive and independent.

Inasmuch as the foregoing results may be indicative of a seeding effect, especially when both programs are considered, further examination of the data is warranted. Two steps are taken in this regard. First, use is made of the improved estimators, as in the previous section; and second, for both unseeded and seeded events the ground and aircraft data are grouped together.

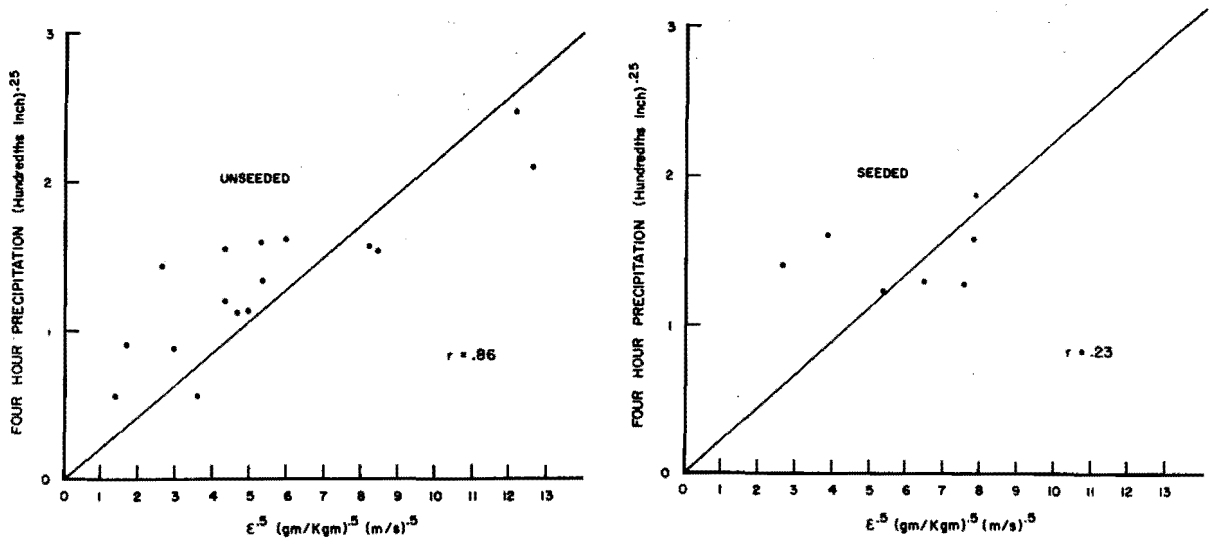

Figure 46. Precipitation (4th root) versus precipitation estimator (square root) for unseeded and warm category seeded orographic events.

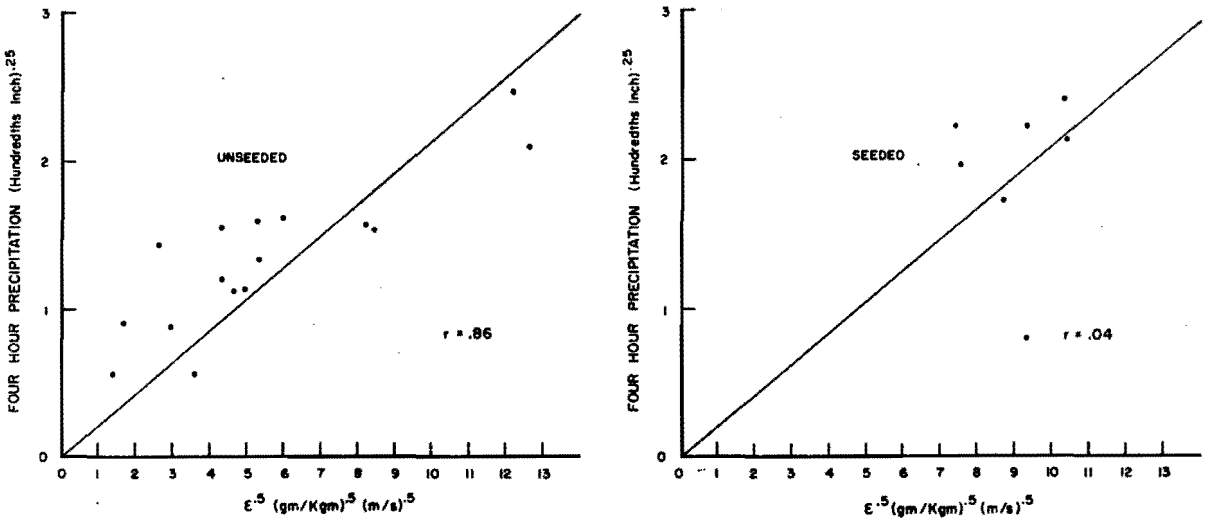

Figure 47. Precipitation (4th root) versus precipitation estimator (square root) for unseeded and cold category seeded orographic events.

Table 10. Aircraft icing events: ground seeding.

Year	Case	S/U	Icing	CBMR	CTMR	ΔMR	V	Estimator	Precip.	Non-Orog.
74	1a	S	LM	2.4	2.2	0.2	27	5	1	
	6a	S	LM	-	-	-	35	-	1	
	7a	S	M	-	-	-	47	-	18	x
	7b	S	M	-	-	-	35	-	16	x
	8a	S	M	2.8	0.6	2.2	26	57	15	
	8b	S	M	3.2	0.9	2.3	27	62	12	
	9a	S	LM	3.0	0.7	2.3	30	69	3	
	9b	S	LM	3.6	1.8	1.8	34	61	6	
	10a	S	LM	4.0	0.8	3.2	34	109	33	
	10b	S	LM	3.4	2.8	0.6	25	15	6	
	12a	S	LM	4.1	2.5	1.6	17	27	11	
	12b	S	M	4.2	1.2	3.0	14	42	3	
	16a	U	M	4.4	0.2	4.2	38	160	19	
	16b	U	LM	4.7	0.2	4.5	33	149	37	
	19a	S	LM	-	-	-	22	-	17	
	19b	S	LM	0.6	0.2	0.4	24	10	33	x
75	1a	U	LM	3.7	0.4	3.3	26	86	3	
	1b	U	M	3.9	2.1	1.8	24	43	1	
	2a	U	MH	-	-	-	23	-	3	
	2b	U	M	-	-	-	23	-	9	
	6a	U	M	5.4	1.6	3.8	19	72	6	
	7a	S	LM	3.2	1.3	1.9	21	40	12	x
	7b	S	LM	-	-	-	13	-	7	x
	14	S	M	3.5	2.0	1.5	19	29	2	
76	1	S	LM	4.6	0.2	4.4	20	88	24	
	6	S	LM	4.2	0.1	4.1	33	135	14	x
	8	U	LM	2.9	1.6	1.3	20	26	22	x

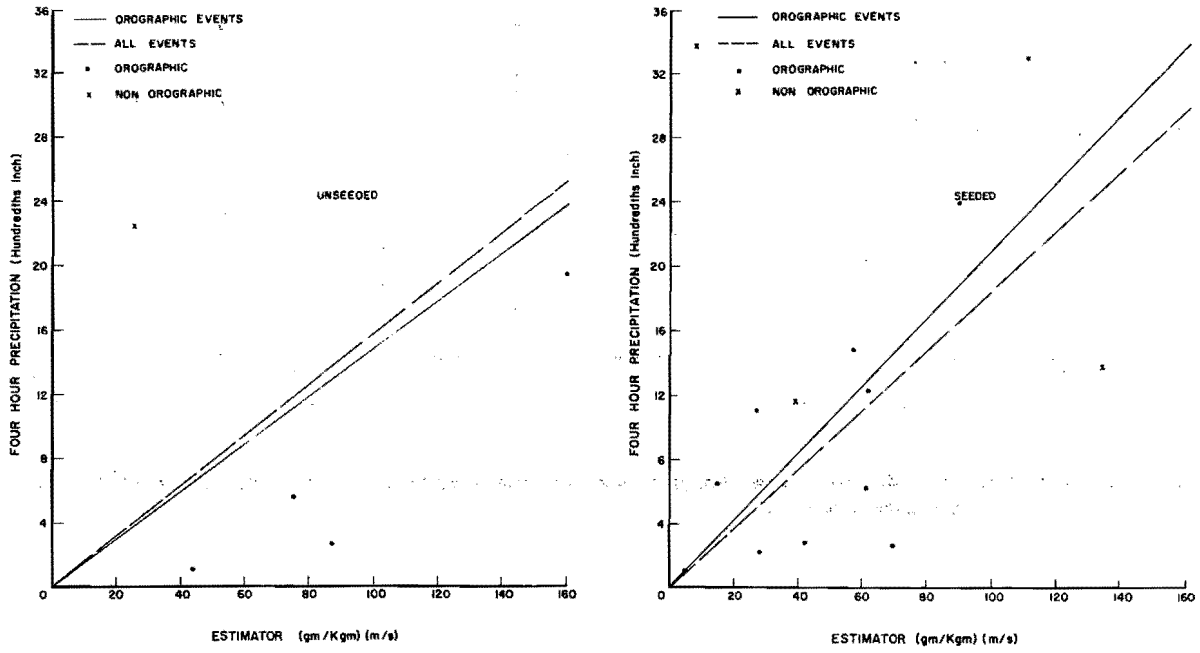

Figure 48. Precipitation versus precipitation estimator for unseeded and seeded orographic events with at least light to moderate aircraft icing during the ground based seeding program.

Precipitation data from the airborne seeding program are made compatible with the ground seeding program so that events from both programs may be combined. To make the precipitation data comparable, the observed rather than standardized precipitation from the airborne seeding program are averaged from only the same 11 gages used in the ground seeding program. Furthermore, the precipitation estimator based upon radar data is adjusted so that the estimators from both programs are compatible. The most important difference between the radar and rawinsonde parameters which affect the estimators is due to the measurement of cloud base height. Typically, cloud bases are lower (and cloud tops are higher) at the rawinsondes site compared to the radar site. A plot of the difference in cloud base heights versus radar cloud base height is shown in Figure 49; a positive difference indicates the cloud bases the lower at the rawinsonde site. Thus a radar cloud base height can be adjusted to coincide with the rawinsonde data, at least in a statistical sense.

As may be found from Table 7, there are four unseeded and four seeded events from the airborne seeding program, which are classified as both orographic and icing events. They are 70-8, 71-14, and 72-18 for both unseeded and seeded, 71-15 for the unseeded portion only, and 70-11 for the seeded portion only. For these events, the modified parameters are listed in Table 11 along with the observed average precipitation for the eleven gages used in the ground seeding program.

In each of three comparisons to follow, the combined ground and airborne unseeded events are used. The seeded events are (1) the ground events, (2) the airborne events, and (3) the combined ground and airborne events.

In Figure 50 the unseeded ground/air events and the seeded ground events are shown. The difference in slope of the regression lines (with zero intercept) for unseeded and seeded events is significant at the 0.05 level.

In Figure 51, the unseeded ground/air events and the seeded air events are shown. Here, with only four seeded events, the difference in slope of the regression lines (with zero intercept) is not significant at the 0.10 level. However, the difference in slope is similar to that for the ground events.

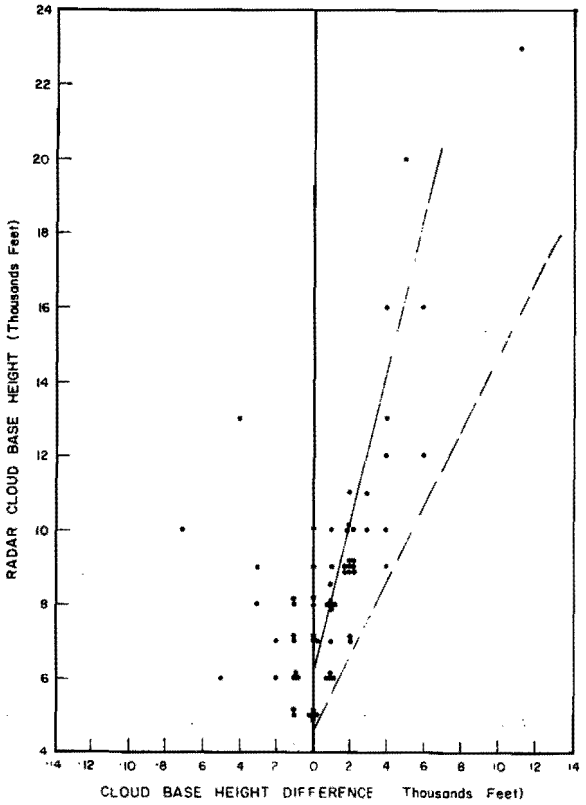

Figure 49. Radar cloud base height versus radar minus the rawinsonde cloud base height.

In Figure 52, the unseeded ground/air events and the seeded ground/air events are shown. The difference in slope of the regression lines (with zero intercept) is significant at the 0.03 level. Thus, the combined programs yield an apparent seeding effect under certain circumstances. According to these results, when light to moderate or greater aircraft icing is occurring upwind of the mountain barrier, a large increase in orographic precipitation may be caused by seeding. These increases may be visualized more clearly when the regression lines of Figure 52 are transformed to a plot of linear precipitation versus a quadratic estimator as shown in Figure 53; for a given value of the estimator, the seeded precipitation is 2.36 times the unseeded precipitation in the class of events characterized as having high supercooled water content.

Table 11. Aircraft icing events: airborne seeding (orographic events, values compatible with groundseeding program).

Year	Case	S/U	CBMR	CTMR	ΔMR	V	Estimator	Precipitation
70	8-1	U	4.8	0.3	4.5	23	106	24.2
	8-2	S	4.5	0.4	4.1	28	114	38.6
	11-2	S	5.5	0.7	4.8	20	96	27.1
71	14-1	U	3.2	1.9	1.3	15	20	0.1
	14-2	S	3.4	2.8	0.6	15	9	0.1
	15-1	U	2.3	1.2	1.1	23	25	1.1
72	18-1	S	4.8	0.6	4.2	20	84	5.6
	18-2	U	4.8	0.6	4.2	20	84	12.3

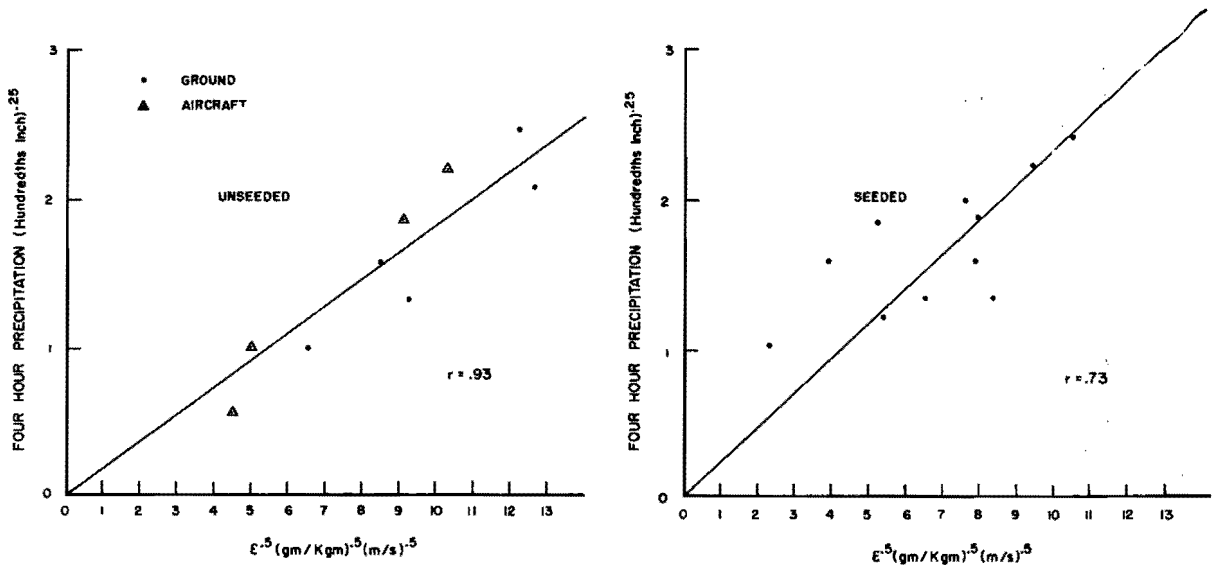

Figure 50. Precipitation (4th root) versus precipitation estimator (square root) for unseeded ground/air orographic events and seeded ground orographic events, with reports of at least light to moderate aircraft icing.

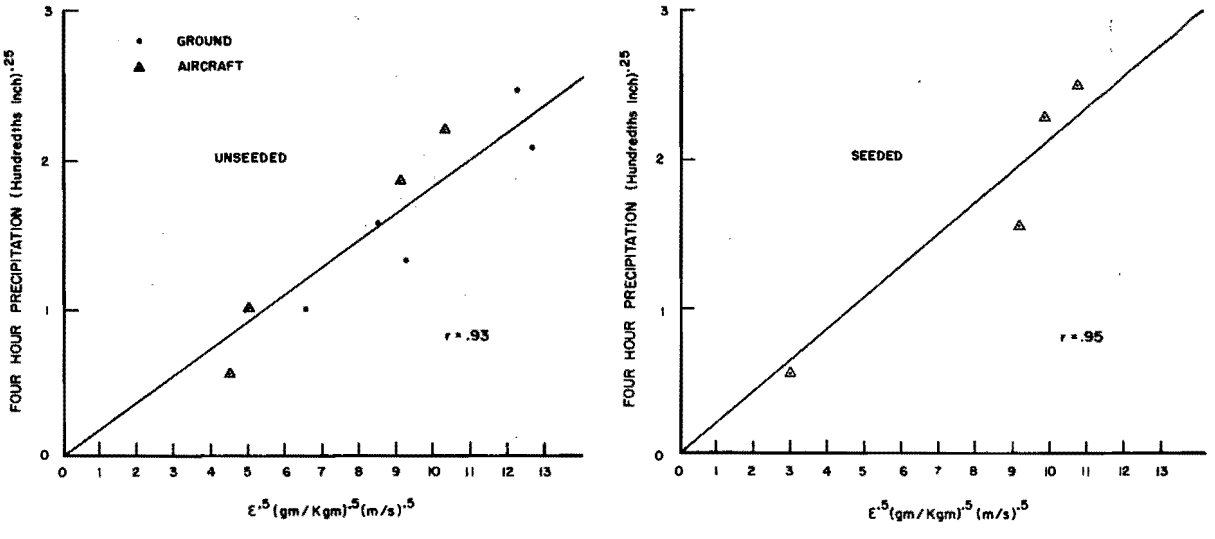

Figure 51. Precipitation (4th root) versus precipitation estimator (square root) for unseeded ground/air orographic events and seeded air orographic events, with reports of at least light to moderate aircraft icing.

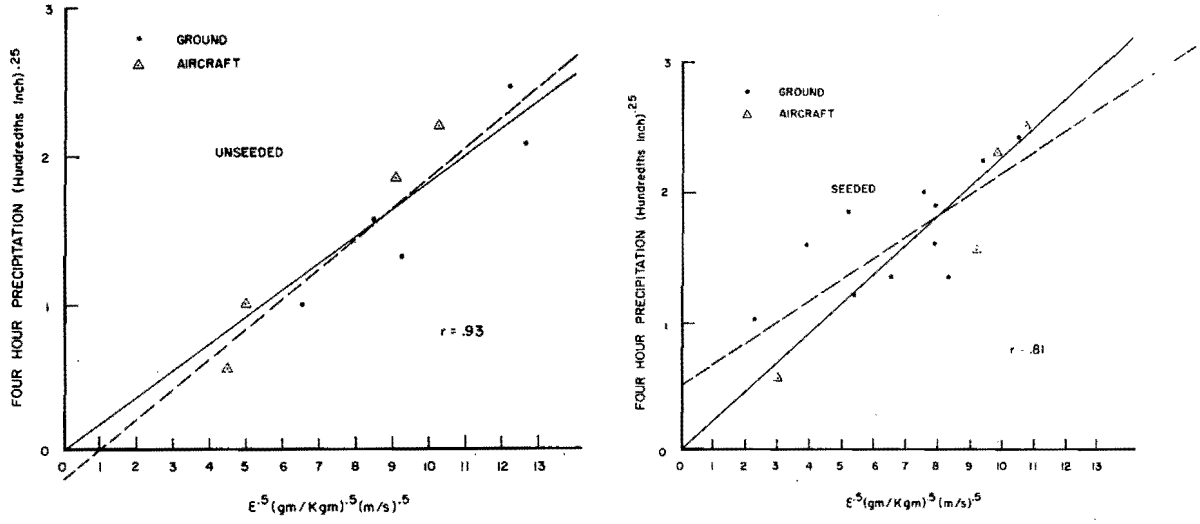

Figure 52. Precipitation (4th root) versus precipitation estimator (square root) for unseeded ground/air orographic events and seeded ground/air orographic events with reports of at least light for aircraft icing events.

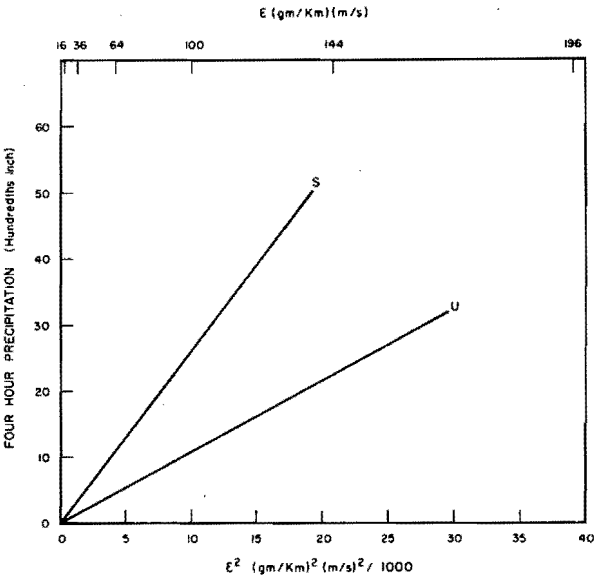

Figure 53. Transformed precipitation and precipitation estimator relationships from Figure 52 with linear precipitation scale, and zero intercepts on the regression lines.

It is of interest to note that the precipitation estimator correlates with precipitation of the combined ground/air unseeded events at the 0.93 level; on the other hand a similar comparison using seeded events (Figure 52) yields a correlation of 0.81. The increased scatter of data in the seeded events may itself be a seeding effect.

In all the foregoing analyses using precipitation estimators, the regression lines have been forced through the origin. In finding a regression relationship, this approach is useful when there are only few data, such as for the seeded events in Figures 46 and 47. On the other hand for the combined air and ground programs there is a larger data base. As may be noted in Figure 52, the intercept for either unseeded or seeded events is other than zero. Therefore, a reanalysis of that data is made accordingly. Analysis of errors for the two separate relationships as compared to a single relationship for both unseeded and seeded events shows that the two separate relationships are better than the single one with a significance level of 0.03.

When relationships with non-zero intercepts are transformed as shown in Figure 54, seeding effects again are apparent. It is noted that the value of the estimator is greater than 100 in only 5 events out of 23. Thus, most of the data lies in the coordinates of the graphs where the results are similar to those of Figure 53. In this range increased precipitation is around 5 to 10 hundredths inch per four hours when meteorological conditions are appropriate. Finally, the fractional increase in precipitation associated with seeding for these events is shown in Figure 55 as a function of the precipitation estimator. At low values of the estimator, the fractional increase in precipitation is large, and decreases steadily with increasing values of the estimator.

These results are somewhat consistent with cloud top temperature concepts. That is, the greatest fractional increases from cloud seeding may be expected when there is a moderately low value of the precipitation estimator. In this situation, the cloud top mixture ratio is apt to be high and the corresponding temperature is relatively warm, which is to say that clouds with warm tops are more suitable for seeding than with clouds with cold tops. On the other hand, as

already indicated, the identification of which clouds are seedable is best done by some direct measure of supercooled water concentration.

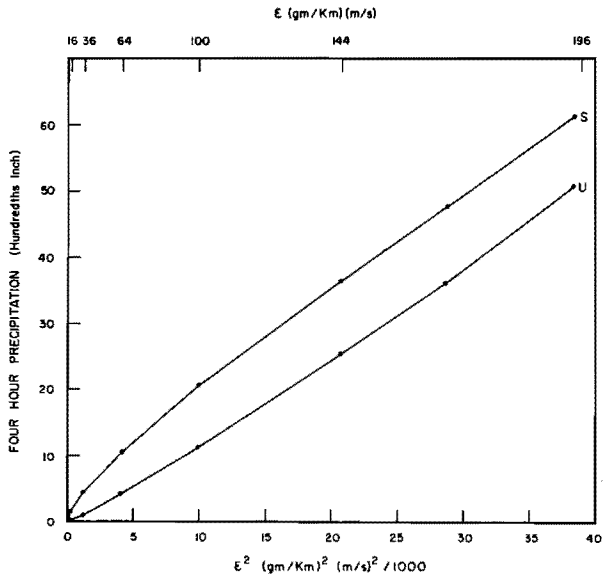

Figure 54. Transformed precipitation and precipitation estimator relationships from Figure 52 with linear precipitation scale, and non-zero intercepts on the regression lines.

To assess the total potential of precipitation augmentation by seeding, both the climatology of the precipitation estimator and the occurrence of relatively high concentrations of supercooled water are needed. The former may be assessed from existing National Weather Service records, but little is known about the frequency, geographical extent of intensity of periods with high supercooled water concentrations over the course of a winter season. Until such data become available, only very crude approximations to the seeding potential can be made. One such estimate can be made on the basis of the airborne program. Out of a total of 80 events there were 14 classified as having light to moderate or greater aircraft icing, or about 17 percent of the events.

The net seeding effect from suitable storms can be estimated by projecting all the precipitation values on Figure 52 first onto the unseeded regression line and then onto the seeded regression line. The value of the estimator for each event is left unchanged. Then the ratio of the seeded to unseeded precipitation as adjusted and summed for all events may be found. This procedure takes into account both the variable seeding effect as a function of the estimator and the observed distribution of the estimator. The result of this calculation is a ratio of 1.85. Thus the net seeding effect is 1.85 times 17 percent, or 32 percent of the winter precipitation. It is interesting to note that the ratio 1.85, according to Figure 55a, occurs at a value of $\epsilon = 95$, or $\epsilon^{.5} = 9.7$. By inspection of Figure 52, it is clear that this value of $\epsilon^{.5}$ is associated with the more intense of the orographic storms. While the percentage of seeding effect increases rapidly with the weaker storms, the net gain of precipitation is apt to be derived from the not so weak storms. For example, with $\epsilon = 95$ and V = 20 kts the cloud top and cloud base mixing ratio difference is 4.75, which is a value typical of low cloud bases in winter. Consequently, the cloud top mixing ratio must be close to zero, or in other words the cloud tops are high and in the cold category, i.e., less than -30°C. Therefore, according to these results, storms with both warm and cold cloud top temperatures may be seeded for precipitation increases provided sufficient supercooled water is present. It appears from these calculations that large increases in winter orographic precipitation may be derived from about one-sixth of the winter storms.

As a final statement concerning the achievement of precipitation increases by seeding, it is emphasized that the foregoing results are *a posteriori* and therefore must be regarded as tentative. Verification of these results should be of high priority. It is therefore postulated that precipitation may be greatly enhanced by artificial seeding when the concentration of supercooled water in winter orographic clouds is high (sufficient to cause light to moderate or greater aircraft icing).

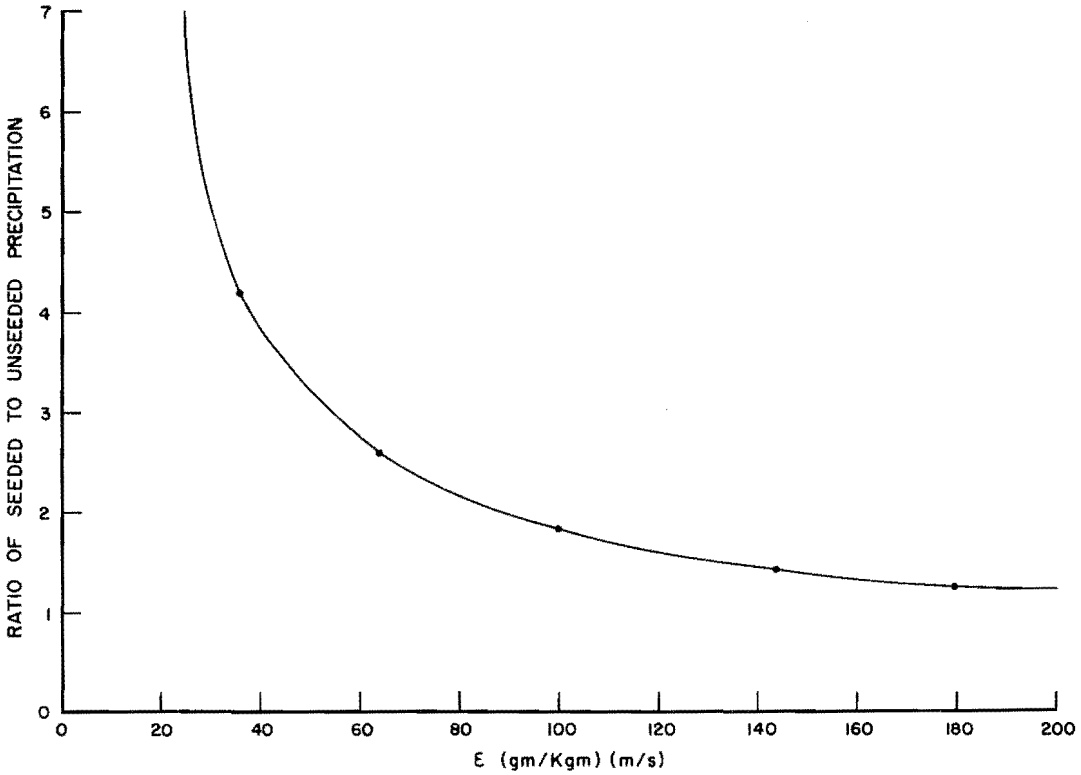

Figure 55a. Ratio of seeded to unseeded precipitation versus the linear estimator for orographic events with light to moderate aircraft icing.

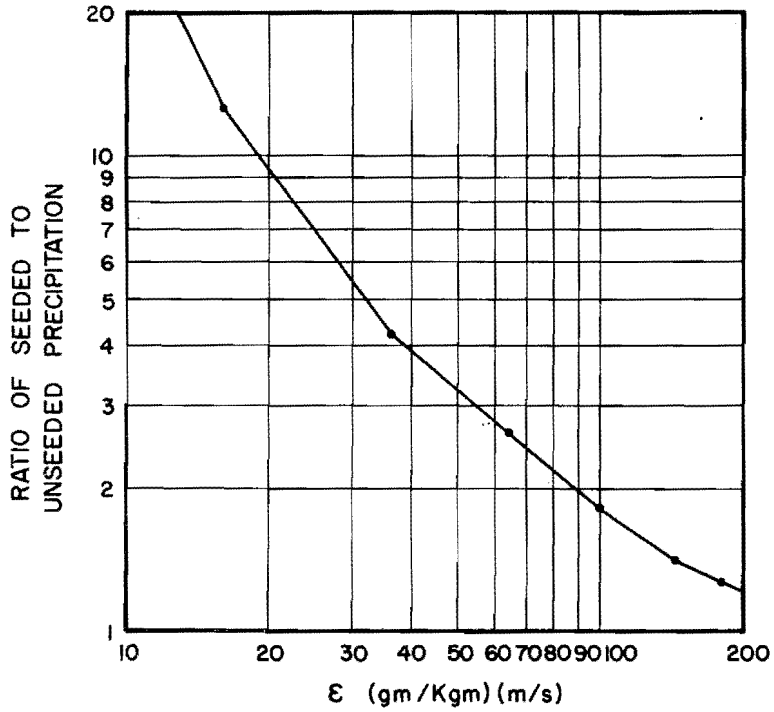

Figure 55b. Logarithmic graph of ratio of seeded to unseeded precipitation versus the linear estimator for orographic events with light to moderate aircraft icing.

8.0 CONCLUSIONS

8.1 Conclusions

In this section the findings which are considered of primary importance will be outlined. Probably the most important finding is that a strong seeding effect is evident in both the airborne and the ground seeding programs, when supercooled water is present in substantial amounts, as indicated by aircraft reports of icing conditions. As *a posteriori* analysis of seeding effects shows that precipitation may be increased several times over its natural amount in individual storm periods. An estimate of the cloud seeding potential yields a winter season increase about thirty percent.

Stratification according to cloud top temperature yielded results which are not regarded as significant. Apparently, the presence of supercooled water is not well indicated by cloud top temperature. However, an analysis of this relationship showed a weak trend toward higher supercooled water amounts at warmer cloud top temperatures. The fact that seeding apparently increases precipitation in supercooled water clouds, but not at warm cloud top temperatures at least in an identifiable amount, tends to support the presence of only a weak relationship. Thus, it would appear that direct measurements of supercooled liquid water as a means of identifying seedability would be highly desirable. Inasmuch as aircraft reports of icing conditions were obtained within the bounds of ordinary, or slightly specialized air traffic routes, no special difficulty should prohibit such measurements. In other words, measurements of supercooled water need not be made in the immediate vicinity of mountains at altitudes hazardous to aircraft.

Other findings of special interest to weather modification projects are several: the use of precipitation estimators is very effective in accelerating the detection of seeding effects; correlation coefficients between a precipitation estimator and precipitation are found typically in the range from 0.70 to 0.95. In these simple estimators, the mixing ratio and wind speed are used. Relationships are improved significantly if the square of a linear estimator is used. Then the fourth root of these parameters is used to achieve normal distributions. Classification of experimental events has proved useful; orographic precipitation is characteristically more predictable than frontal, cyclonic, or convective. Non-orographic precipitation is more variable, less representative and usually greater than the orographic. When a few non-orographic events are combined with many orographic ones, the results may be unrealistic.

In the analysis of data, it was found that cloud top temperatures could be well defined by the top of ice saturation, at least in most instances. Vertical incidence radar was used as a basis of comparison. It was also found that cloud top temperatures, governed by the humidity field, vary greatly over relatively short periods of time. In two hours the standard deviation of the cloud top temperature is 5.5°C; in four hours it is 13°C and in six hours, 22°C.

Two additional points are noteworthy. One is that cloud top temperatures found from rawinsondes, are greatly in error if solar shielded rawinsondes were not used, as was the case prior to about 1971 or 1972. Another point is that when one is free to choose the physical limits, especially two sided ones within which an effect is supposed to occur, an otherwise not statistically significant variation becomes apparently significant. It is the exclusion of apparently adverse seeding effects by the precise specification of limits that augments the variation to a more favorable amount. This problem is present even in ranges wherein a physical basis is present.

8.2 Recommendations

The primary recommendation derived from this program is that the identification of suitable clouds for seeding in winter orographic storms should be carried out by aircraft, equipped to measure supercooled water concentrations. The seeding itself can be carried out from either the air or ground. Although the ground seeding program yielded more definitive results than the air seeding program (due to the number of suitable events), effects of seeding at later times than that intended is not known. In the case of ground seeding such after effects are apt to be more pronounced than with airborne seeding. However, the critical factor appears to be the identification of suitable clouds for seeding.

It is suggested that this approach to cloud seeding be used in both operational and experimental programs. That is, sufficient measurements of supercooled water along with other quantities such as precipitation should be made on a regular basis both for the identification of seedable clouds and for the evaluation of the programs.

Another recommendation is that past experimental projects should be reexamined to ensure that the cloud top temperatures used are appropriate, i.e., that solar shield rawinsondes were used and that a sufficient frequency of releases were made. Also, further examination of the choice of limits-of-effect should be made so that noise type variations are not bracketed and then appear as a seeding effect. In projects where supercooled water or closely related measurements are available, a reanalysis should be made with the presence of substantial supercooled water as a basis of stratification.

REFERENCES

Chadwick, D.G. 1968. USU remote total precipitation telemetry station. Bureau of Reclamation PR-WG30-6, Contract 14-06-D-6003, Denver, Colorado.

Chappell, C.F. 1971. Modification of cold orographic clouds. Department of Atmos. Science. Colorado State University, PhD dissertation. 196 p.

Chappell, C.F., J.E. Fletcher, G.W. Reynolds, W.N. McNeill and R. Campbell. 1971. Development of cold cloud seeding technology for use in precipitation management. Final Report PR-WG80-2, Bureau of Reclamation, Contract No. 14-06-D-6820, Denver, Colorado. 96 p.

Chappell, C.F.., J.E. Fletcher, W.N. McNeill, R.H. Campbell, G. Wooldridge, L. Balick and F. Johnson. 1972. Development of cold cloud seeding technology for use in precipitation management—May 15th Interim Progress Report. Bureau of Reclamation Contract No. 14-06-D-7184. 47 p.

Chappell, C.F. and F.L. Johnson. 1974. Potential for snow augmentation in cold orographic clouds. J. Appl. Meteor., 374-382.

Elliott, R.D., R.W. Shaffer, A. Court, J.F. Hannaford. 1976. Colorado River Basin Pilot Project—Comprehensive Evaluation Report. U.S. Bureau of Reclamation Contract No. 14-06-D-7332. 641 p.

Gifford, F.A. 1968. An outline of theories of diffusion in the lower layers of the atmosphere. Meteorology and Atomic Energy, Air Resources Laboratory, NOAA. pp. 97-114.

Grant, L.O. and P.W. Mielke, Jr. 1967. A randomized cloud seeding experiment at Climax, Colorado. 1960-1965. Proc. of 5th Berkeley Symposium in Math, Stat., and Prob., 5, pp. 115-131.

Henderson, T.J., G.F. Darrigo, R.L. French and R.J. Fraser. 1970. Wasatch Airborne Seeding Programs. Final Report to Utah Water Research Laboratory, Logan, Utah, under Bureau of Reclamation Contract No. 14-06-D-6820. 119 p.

Hill, G.E. 1973. Development of cold cloud seeding technology for use in precipitation management—Nov. 15 Interim Progress Report. Bureau of Reclamation Contract No. 14-06-D-7184. 52 p.

Hill, G.E. 1974. Development of cold cloud seeding technology for use in precipitation management—Nov. 15 Interim Progress Report, Bureau of Reclamation Contract No. 14-06-D-7184. 34 p.

Hill, G.E. 1974. Results of a cold cloud seeding experiment in the Northern Wasatch Mountains. Amer. Meteor. Soc. 4th Conf. on Weather Mod. Ft. Lauderdale, Florida. pp. 462-467.

Lopez, M.E. and C.K. Nason, 1967. Normalization of truncated precipitation series. Sci. Rep. No. 1, Contract No. 14-06-D-5962. U.S. Bureau of Reclamation, W.E. Howell inc. Lexington, Mass. 19 p.

Juisto, J.E. 1971. Crystal development and glaciation of a supercooled cloud. J. Researches Atmospheriques, vol. 5, 69-85.

Juisto, J.E. and R.K. Schmitt. 1970. A model of supercooled cloud microphysics. Proc. of the Second Nat. Conf. of Weather Modification. Santa Barbara, California. pp. 41-44.

McNeill, W.N., R.H. Campbell, G.L. Wooldridge, L.K. Balick and F. Johnson. 1972. Development of cold cloud seeding technology for use in precipitation management—Nov. 15th Interim Progress Report. Bureau of Reclamation Contract No. 14-06-D-7184.

Peterson, K.R. 1968. Continuous point source plume behavior out to 160 miles. Journal Appl. Met., 7, 217-226.

Turner, D.B. 1969. An outline of theories of diffusion estimates. National Air Pollution Control Administration, Public Health Service, U.S. Dept. of Health, Education and Welfare. pp. 15-42.

A.0 APPENDIX A

A.1 Airborne Seeding Program

During the airborne seeding program, a pilot report of each seeding flight was prepared. One such report is reproduced in Figure 56. It is from these reports that the airborne seeding events are classified as to degree of aircraft icing. Following this sample report, a list of icing conditions extracted from these pilot reports is given in Table 12. In essence the extractions are quotes. Fourteen events classified as light to moderate icing or greater are circled. Five of these events are classified as orographic with complete data (precipitation and Cache Peak rawinsonde). These events are doubly circled. Case 70-11 is orographic during the seeded period only and 71-15 during the unseeded period only; the other three are orographic during both the unseeded and seeded periods.

A.2 Ground Seeding Program

To obtain data on aircraft icing during the ground seeding program it is necessary to use pilot reports by commercial and military flights. In Table 13 such reports as available are listed for periods before, during and after each event. The time, approximate location and altitude is given along with the pilot characterization of icing. A list of locations is provided at the end of the table. These reports are then given an overall classification for each four hour period as in the airborne program. In making the classification several factors are considered. The time and altitude of the report are entered onto graphs of cloud bases and tops so that the intensity of icing may be evaluated according to cloud pattern and time of event.

Test case #71-9
Date 11th, Jan. 1971
Seeding track B-3
Seeding start time 1900 local
Seed second half. Test period begins at 1500 local
Seeding altitude 11,000 MSL
Seeding rate 2 grams per minute
Forecast winds 225 magnetic at 25 nauts
Take-off 1849 Land 2112
Total flight time 2.4 hours
Seeding start time 1900 actual
Agl seeding material consumed 270 grams
Alert received 1510

Remarks:

Take-off was made using runway 16, winds were from 140 degrees at 5 nauts. Weather conditions were 5,000 overcast with visibility greater than 30 miles in all directions. Surface temperature was plus 4 degrees centigrade. The runway and taxi ways were standing pools of water and were icy in spots.

The temperature at seeding altitude remained constant at -10C during the seeding flight but the temperature showed a warming trend at the end of the flight.

The seeding flight was conducted in and out of cloud, always near the top of the overcast. Higher buildups were observed to the east. Very light rime ice was building while in cloud and very light turbulance was observed during that time spent in the clouds. Light snow showers were noticed in the cloud and icy crystal were apparent during the flight above the overcast. There were no signs of a higher overcast as was observed during test case #8.

Light snow showers were encountered during our descent, but there was no precip at the airport upon landing. Cloud bases remained at 9,000 feet during the entire flight.

The overcast layer was fairly heavy and solid, throughout the flight it was never possible to observe the ground through breaks in the overcast or through light cloud.

The flight went off very smoothly, presenting no problems. The fuel adjustment apparently resolved the problems with the right engine as encountered on the prior test case.

Figure 56. Sample seeding—aircraft report.

Table 12. Aircraft icing reports: airborne seeding program.

	Event	Report
70	1	None
	2	None
	3	Some light rime ice
	4	None
	5	Very light rime
	6	Light rime
	7	Very light ice
	(8)	(Two PIREPS OGD) Moderate rime
	9	Some light rime
	10	Light rime
	(11)	Light to moderate rime ice led to break in seeding for 18 minutes to descend and de-ice; (PIREP OGD): moderate to heavy ice, losing power
	12	Light ice
	13	Light ice
	14	Very light ice
	15	Some light clear ice
	(16)	Light to moderate rime ice; (PIREP SLC light to moderate ice)
	17	Light rime
	18	Very light rime
71	1	Light rime
	(2)	Light to moderate: total to 3 inches built up on air frame; de-icing equipment proved adequate
	3	Light to moderate icing, but limited to isolated connective activity
	4	None
	5	None
	6	None
	7	Light: 3/8 inch rime accumulation
	8	None
	9	Very light rime
	10	None
	11	Very light
	12	Light rime only during climb
	13	None
	(14)	Two inches of rime/clear in 30 minutes; necessary to descend
	(15)	Moderate: two inches in 50 minutes; flight discontinued due to ground based communications problem
	16	Light clear icing
	17	Light clear icing
	18	Very light icing
	19	None
	20	Light icing briefly
	(21)	Heavy rime ice: icing rate was probably an ince every 15 minutes
	22	Light icing
	23	Light icing
	(24)	1¼ inch of ice during first half; very little, second half
	25	None
	26	None
	27	None
	28	None
	29	Very light ice
	30	Very light ice
	31	None
	32	Very light ice
	33	Very light ice
	34	None
72	1	None
	2	No flight
	(3)	Moderate aircraft icing; aborted due to radio failure
	4	None
	5	Very light icing
	6	None
	7	None
	8	None
	9	None
	10	None
	11	No flight
	12	None
	13	No flight
	14	Light ice: about 1/8 inch per hour
	(15)	Ice build-up fast in cloud; numerous PIREPS of heavy icing N and NW of Ogden from 12K to 20K ft.
	(16)	Light icing during the time in clouds; accumulation of about 1 inch
	17	None
	(18)	Over 1 inch accumulation of ice during first hour
	(19)	Initial icing very fast; not much icing thereafter
	20	None
	21	None
	22	Light icing
	23	Light icing
	24	Very light
	25	No icing statement made; flight aborted early
	(26)	Accumulation of about 1 inch of ice
	27	Not much aircraft icing

Another factor considered in classifying icing is the time of the event itself. During the daytime an absence of reports may be interpreted as meaning no significant icing (or turbulance); at night an absence of reports simply means no aircraft are flying in the vicinity. In Figure 57 a plot of number of PIREPS versus time is shown. It is clear that few reports are available between about 0500 and 1300 GMT. On the other hand a much larger number of reports are available between about 1400 and 0300 GMT. Thus an absence of reports in this latter period is indicative of little significant icing.

In any case, only events characterized by significant icing based upon actual reports (LM or greater) are classed as having high supercooled water. As in the airborne seeding events, those classified as light to moderate or greater aircraft icing are circled. From these circled events, ones classified as orographic with complete data and identifiable cloud bases and tops (see Table 10) are doubly circled.

Table 13. Aircraft icing reports: ground seeding program.

FY	Event	Date	Time (GMT) 4 Hour Period	Icing Class	Time (GMT)	Location	Rate	Altitude Thousand Feet Above Sea Level
74	1	Nov. 27	2100-0500	(1) LM	1839	BYI	MDT	12
				2 O	1840	SUN	MDT	12
					2208	OGD	LGT-MDT	10-12
					0250	SLC	None	
	2	Dec. 12	0800-1600	1 –	0245	SLC	None	
				2 –	0310	SLC	None	
	3	Dec. 13	0700-1500	1 –	1405	SLC	None	
				2 –	1634	SLC	None	
					1800	SLC-TWF	MDT	13
	4	Dec. 22	0700-1500	1 –	2150	SLC	None	18
				2 –	0420	SLC	None	9
					1452	DTA	MDT	12
					1540	OGD	LGT	
					1645	SLC	LGT	
					1650	SLC	0.5 inch	10-13
					1755	SLC	V. LGT	
	5	Dec. 23	0130-0930	1 –	0143	MLF	MDT	12
				2 –	0143	MLF	None	13
					0150	MLF	MDT	13
	6	Dec. 28	2130-0530	(1) LM	1555	SLC	LGT	7-16
				2 –	1555	SLC	n.i.r.	
					1650	SLC	MDT	7-19
					1743	SLC	LGT	7
					1743	SLC	LGT	13-15
					2320	SLC	MDT	11
					2320	SLC	n.i.r.	11
	7	Dec. 29	2200-0600	(1) M	1905	FFU	MDT	13-21
				(2) M	1905	SLC	n.i.r.[a]	
					2108	SLC	n.i.r.	
					2146	SLC	LGT-MDT	12-18
					2220	HIF	LGT-MDT	13-16
					2256	SLC	LGT	11
					2300	SLC	MDT	18-19
					2358	DTA	MDT	14
					0010	OGD	MDT	12
					0646	SLC	MDT	12
	8	Jan. 7	1600-0000	1 M	1529	FFU	LGT	20
				2 M	1545	SGU-DTA	MGT	6-12
					1720	SLC	MDT	15-18
					1940	FFU	MDT	13-15
					2209	ELY	MDT	5-16
	9	Jan. 12	1200-2000	(1) LM	1400	SLC	MDT	5-24+
				(2) LM	1412	SLC	MDT	5-20
					1430	SLC	None	14
					1700	SLC	LGT	13
					1845	SLC-MLD	MDT	14
					2210	PIH-IDA	LGT	9
	10	Jan. 13	1930-0330	(1) LM	1530	SLC	n.i.r.	
				(2) LM	1600	SLC	n.i.r.	
					2307	BYI	MDT	12
					0130	OGD	LGT-MDT	12

[a]n.i.r. means no ice report in PIREP.

Table 18. Continued.

FY	Event	Date	Time (GMT) 4 Hour Period	Icing Class	Time (GMT)	Location	Rate	Altitude Thousand Feet Above Sea Level
74	11	Jan. 17	1530-2330	1 L	1445	DPG	LGT	14
				2 L	1530	HIF	LGT-MDT	10-12
					1648	LGU	LGT	17
					1715	HIF	LGT	7-16
					1847	OGD	LGT	11
					1850	FFU	LGT	22-24
					1905	SLC	1 inch	18
					2006	FFU	LGT	19
					2336	SLC	LGT	11
					0010	SLC	LGT	11
					0145	PIH-SLC	LGT-MDT	9-11
	12	Jan. 19	1630-0030	(1) LM	1508	SLC	None	5-13
				(2) M	1640	SLC	None	5-16
					1745	SLC	MDT	5-13
					1958	OGD	None	14
					2046	OGD	LGT	11
					2240	OGD	MDT	12
					2240	SLC	MDT	9-14
					2340	SLC	MDT	7-10
					0100	DTA	Trace	13
	13	Jan. 20	2300-0700	1 O	1845	HIF	Trace	6-14
				2 –	1949	MLF	LGT	11
					2040	DTA	None	11
					2040	HIF	None	5-26
					0035	SLC	None	14
					0047	SLC	None	25
	14	Jan. 26	0000-0800	1 L	2225	IDA-PIH	LGT	8
				2 L	2342	OGD	LGT	12
					0049	SLC	n.i.r.	12
					0210	BYI	LGT-MDT	15
					0515	BOI-SLC	LGT	16
	15	Jan. 27	2230-0630	1 L	2145	SLC	Trace	10-12
				2 O	2145	4SV	LGT	12
					0145	FFU	LGT	9-11
					0357	SLC	None	5-19
	16	Jan. 31	2130-0530	(1) M	1715	SLC-FFU	None	5-6
				(2) LM	1745	SLC	None	6-8
					1855	SLC	None	11
					2136	SLC	None	5-15
					2155	SLC	None	5-12
					2155	SLC	LGT	14
					2201	FFU	None	15
					2245	SLC	LGT-MDT	12-19
					2245	PIH	HVY	24
					0020	SLC	LGT-MDT	12
					0046	OGD	MDT	16-21
					0047	OGD	MDT-HVY	13-23
					0047	OGD	HVY	17
					0100	OGD	MDT-HVY	13-23
					0152	MLD	None	12
					0215	OGD	LGT	12
					0315	BVL	MDT	24
					0402	HVE-SLC	LGT-MDT	18
					0600	MLD	LGT	18

Table 13. Continued.

FY	Event	Date	Time (GMT) 4 Hour Period	Icing Class	Time (GMT)	Location	Rate	Altitude Thousand Feet Above Sea Level
74	17	Feb. 17	1630-0030	1 VL 2 O	1905 several	SLC SLC vcnty.	LGT n.i.r.	9
	18	Feb. 19	1300-2100	1 L 2 L	1415 1450 1625 1930 1930 2005 2129 2151 0023 0106	SLC SLC OGD RKS SLC SLC SLC-OGD SLC SLC SLC	n.i.r. LGT-MDT LGT LGT n.i.r. n.i.r. None V. LGT LGT n.i.r.	 13 17 12 DURGD DURGC 6-12 6-26 16 DURGC
	19	Feb. 22	1800-0200	(1) LM (2) LM	1320 1405 1540 1741 2010 2025 2210 2346 0057 0443	MLD SLC HIF TWF SLC OGD SLC OGD HIF SLC	LGT n.i.r. LGT n.i.r. n.i.r. MDT n.i.r. LGT-MDT n.i.r. n.i.r.	12 DURGC DURGC 13-14 13 12 16 13
75	1	Feb. 7	1700-0100	(1) LM (2) M	1405 1430 1615 1616 1627 2056 2225 2225 0105	OGD OGD HIF SLC SLC SLC MLD MLD SLC-MLD	LGT LGT-MDT MDT MDT V. LGT LGT MDT-HVY MDT-HVY MDT-HVY	9-11 13-16 11 10-12 12 12 6-15 6-15 6-16
	2	Feb. 10	0030-0830	(1) MH (2) M	2130 2315 2315 0035 0205 0449 1420	SLC SLC SLC FFU SLC SLC SLC	None LGT V. LGT LGT HVY n.i.r. LGT-MDT	10 17 12 13 10 7 6-17
	3	Feb. 12	1600-0000	1 O 2 O	1802 1802	DTA BYI-SLC	n.i.r. None	8 12
	4	Feb. 20	0000-0800	1 VL 2 –	2326 0102 0310	PIH-SLC HIF HIF	None None LGT	13 9 16-24
	5	Feb. 27	1530-2330	1 VL 2 VL	1349 1500 1500 1504 1640 1718 2210 2210	SLC-DTA HLN-SLC SLC OGD-MLD SLC-DTA SLC SLC LGU	None None None LGT V. LGT None LGT None	 23 6-23 6-12 12 6-12 12 13
	6	Feb. 28	1700-0100	(1) M 2 O	1515 1840 1914	LGU SLC-RKS RKS	MDT HVY None	14 9+ 14

Table 13. Continued.

FY	Event	Date	Time (GMT) 4 Hour Period	Icing Class	Time (GMT)	Location	Rate	Altitude Thousand Feet Above Sea Level
75	7	Mar. 6	1800-0200	① LM	1235	FFU	HVY	14
				② LM	1358	SLC	LGT	6-23
					1615	FFU	LGT	12
					1625	MLD	LGT	11
					1632	DTA	MDT	12
					2156	SLC	LGT	7
	8	Mar. 10	1200-2000	1 L	1300	SLC-MLD	LGT	7
				2 L	1800	SLC	LGT	DURGC
					1915	SLC	LGT	8
	9	Mar. 16	2300-0300	1 VL	1758	SLC	n.i.r.	7-14
					1818	FFU	LGT	5-8
					1825	OGD	LGT	14
					2017	SLC	MDT	8-11
					0000	SLC	None	5-13
					0026	PUC	LGT	13
					0110	HIF	None	DURGD
	10	Mar. 18	0330-0730	1 O	2025	HIF	None	16
	11	Mar. 20	1745-2145	1 O	1351	SLC	n.i.r.	6-14
					1624	SLC	n.i.r.	16
					2100	DTA	n.i.r.	16
					2259	FFU	n.i.r.	23
	12	Mar. 22	0115-0515	1 O	1900	OGD	n.i.r.	8
					1911	HVE	n.i.r.	12
					1932	MLD	LGT	11
					0018	MLF	LGT	28
					0100	SLC	n.i.r.	8
					0204	SLC	n.i.r.	8
	13	Mar. 22	1615-2015	1 VL	1545	SLC	n.i.r.	18
					1604	MLD	n.i.r.	17
					1729	SLC	V. LGT	6-28
					1933	LGU	n.i.r.	22
	14	Mar. 24	1545-1945	① M	1206	DTA	LGT	12
					1320	SLC	LGT	9-12
					1950	FFU	MDT	12
					2115	SLC	HVY	6-15
					2115	SLC	MDT-HVY	10
	15	Mar. 25	1245-1645	1 VL	1309	SLC-PIH	V. LGT	11
					1355	SLC	LGT	16
					1355	SLC	None	13
					1620	BVL	LGT	13
					1620	FFU	LGT	12
					1909	MLD	None	13
76	1	Feb. 9	0300-0700	① LM	2320	SLC	MDT	10-18
					0330	FFU-SLC	LGT	11-13
					0330	SLC	MDT	7
	2	Feb. 14	2000-0000	1 VL	0245	FFU	LGT	10-13
	3	Feb. 15	1930-2330	1 O	1800	HIF	LGT	21
	4	Feb. 16	2100-0100	1 VL	2010	PVU	n.i.r.	8
					2025	BVL	n.i.r.	6
					2025	FFU	n.i.r.	6
					2028	SLC	n.i.r.	6-12
					2050	SLC	LGT	9
					0145	FFU	n.i.r.	26

Table 13. Continued.

FY	Event	Date	Time (GMT) 4 Hour Period	Icing Class	Time (GMT)	Location	Rate	Altitude Thousand Feet Above Sea Level
76	5	Feb. 20	0300-0700	1 O	2113 2349	SLC PUC	n.i.r. n.i.r.	13-15
	6	Feb. 29	0530-0930	① LM	0013	SLC	¼ inch	16
	7	Mar. 1	2145-0145	1 O	1740 1800 1921 2350	SLC SLC SLC SLC	n.i.r. LGT-MDT n.i.r. n.i.r.	6 8-18 5-7 10-13
	8	Mar. 14	1900-2300	① LM	1721 2058 2105 2121	SLC-BYI MLD FFU SLC	V. LGT MDT n.i.r. n.i.r.	12 13 21 22
	9	Mar. 19	1400-1800	1 L	1700 1753 1825 1928	SLC SLC SLC OGD	LGT LGT n.i.r. n.i.r.	10-13 16 10 8
	10	Mar. 27	2015-0015	1 O	No reports			

LIST OF STATION LOCATIONS

BOI	Boise
BVL	Bonneville
BYI	Burley
DPG	Dugway
DTA	Delta
ELY	Ely
FFU	Fairfield
HIF	Hill AFB
HLN	Helena
HVE	Hanksville
IDA	Idaho Falls
LGV	Logan
MLD	Malad
MLF	Milford
OGD	Ogden
PIH	Pocatello
PVC	Price
PVU	Provo
RKS	Rock Springs
SGU	St. George
SLC	Salt Lake City
SUN	Sun Valley
TWF	Twin Falls
4SV	Strevell

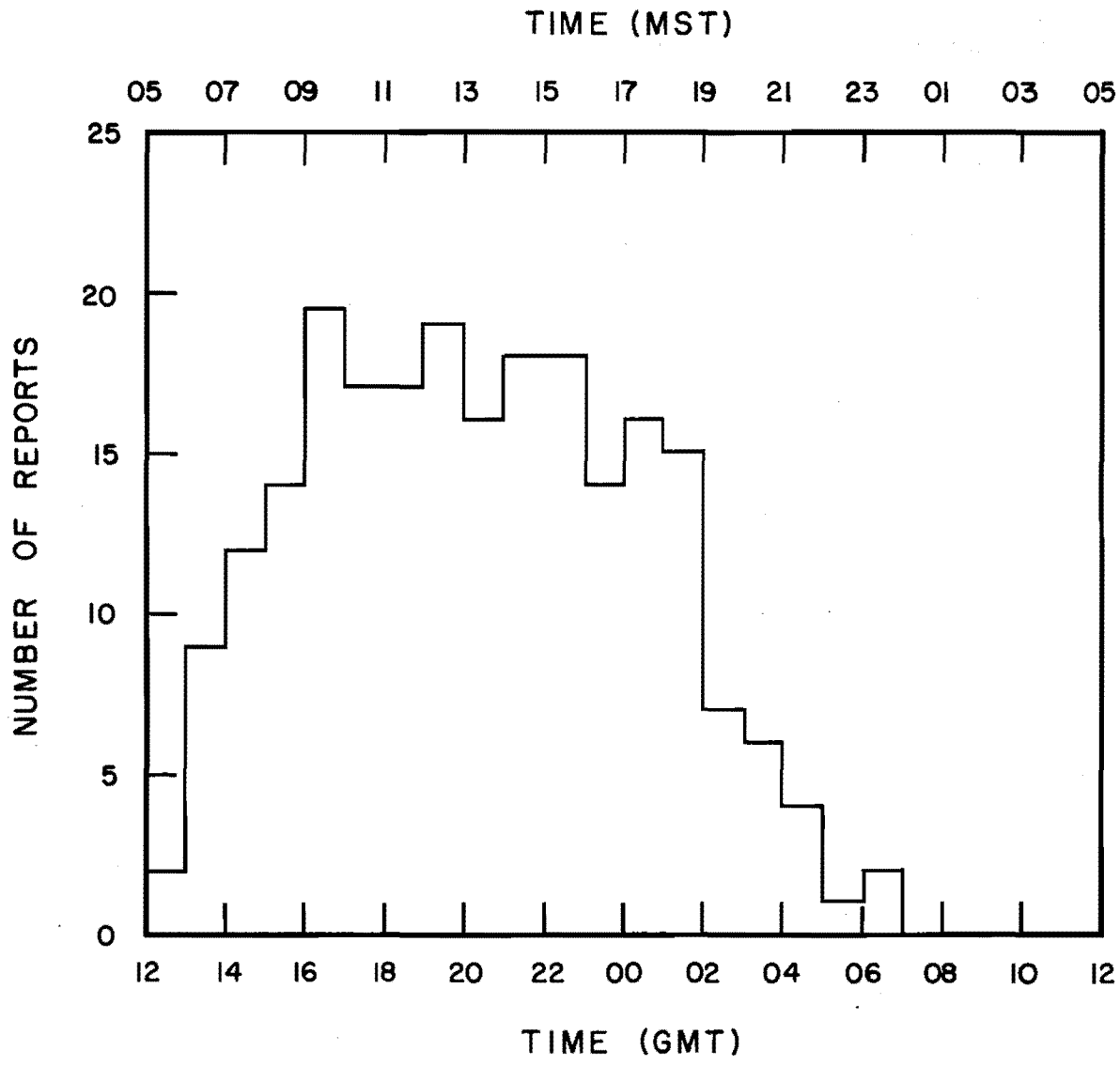

Figure 57. Hourly frequency of aircraft reports (PIREP).

B.0 APPENDIX B

A list of personnel and the area of contribution to the research are given below. Personnel associated with previous projects are not listed here. The period covered herein is July 1, 1971 to the time of completion of the project. Personnel associated with the airborne seeding program are listed as follows:

Research staff (including full-time graduate students):

Name	Specialty	Assignment
Balick, Lee	Meteorologist	Data analysis, diffusion calculations
Bindrup, Verl K.	Technician	Field installations, maintenance
Campbell, Ronald H.	Meteorologist (G.S.)	Data Processing
Chadwick, Prof. Duane G.	Elec. Engineer	Precipitation sensors, radar
Chappell, Dr. Charles F.	Meteorologist	Project Leader 1971-72
Dittmer, Kent	Programmer (G.S.)	Computer programming
Fletcher, Prof. Joel E.	Chemist	Precipitation chemistry
Griffin, Donald L.	Elec. Engineer	Telemetry system
Harrelson, H.E.	Technician	Radar, field work
Hill, Dr. Geoffrey E.	Meteorologist	Project Leader 1972-77
Johnson, Floyd	Meteorologist (G.S.)	Cloud microphysics, rawinsonde
May, Joyce	Data Specialist	Data Processing
McNeill, William N.	Meteorologist	Field program supervisor, rawinsonde
Merritt, Harold	Senior Technician	Seeders, radar, rawinsonde
Morgan, Dr. Neil	Research Assistant	Computer programming
Sleight, Gayla	Research Associate	Data processing
Rao, Dr. Ramana	Meteorologist	Data analysis
Reynolds, Dr. George W.	Meteorologist	Data analysis
Woffinden, Duard S.	Elec. Engineer	Field electronics, seeders, rawinsonde
Wooldridge, Dr. Gene	Meteorologist	Diffusion

Student assistants:

Name	Assignment
Gerber, Richard	Precipitation chemistry
Hayman, Charles	Electronics
Jorgensen, Jeff	Computations
Leatham, Larry	Precipitation chemistry
Slusser, William	Ice nuclei analysis
Stenquist, Lee	Field calibrations
Thomas, Lynn	Field calibrations
Thornley, Paul	Seeders, ice crystal replicator

Personnel associated with the ground seeding program are listed as follows:

Name	Specialty	Assignment
Bindrup, Verl K.	Technician	Field installations, maintenance, rawinsonde
Griffin, Donald L.	Elec. Engineer	Telemetry system
Hill, Dr. Geoffry E.	Meteorologist	Project Leader
McNeill, William N.	Meteorologist	Rawinsonde
Merritt, Harold	Senior Technician	Seeders
Rao, Dr. Ramana	Meteorologist	Data preparation
Woffinden, Duard S.	Elec. Engineer	Field electronics, seeders, rawinsonde